1-1-1990

Sensitization of vesicles to pH and glucose/

Brian Patrick Devlin
University of Massachusetts Amherst

SENSITIZATION OF VESICLES TO PH AND GLUCOSE

A Dissertation Presented

by

BRIAN PATRICK DEVLIN

Submitted to the Graduate School of the
University of Massachusetts in partial fulfillment
of the requirements for the degree of

DOCTOR OF PHILOSOPHY

September 1990

Polymer Science and Engineering

SENSITIZATION OF VESICLES TO PH AND GLUCOSE

A Dissertation Presented

by

BRIAN PATRICK DEVLIN

Approved as to style and content by:

David A. Tirrell, Chair

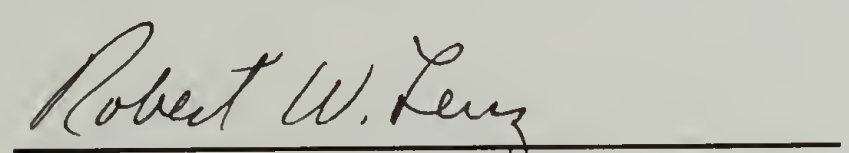

Robert W. Lenz, Member

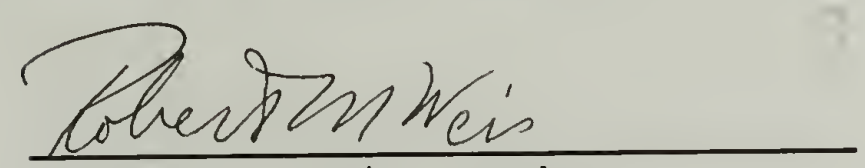

Robert M. Weis, Member

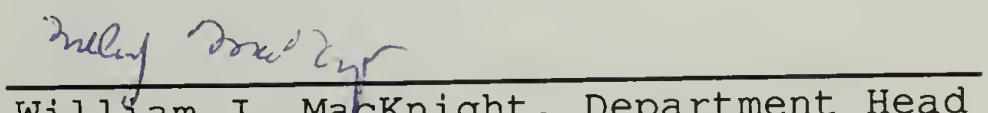

William J. MacKnight, Department Head
Polymer Science and Engineering

ACKNOWLEDGEMENTS

I would like to take this opportunity to acknowledge the people who helped me throughout my graduate career.

First and foremost, I would like to thank my thesis advisor, Dr. David Tirrell, for giving me guidance and freedom in my research. He set a great example of a scientist for me to try modeling myself after.

I am deeply indebted to Dr. Mike Ferritto for the help he gave me with my research. Many problems were ironed out after discussing them with Mike. In addition, he was a great friend, roommate, and weight lifting partner. I will miss our daily conversations. I would also like to extend gratitude to Dr. Doug Wicks and Kevin McGrath for their friendship and the many valuable discussions I had with each of them.

I would like to acknowledge Dr. David Gross for the use of the fluorescence microscope and to Alex Jesurum for his assistance in using the microscope.

Finally, I would like to thank my parents, Michael and Dorothy for giving me the drive, support, and discipline it took to attain this degree.

ABSTRACT

SENSITIZATION OF VESICLES TO PH AND GLUCOSE

SEPTEMBER 1990

BRIAN PATRICK DEVLIN, B.S., PENNSYLVANIA STATE UNIVERSITY

Ph.D., UNIVERSITY OF MASSACHUSETTS

Directed by: Professor David A. Tirrell

The structural reorganization of vesicle membranes that occur due to a pH dependent complexation of the membranes with poly(2-ethylacrylic acid) (PEAA) was investigated. The kinetics of the reorganization were examined by monitoring the changes in the turbidity of vesicle suspensions that occurs during the reorganization. The response of the rate of reorganization to pH, temperature, and membrane composition was studied. It was found that the reorganization behaved similarly to the solubilization of phosphatidylcholine vesicle by apolipoproteins. Permeability changes accompanying the process were recorded by monitoring the fluorescence changes of vesicle suspensions containing a fluorescent marker. The rate of change in permeability was found to be fast relative to the rate of structural reorganization.

PEAA was labeled with the dansyl chromophore. Fluorescence microscopy was used to visualize the interaction of the labeled polymer (DnsPEAA) with egg yolk phosphatidylcholine vesicles. Adsorption of DnsPEAA onto vesicle surfaces produced a concentration of fluorescence on the vesicles. Following acidification of these samples,

vesicles reorganized into many smaller particles with a diffusion of fluorescence.

The reorganization was sensitized to the presence of glucose by incorporating the enzyme, glucose oxidase, into vesicles suspensions containing PEAA. The rate of permeability increase of membranes could be controlled by adjusting the concentrations glucose, enzyme, oxygen and PEAA.

TABLE OF CONTENTS

Page

APPENDICES

LIST OF TABLES

LIST OF FIGURES

Page

CHAPTER I

INTRODUCTION

A. Phospholipid Vesicles

Biological membranes surround cells and provide the compartment for the microenvironment of the cell. They mediate the important cellular functions of fusion, recognition, endocytosis, exocytosis, intercellular interaction, excitability, translocation, transport and osmosis.[1] Much of our understanding of membranes and their processes is derived from the study of membrane models. Membranes of plant and animal cells are typically composed of 40-50% lipids and 50-60% proteins. Because of the critical role of lipids in cell membranes, phospholipid vesicles have been extensively investigated as models.[2-5]

Phospholipids are double chain surfactants possessing a polar phosphodiester head group and nonpolar hydrocarbon tails. When long chain diacyl phospholipids of the correct geometry are hydrated and agitated above the transition temperature (T_m) of the lipid, the lipid molecules reorganize into a series of concentric bilayer membranes usually consisting of 6 to 9 bilayers separated by layers of water (see Figure 1.1).[6,7] These structures, termed multilamellar vesicles (MLV's), range in size from 0.1 to

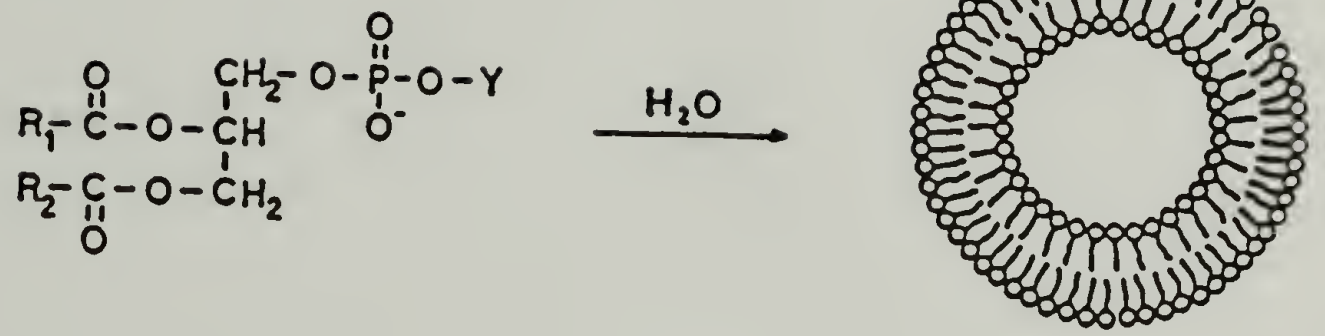

Figure 1.1 Formation of vesicular structures via the dispersion of phospholipid molecules in aqueous solution.

5μm.[8,9] Suspensions of MLV's appear turbid due to the scattering of incident light. Small unilamellar vesicles (SUV's) [10] of a more narrow size distribution can be prepared through sonication of MLV suspensions. The SUV's have diameters ranging from 20 to 50 nm.[11] Many procedures have been developed to prepare vesicles of a specified structure although ease of preparation favors the use of MLV's in many instances.[12] The unique structure of vesicles arises from the amphiphilic nature of the phospholipid molecule. The hydrophobic acyl chains associate in a lamellar array to minimize the number of water contacts leaving the polar head groups of the lipids exposed to the aqueous phase. The separation of aqueous layers by a non-polar bilayer enables the entrapment of drugs, proteins, and other biologically active substances.[13-18]

MLV's composed of a single pure phospholipid are characterized by a temperature dependent, endothermic, reversible order-disorder transition that occurs over a narrow temperature range centered around the "melting temperature" (T_m) for the particular lipid. Below T_m, the polymethylene acyl chains exist in an all trans conformation. Raising the temperature above T_m induces a few bonda along the acyl chains adopt the gauche conformation resulting in lateral expansion and a decrease in thickness of the bilayer.[19-22] The phase transition temperature is dependent on the structure of the headgroup (**Y**) and the length and degree of saturation of the diacyl chains(**R**) (see

Figure 1.1).[23-29] This transition temperature can be measured by high sensitivity differential scanning calorimetry.

Liposomes formed from dipalmitoyl phosphatidylcholine (see Figure 1.2) display a sharp transition at 41.4°C.[30] The main transition properties are shown for various saturated phosphatidylcholines in Table 1.1 [30].

Table 1.1 Melting transitions (T_m) of some saturated phosphatidylcholines.

Lipid	# of methylenes in R	T_m(°C)
DLPC	10	-1.8
DMPC	12	23.9
DPPC	14	41.4
DSPC	16	54.9

While the phase behavior of vesicles consisting of a single phospholipid appears relatively simple, the phase behavior of lipid mixtures is much more complicated. It has been established that domains of lipids can exist in biomembranes and phase separations can occur in mixed lipid bilayers.[31-34] The phase behavior of DLPC, DMPC, DPPC, and DSPC binary mixtures has been examined.[30] It was found that for lipid mixtures involving up to a difference of four methylene groups in the hydrophobic chains there was some degree of miscibility. DSC of these mixtures gave a single broad peak centered at a temperature between the melting temperatures of the pure components. The acyl chain

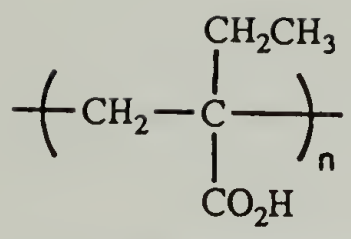

Poly(2-ethylacrylic acid) (PEAA)

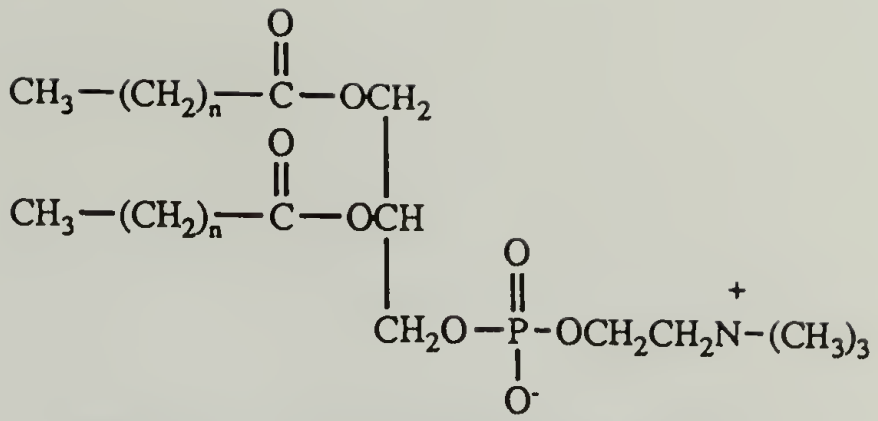

n=10 Dilauroyl phosphatidylcholine (DLPC)
n=12 Dimyristoyl phosphatidylcholine (DMPC)
n=14 Dipalmitoyl phosphatidylcholine (DPPC)
n=16 Distearoyl phosphatidylcholine (DSPC)

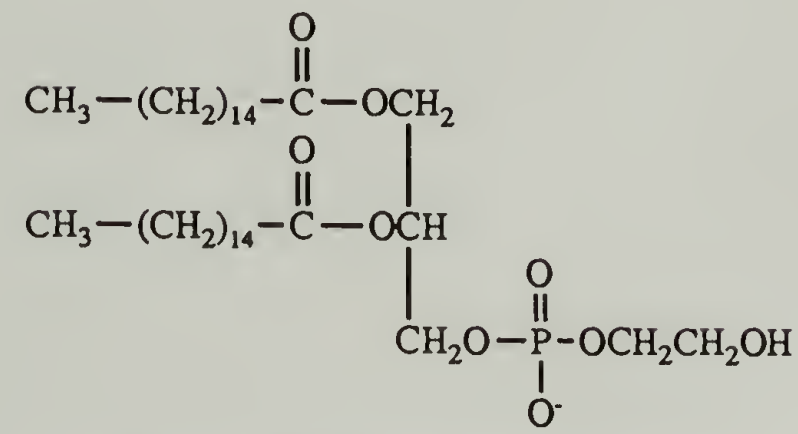

Dipalmitoyl phosphatidylglycerol (DPPG)

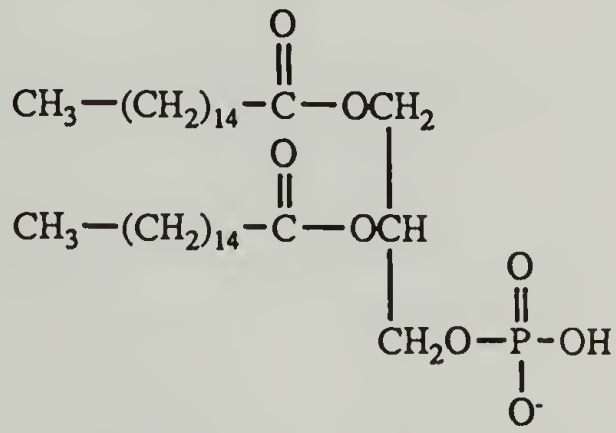

Dipalmitoyl phosphatidic acid (DPPA)

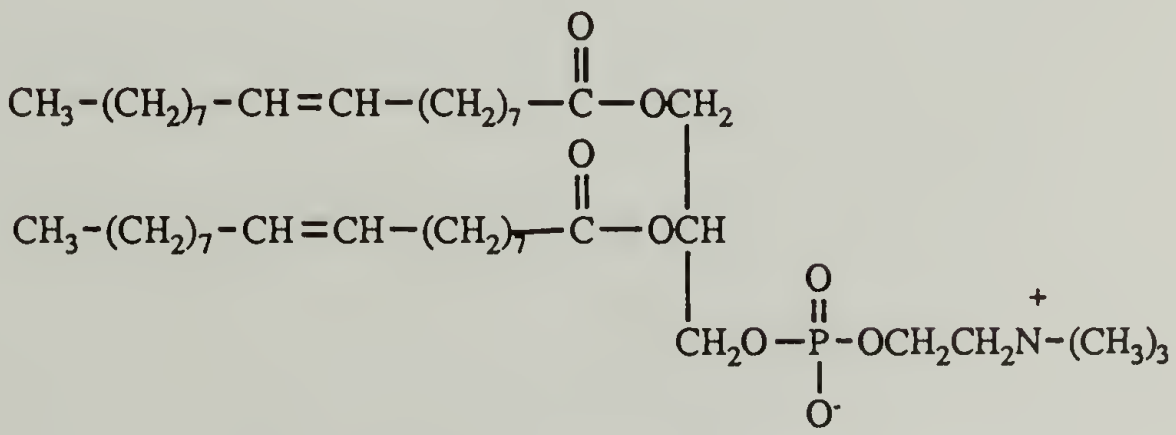

Dioleoyl phosphatidylcholine (DOPC)

Figure 1.2 Chemical structures with abbreviations of materials used in vesicle investigations.

length of DSPC differs from that of DLPC by six carbons. Consequently, DLPC/DSPC mixtures show a degree of immiscibility. DSC thermograms of DLPC/DSPC mixtures exhibit an endotherm characteristic of DLPC with a broad endotherm that moves to higher temperature with increasing DSPC content.[30](see Figure 1.3)

Lyso-phosphatidylcholines (lyso-PC's) are a class of phosphatidylcholines which are partially hydrolyzed, and have only one acyl chain (see Figure 1.1, R_1 or R_2 = H). This chemical structure imparts a wedge-shaped geometry to the molecule. Because of this geometry, lyso-PC's form micelles rather than vesicles when dispersed in water.[35] In mixtures of lyso-PC's and phosphatidylcholines, lyso-PC destabilizes the bilayer structure. Permeability studies by Mandersloot *et al.* demonstrated a dramatic increase in permeability of egg-PC vesicles when the lyso content exceeds 22.5%.[36]

In contrast to lyso-PC's, cholesterol exhibits a bilayer stabilizing force when mixed with PC. It is well known that cholesterol reduces the average molecular surface area, reduces membrane permeability, alters lateral diffusion for lipids and modulates acyl chain order.[12] DSC studies of DPPC/cholesterol mixtures establish that at a cholesterol content greater than 5 percent, the endothermic peak of the mixture can be analyzed as the sum of two peaks, a broad one and a narrow one.[37] The broad peak is centered at 41.0-41.6°C up to 20 mole percent cholesterol and then moves up to

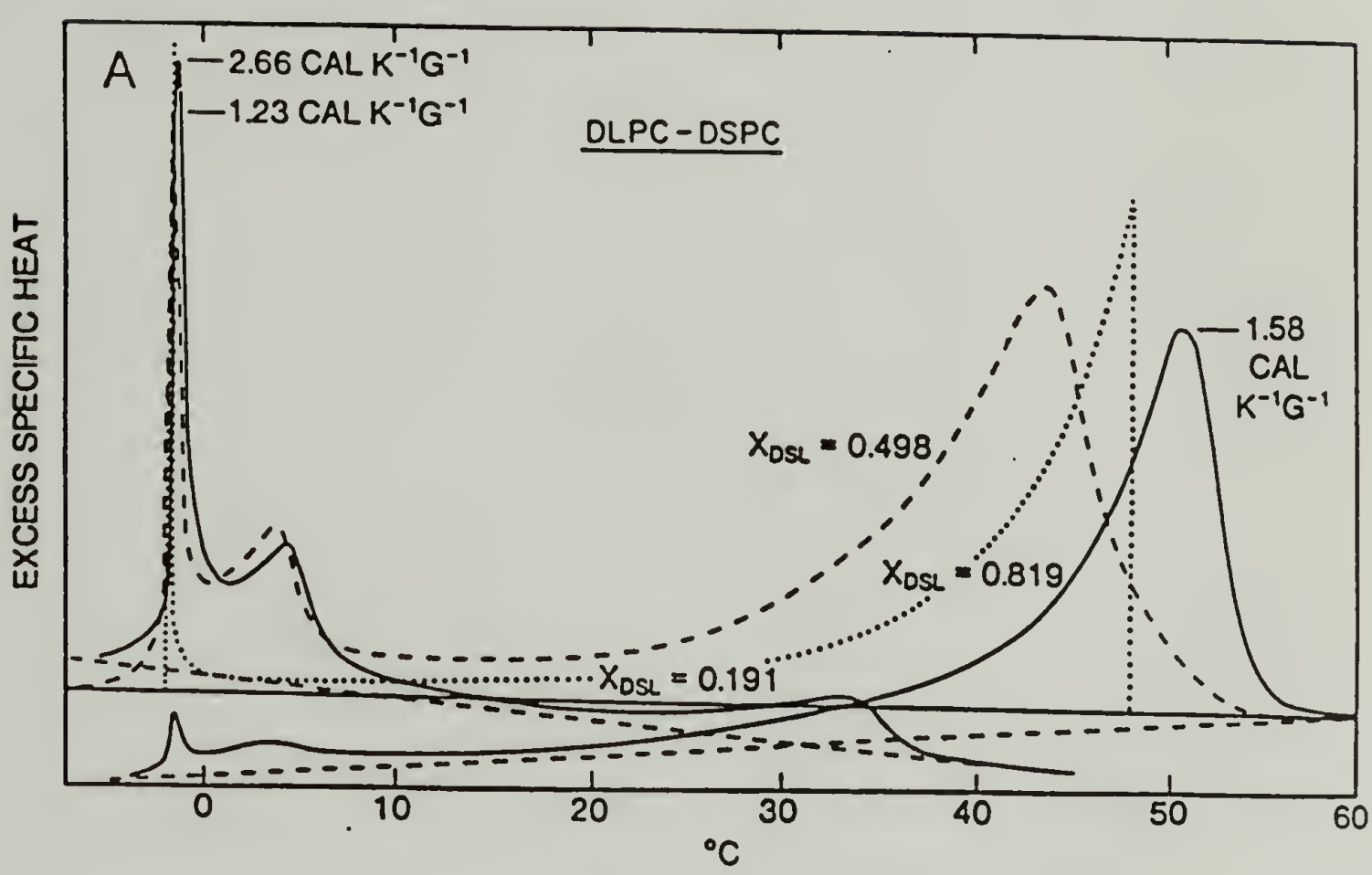

Figure 1.3 Differential scanning calorimetry scans of DLPC/DSPC mixtures. From Mabrey, S.; Sturtevant, J.M., *Proc. Natl. Acad. Sci.*, **73(11)**, 3862 (1976).

45.6°C at 33 mole percent. An endotherm remains present up to 50 percent cholesterol incorporation.

B. Solution Conformation of Poly(carboxylic acid)s

The conformation of a poly(carboxylic acid)s in aqueous solution depends upon the extent of ionization of the carboxyl groups attached to the polymer. At high pH, the polymer exists as an extended coil to reduce electrostatic repulsions between neighboring carboxyl groups arising from the high degree of ionization of the chain. As the pH is depressed to near the pK_a of the carboxylate groups on the polymer, many of the groups become neutralized and the polymer chain collapses into a globular form due to the internal hydrophobic attractive forces of the chain overcoming the decreasing electrostatic repulsions (see Figure 1.4). For poly(acrylic acid), the reversible change in hydrodynamic radius of the chain is linear with pH [38-41]. For poly(methacrylic acid), the change in hydrodynamic radius with pH is non-linear with pH[42-50]. The presence of an extra methyl group causes the polymer to unfold in a more cooperative manner with increasing pH because of stronger intramolecular hydrophobic attractions. Thomas determined by fluorimetry that this transition occurs around pH 5.0, although the precise transition pH is dependent on the ionic strength of the solution.[51]

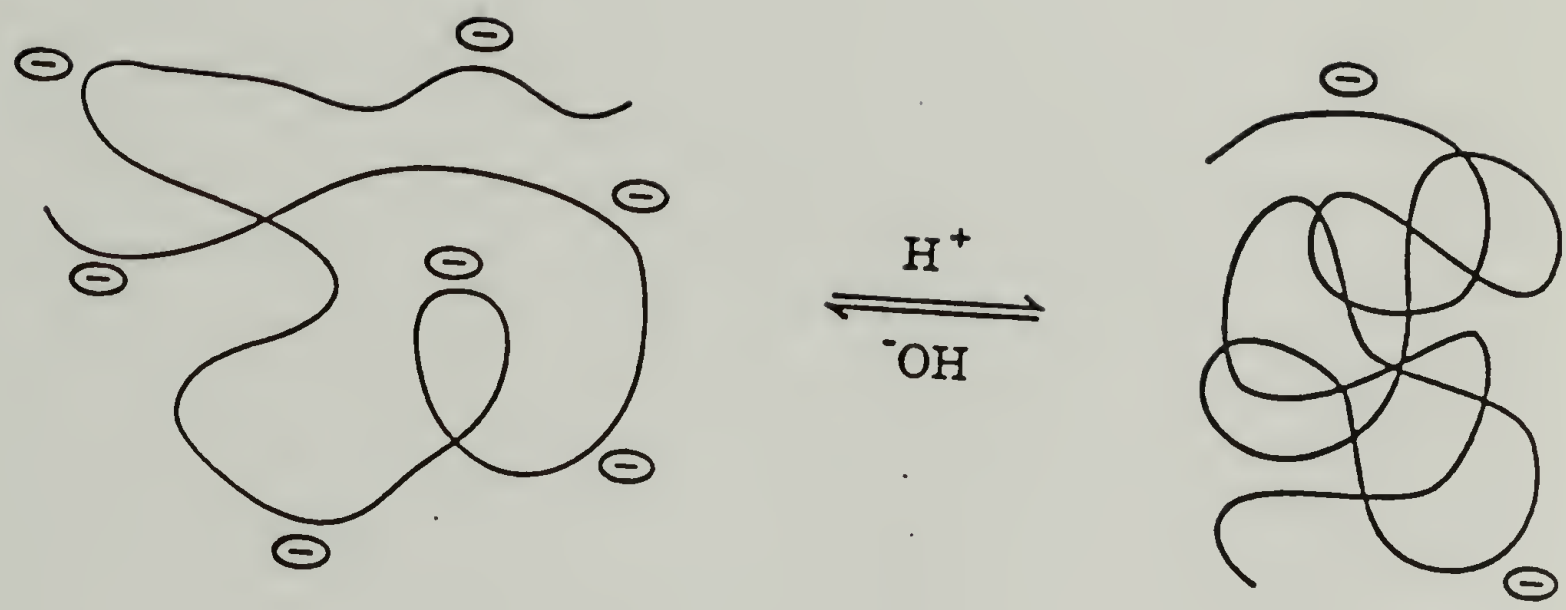

Figure 1.4 The reversible pH-induced conformational transition of PEAA.

Poly(2-ethylacrylic acid) exhibits an even more cooperative unfolding with increasing pH. The presence of the extra methylene group imparts additional hydrophobic character to the chain and raises the pK_a of the acid groups. Viscometric[52], potentiometric[53,54], ^1H NMR[52], fluorimetric[55-57], and dynamic light scattering[58,59] methods have been used to study the conformational transition of PEAA. The conformational transition has been determined to occur around pH 7.0.

The hydrophobic globule form of poly(methacrylic acid) has been shown to solubilize simple hydrocarbons. Below a degree of ionization of 0.1, the solubility of simple n-alkanes and polycyclic aromatic hydrocarbons in poly(methacrylic acid) solutions is dramatically increased and is linearly dependent on the concentration of the polymer.[60,61] Additionally, the solubility was shown to be dependent on the molecular weight up to a value of one million.[61] This ability to solubilize non-polar compounds is not exhibited by poly(acrylic acid) owing to the decreased hydrophobicity of poly(acrylic acid).[60,61]

C. Poly(carboxylic acid)-Vesicle Interactions

As mentioned previously, the unique structure of liposomes yields the ability to entrap many different types of solutes in the aqueous cavity of the liposome. This function is attractive for the possible use of vesicles as

drug carriers. One parameter which this use depends on is the ability to sensitize the release of the vesicle contents to the areas of need within the body. The pH of blood and tissue fluids, normally 7.4, has been reported to drop to 6.9 in tumor sites and may be reduced to as low as 6.2 by the addition of $NaHCO_3$, glucose, or CO_2.[62,63] There has been some work on the design of pH-sensitive liposomes by the incorporation of pH sensitive functional groups into the vesicle bilayer.[64,65] In these systems, complete release of entrapped fluorescent dyes was observed upon acidification of the vesicle solutions.

Tirrell *et al.* demonstrated the pH and temperature dependent destabilization of PC vesicles through the interaction of the vesicles with polyelectrolytes.[66-68] It was discovered that there was a highly pH-dependent complexation of certain poly(carboxylic acid)s with the vesicles. The critical pH for the interaction of PAA, PMAA, and PEAA was found to be 4.6, 5.3, and 6.9 respectively. The increased pH of interaction with increasing length of alkyl substituent parallels the trend of increasing pK_a for these polymers. Although PAA and PMAA did cause some perturbation of the vesicular structure, it was found that poly(2-ethyl-acrylic acid) (PEAA) caused complete destabilization and reorganization of the lipid bilayer. DPPC vesicles suspended in a solution of PEAA are stable at pH 7.4. However, at a temperature above the T_m of the lipid, decreasing the pH of the solution below 7.0 induces a bilayer-destabilizing

interaction of the PEAA chains with the vesicle surface. During this reorganization, initially turbid vesicle suspensions become transparent due to a decrease in particle size. A plot of optical density versus pH for this system shows a dramatic decrease in optical density which is centered around pH 6.9 (see Figure 1.5).[67] The exact critical pH for the reorganization can be controlled by changing the polymer tacticity.[68] DSC studies show a transition from a narrow endotherm for the vesicles in the presence of PEAA at pH 7.4 which broadens as the pH is lowered until eventually no peak is observed concurring with the optical density measurements.

The optical density of the PEAA/vesicle system falls due to a decrease in particle size of the lipid containing particles (see Figure 1.6). This was studied in detail by Borden et.al..[55] Transmission electron micrographs of PEAA/DPPC systems were examined at various steps in the reorganization process, and demonstrated the conversion of vesicles into a mixed micellar structure having dimensions of 54±6 Å in thickness and 160±50 Å in length. These sizes are confirmed by light scattering measurements. Similar mixed micelles are proposed for mixtures of dipalmitoyl phosphatidylglycerol with PAA, [69] and are also formed by the interaction of PC vesicles with apolipoproteins, bile salts, and detergents.[70-72]

The effect of this reorganization is seen more dramatically when monitoring the release of an entrapped dye.

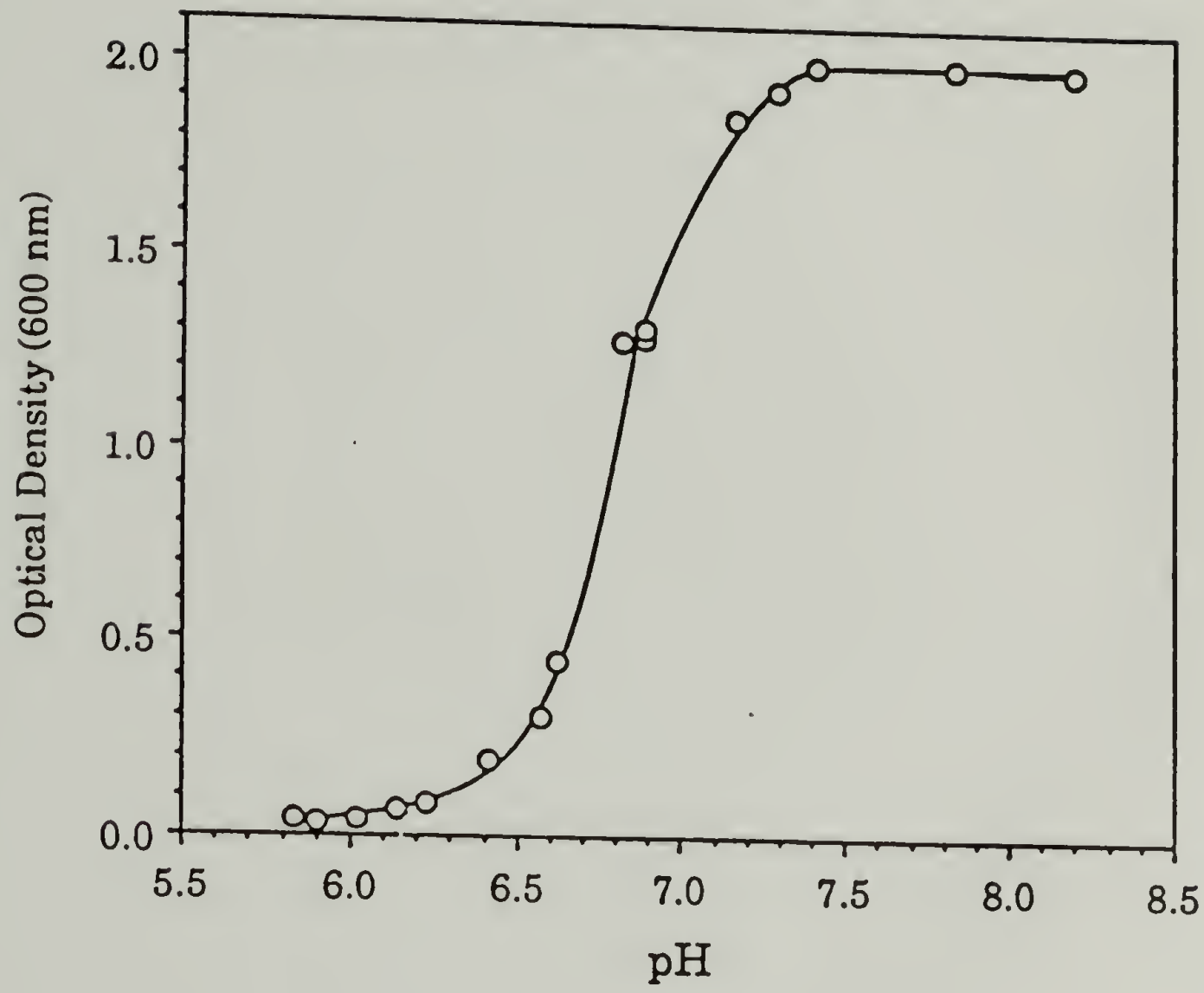

Figure 1.5 Optical density measurements on 0.02M phosphate buffered suspensions of DPPC MLVs prepared in the presence of PEAA. Concentration of both PEAA and DPPC was 1.0 mg/ml. From Tirrell, D.A.; Takigawa, D.Y.; Seki, K., *Ann. N.Y. Acad. Sci.*, **446**, 237 (1985).

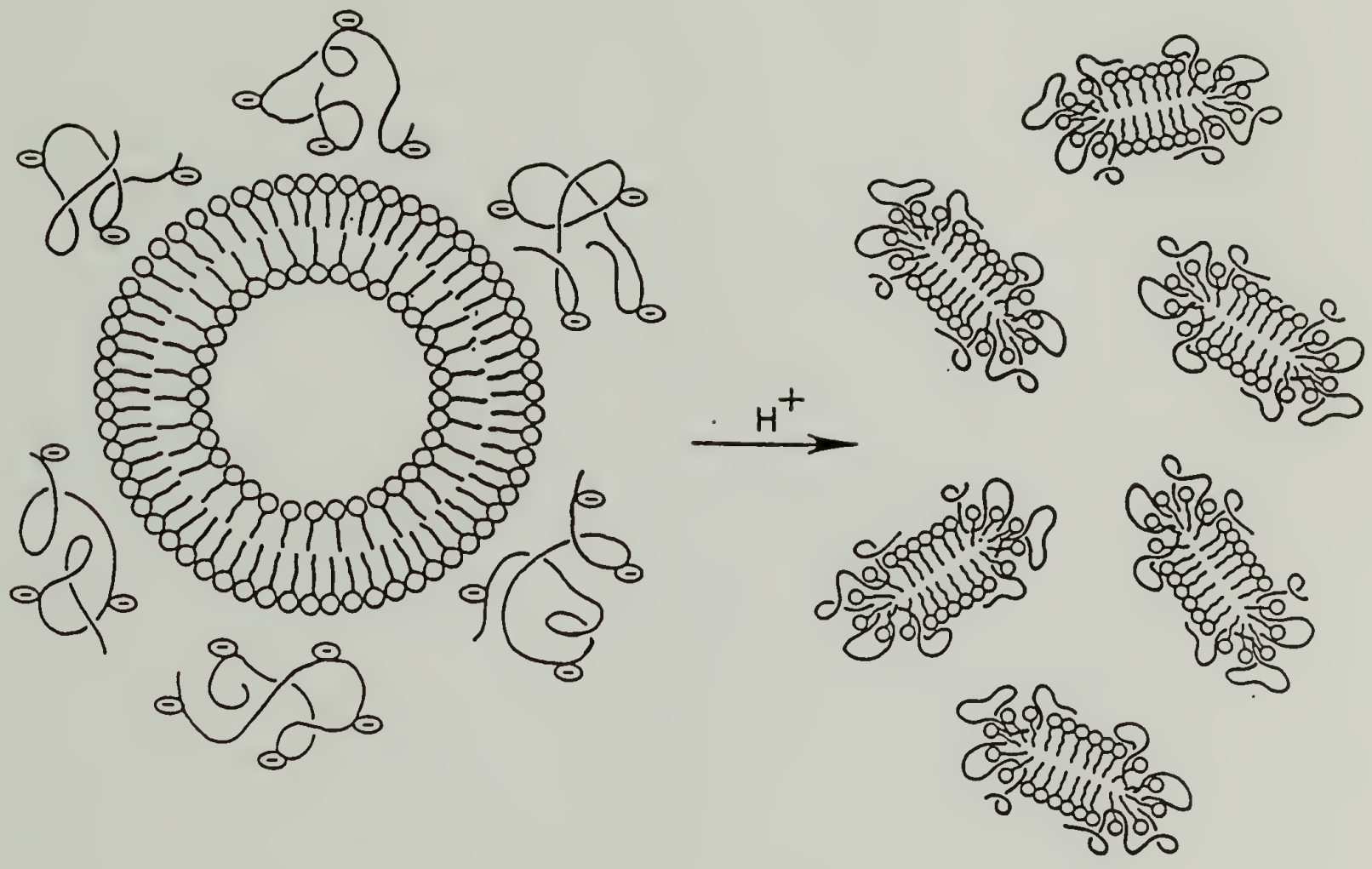

Figure 1.6 The pH-induced structural reorganization of phospholipid vesicles into mixed micelles by PEAA.

Figure 1.7 shows the fluorescence of a suspension of egg yolk phosphatidylcholine (EYPC) SUV's with entrapped 6-carboxy-fluorescein in the presence of PEAA.[67] At pH 7.4, there is a small increase in fluorescence due to leakage of the fluorescent dye. However, when the pH is lowered to 6.5 there is a complete concomitant release of the dye. The change in permeability is attributed to the interaction with the globular form of PEAA.

More recently, Ferritto has demonstrated that the interaction and reorganization of PC vesicles could be controlled photochemically.[73] The photochromic groups, spirobenzopyran and azobenzene, were chemically attached pendant to PEAA samples. Azobenzene modified PEAA samples interacted strongly with vesicles when kept in the dark. Conversely, the interaction of the spirobenzopyran-modified polymer was triggered by exposure to light.

D. Glucose Oxidase and Glucose-sensitive Systems

It was shown previously that disruption of vesicle membranes by PEAA is accompanied by rapid, quantitative release of vesicle contents.[67] The macromolecular signaling process has been sensitized to pH[67], temperature[68], and light[73]. It is of interest to sensitize the process to the presence of a neutral solute such as glucose. One can imagine therapeutic applications of this in self regulated insulin delivery or diagnostic uses in

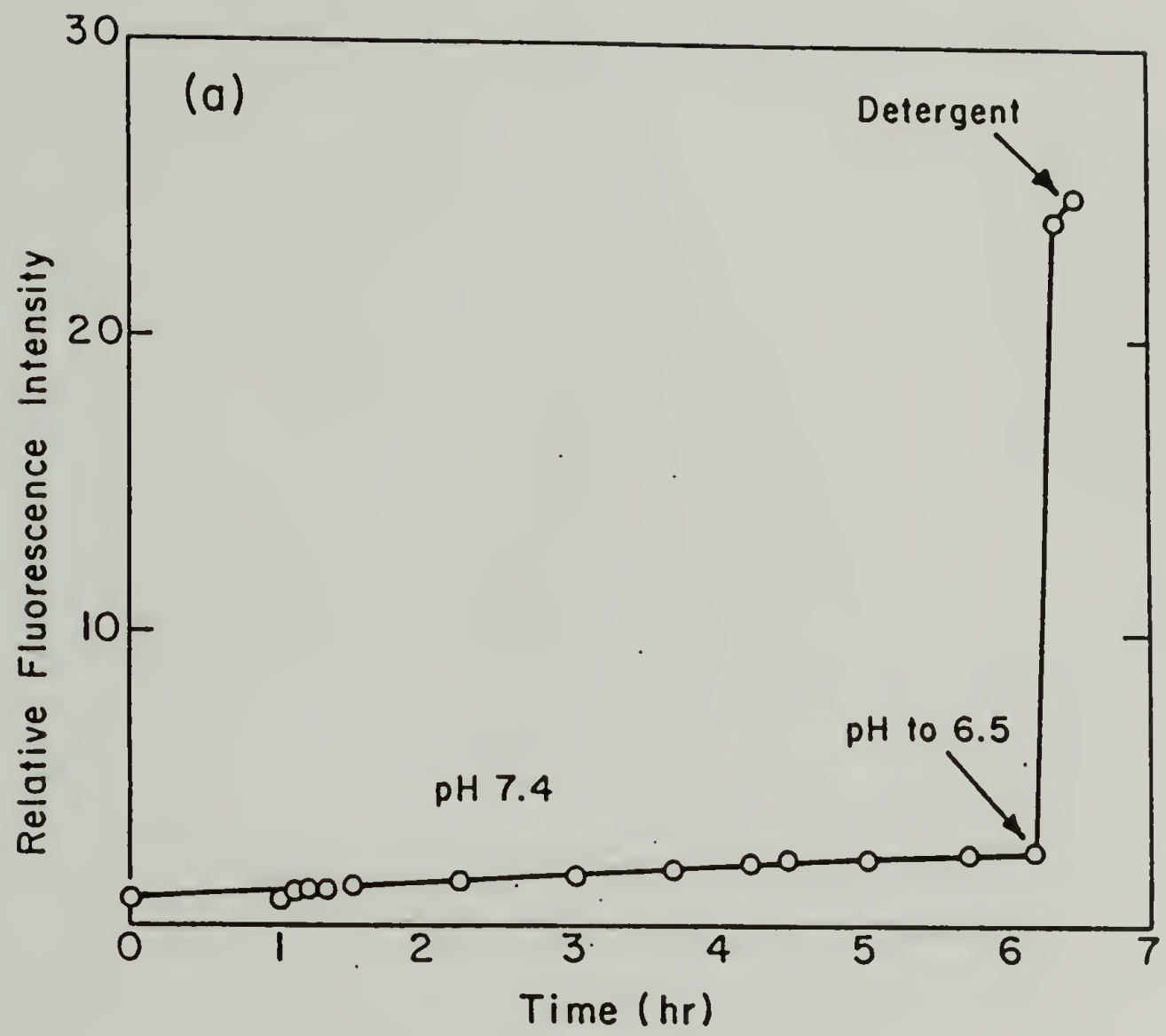

Figure 1.7 The release of 6-carboxyfluorescein from EYPC single unilamellar vesicles. Release is brought about by acidification from pH 7.4 to 6.5 in the presence of PEAA. From Tirrell, D.A.; Takigawa, D.Y.; Seki, K., *Ann. N.Y. Acad. Sci.*, **446**, 237 (1985).

monitoring of glucose concentrations in physiologic fluids. The reorganization of vesicles by PEAA is ultimately controlled by the production of protons in the system (i.e. addition of acid), and one can generate protons by the enzymic oxidation of glucose.

The enzyme, glucose oxidase (GO), was discovered by Muller in 1928 in *Aspergillus niger* and *Penicillum glaucum*.[74] Muller found that the enzyme catalyzes the oxidation of glucose to gluconic acid by means of molecular oxygen. Later, it was demonstrated that during the oxidation, oxygen was reduced to hydrogen peroxide.[75,76] The overall reaction is:

$$C_6H_{12}O_6 + H_2O + O_2 \longrightarrow C_6H_{12}O_7 + H_2O_2$$

The enzyme is fairly specific for glucose over other sugars. Table 1.2 shows the relative selectivity of GO for glucose.[77]

GO as isolated from *Aspergillus niger* was determined by sedimentation experiments to have a molecular weight of approximately 154,000.[78] It was determined from absorption measurements that there were two moles of the coenzyme, flavin adenine dinucleotide (FAD) present for every mole of oxidase.[79] The mechanism by which the coenzyme participates in the oxidation of glucose was shown by tracer experiments with $^{18}O_2$ and H_2O^{18} (see Figure 1.8).[80]

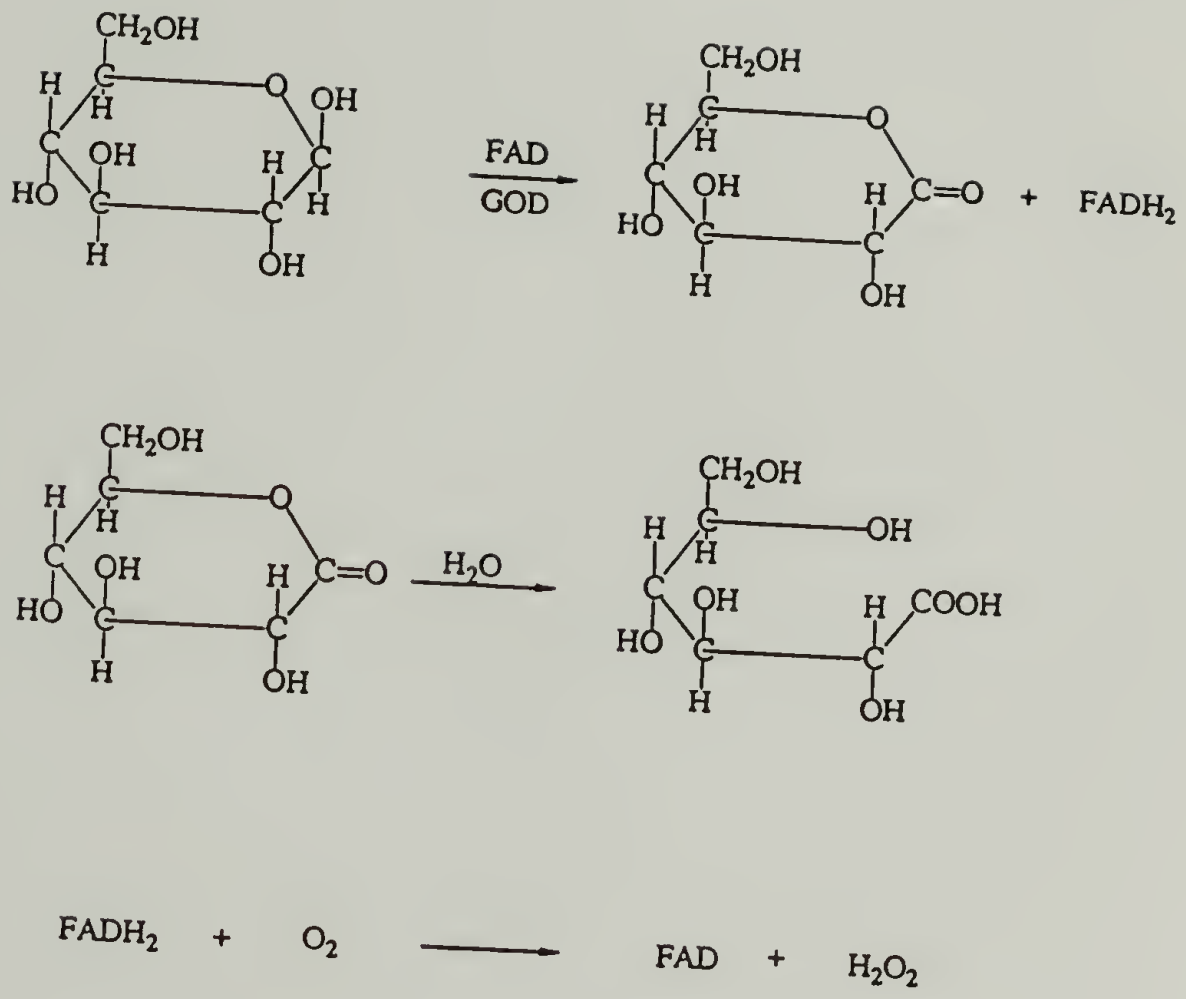

Figure 1.8 Mechanism of the enzymatic reaction of glucose and glucose oxidase.

Table 1.2 Relative rates of glucose oxidation by glucose oxidase from *Aspergillus niger*.[78]

Sugar	Rel. Rate[a]
D-Glucose	100
L-Glucose	0
2-Deoxy-D-glucose	20
4-O-Methyl-D-glucose	15
6-Deoxy-D-glucose	10
4-Deoxy-D-glucose	2
D-Mannose	1
3-Deoxy-D-glucose	1
6-O-Methyl-D-glucose	1
D-Galactose	0.5
5-Deoxy-D-glucose	0.05
D-Allose	0.02
3-O-Methyl-D-glucose	0.02

[a]Rates were determined manometrically by the uptake of O_2.

As with other enzymes, the activity of GO is dependent on temperature and pH. The pH at which the enzyme is most active is 5.6 and variations of phosphate and acetate buffer concentrations between 0.03 M and 0.25 M do not influence the rate of oxygen consumption. The enzyme becomes unstable above a pH of 8.0 although at that pH, the presence of glucose exerts a protective action.[81] The enzyme becomes more active with an increase in temperature up to approximately 40°C where the activity begins to degrade.

As mentioned, oxygen is an integral part of the oxidation scheme, and serves as the ultimate hydrogen acceptor. The concentration of oxygen in solution greatly affects the rate of oxidation of glucose. In oxygen saturated solutions, GO oxidizes glucose 2.5 times faster

than in solutions equilibrated in air. Other hydrogen acceptors have been shown to work with glucose oxidase such as 2,6-dichlorophenolindophenol[81], but the rate of glucose oxidation is only 3.3% of that in the presence of oxygen.[82]

E. Glucose-Sensitive Insulin Delivery Systems

The conventional insulin injection treatment of diabetes gives poor control of blood sugar levels when compared to the normal homeostatic system. Abnormal glucose levels may be the cause of many of the degenerative diseases associated with diabetes.[83] Research has been active in this field to provide a regulated insulin delivery system. Four approaches have been taken toward this goal: 1) transplantation of pancreatic islet cells 2) development of polymer membranes that swell in response to glucose 3) development of insulin infusion pumps and 4) binding of a chemically modified insulin to lectins.

The transplantation of islet cells surrounded by polymer membranes has shown encouraging results.[84,85] The membrane allows transport of insulin and glucose but restricts the passage of immunoglobulins that would reject the cells. A computerized insulin infusion pump has been devised that delivers precise doses of insulin in response to low blood sugar levels mimicking the body's natural function.[86] However, work is still being done to reduce the size of such systems and improve the life of the glucose sensors.

Horbett developed a glucose responsive membrane from a crosslinked poly(dimethyl amino methacrylate).[87] GO was entrapped in the membrane. Glucose entering the membrane was oxidized to gluconic acid and protonated the polymer causing it to swell due to electrostatic repulsions. The increased pore size of the membrane allowed insulin to permeate across the membrane. Ishihara took a similar approach using two membranes.[88] GO was entrapped in a poly(acrylamide) gel acting as a glucose sensor. A second membrane contained the nicotinamide moiety that acted as a regulator of insulin permeation by means of an oxidation reaction with hydrogen peroxide. In the fourth approach, Jeong used a glycosylated insulin bound to Concanavalin A inside a microcapsule.[89] The competitive binding of glucose onto the lectin released the modified insulin.

F. Goals and Overview

Tirrell and coworkers have shown that initially pH-insensitive phosphatidylcholine vesicles could be made sensitive to small changes in pH by the addition of poly(2-ethylacrylic acid).[67] It was found that the critical pH for the vesicle reorganization corresponded to the critical pH for the conformational transition of PEAA. The process was shown to involve two stages.[55] There is an increasing complexation of PEAA with the bilayer with decreasing pH followed by structural reorganization of the vesicle into

polymer/lipid mixed micelles with quantitative release of any entrapped materials upon further reduction in pH.

Although much is understood about the mechanism of the process, little is known about the rate of the process, how the rate is affected by environmental factors, and the relationship between the permeability and the reorganization of the membrane. Additionally, there is a need to generalize the switching process. The process has been sensitized to changes in pH[67], temperature[68], and to light[73]. It would be of interest to include sensitization to glucose.

The structural reorganization of vesicles into mixed micelles is characterized by a large decrease in the turbidity of the vesicle suspension due to the decrease in particle size. It should be possible to follow the reorganization kinetically. A kinetic study of the reorganization, and determination of the parameters that affect its rate, should provide valuable insight into the process. Dye release will be studied kinetically so that a comparison can be made between the rates of membrane permeabilization and reorganization.

The initial and final states of the reorganization process have been characterized by electron microscopy.[55] To view the transition between the two states, light microscopy will be employed. A fluorescently labeled PEAA will be synthesized so that fluorescence microscopy can be utilized. Fluorescence microscopy is a type of light microscopy that is sensitive only to fluorescent objects.

Using this technique, the location of the fluorescent PEAA can be followed. Comparison of conventional and fluorescence micrographs will provide valuable information about the transition of vesicles into mixed micelles and the incorporation of PEAA into the mixed micelles.

With the ability to release entrapped materials in response to pH one may envision possible therapeutic or diagnostic uses for vesicles in systems where the pH changes. The number of these types of uses becomes greater the more the process is generalized to other stimuli other than pH. It would be of interest then to be able to sensitize vesicles to as many stimuli as possible. The conversion of glucose to gluconic acid by the enzyme glucose oxidase provides an indirect way of sensitizing PEAA/vesicle systems to glucose. Measurement of the rate of pH depression with systematic variation of parameters that affect the enzymic reaction will provide information about the factors affecting the pH depression. This information will be coupled with dye release experiments to determine the rate of release of vesicle contents in response to the presence of glucose. Understanding of this system should extend to the use of proton producing enzymic reactions, in general, to effect the disruption of vesicles in response to other stimuli.

CHAPTER II

EXPERIMENTAL SECTION

A. Routine Measurements

Proton and carbon nuclear magnetic resonance spectra were recorded at 200 MHz and 50 MHz respectively on a Varian XL-200 spectrometer. Chemical shifts are reported as parts per million downfield from tetramethylsilane.

All melting points were recorded on a Fisher-Johns melting point apparatus and are uncorrected.

Copolymers were purified by ultrafiltration in a water/methanol (75:25) solution employing a S1Y3 spiral wound membrane cartridge from Amicon (molecular weight cutoff 3000; 1 square foot membrane area). The polymer solutions were pumped through the membrane cartridge by a Masterflex peristaltic pump at a rate of approximately 1 L/hr, maintaining a pressure of 20-25 psi over the membrane. Methanol was removed under reduced pressure on a rotary evaporator and the polymer was isolated by freeze drying.

Solution pH of all samples were measured with a Corning 155 pH/ion analyzer equipped with an Aldrich combination ultra-thin electrode. The pH meter was calibrated with pH 4 and pH 10 standardized buffers. Optical density and

absorbance measurements were obtained with a Beckman DU-7 UV/VIS spectrometer in 1 cm quartz sample cells. A water-jacketed cell holder connected to a Lauda RM-6 circulating bath was used when constant temperature measurements were desired. Temperature was controlled to ±0.1°C

Inherent viscosity measurements were determined with a Cannon-Fenske viscometer (model 50-L128) placed in a water bath with the temperature regulated to ±0.1°C by a Lauda MT constant temperature circulator.

Fluorescence measurements were performed on a Perkin-Elmer MPF-66 fluorescence spectrophotometer using 1 cm cells. A water jacketed cell holder connected to a Lauda K4R circulating bath was used when constant temperature measurements were desired. Temperature was controlled to ±0.1°C.

Elemental analyses measurements were determined at the Microanalysis Laboratory at the University of Massachusetts at Amherst.

B. Materials

All reagents and their sources are listed below. The reagents were used as received unless indicated otherwise. Letter codes indicate the source of the material.

2,2'-Azobis(2-methylpropionitrile), (AIBN), recrystallized from methanol, mp 101.5-102.5 °C (dec), lit.[90 mp 102-103°C (dec) (A).

Calcein (S)

Cellulose dialysis tubing, MW 2000 cutoff, rinsed with distilled water prior to use.(F)

Chloroform, HPLC grade (F)

Cholesterol, 98% (A)

Dansyl chloride, 98% (A)

1,3-Dicyclohexylcarbodiimide, 99% (DCC) (A)

Diethyl ether (F)

Diethyl ethylmalonate, 99% (A)

Diethylamine, 98% (A)

Dimethylformamide, ACS reagent grade (A)

L-α-Dilauroyl phosphatidylcholine, 99% (S)

3,3'-Dimethoxybenzidine, 97% (o-dianisidine) (A)

L-α-Dimyristoyl phosphatidylcholine, 99% (S)

L-α-Dioleoyl phosphatidylcholine, 99% (S)

L-α-Dipalmitoyl phosphatidic acid, sodium salt 98% (S)

L-α-Dipalmitoyl phosphatidylcholine, 99% (S)

L-α-Dipalmitoyl phosphatidylethanolamine, 99% (S)

L-α-Dipalmitoyl phosphatidylglycerol, 99% (S)

L-α-Distearoyl phosphatidylcholine, 99% (S)

Egg yolk phosphatidylcholine (EYPC) (S)

Ethanol, absolute (P)

Ethyl acetate, ACS reagent grade (F)

Ethylenediamine, 99% (A)

Formaldehyde (37% w/w in water) (F)

D-Glucose, ACS reagent grade, (A)

Glucose oxidase, type X from Aspergillus niger (S)

n-Hexane (F)

Hydrochloric acid (F)

Hydrochloric acid, 0.100 ± 0.001N volumetric standard solution (F)

Lysophosphatidylcholine palmitoyl, 99% (S)

Methanol, ACS reagent grade (F)

Peroxidase,Type II from horseradish (S)

Sepharose CL-2B (P)

Sodium hydroxide, pellets (F)

Sodium hydroxide, 0.100 ± 0.001N volumetric standard solution (F)

Sodium phosphate dibasic (F)

Sodium phosphate monobasic (F)

Sulfuric acid (F)

Triethylamine (A)

Triton X-100, scintilation grade (Am)

Sources

(A) Aldrich Chemical Co. (Milwaukee, WI)

(Am) Amersham Corporation (Arlington Heights, IL)

(F) Fisher Scientific (Boston, MA)

(P) Pharmco Products (Dayton, NJ)

(S) Sigma Chemical Co. (St. Louis, MO)

C. Preparations

1. Preparation of monomers and intermediates

a. 2-Ethylacrylic acid (EAA).2-Ethylacrylic acid was synthesized by the procedure reported by Ferritto, Ponticello and Tirrell. [91]

b. 5-Dimethylaminonapthalene-1-(N-(2-aminoethyl)) sulfonamide (DnsEDA).Ethylene diamine (EDA) (1.78 g, 29.7 mmol) was placed in a 50 ml round bottom flask. Dansyl chloride (DnsCl) (2.0 g, 74.1 mmol) was dissolved in 45 ml diethyl ether and placed in an addition funnel. The EDA was stirred rapidly and cooled in an ice bath as the DnsCl solution was added dropwise. The yellow color of the DnsCl disappeared immediately upon contact with the EDA and a greenish white precipitate developed. After addition was complete, the ether was removed on a rotary evaporator. The green oil that remained was dissolved in ethyl acetate (75 ml) and extracted twice with water (50 ml) adjusted to pH 12. The organic phase was then extracted twice with 0.1 N HCl (50 ml). The aqueous phases were combined, adjusted to pH 12 with 40% NaOH, and extracted with ethyl acetate (200 ml). The organic phase was dried over sodium sulfate and filtered. The solution volume was reduced to approximately 50 ml. The greenish-white needle-shaped crystals that formed were collected by filtration. Additional product was

recrystallized by the slow addition of hexane. Thin layer chromatography (TLC) (silica gel, 250 μm) in $CHCl_3/MeOH/H_2O$ (65:25:4) showed a single spot R_f 0.65 that was fluorescent and ninhydrin positive. Yield 1.17 g, 54%. Anal. calcd. for $C_{14}H_{19}N_3O_2S$: C, 57.32; H, 6.53; N, 14.30. Found: C, 57.29; H, 6.37; N, 14.14. Lit.[92]: C, 57.24; H, 6.53; N, 13.71. ^1H NMR (200 MHz, CD_3OD)δ: 2.55(t,2H), 2.86(m, 8H), 7.26(d, 1H), 7.58(m, 2H), 8.21(d, 1H), 8.34(d, 1H), 8.55(d, 1H).

2. Preparation of polymers

a. Poly(2-ethylacrylic acid) (PEAA). 2-Ethylacrylic acid (60.0 g,0.6 mol) was placed in Schlenk type flask with azobis(isobutyronitrile) {AIBN} (0.492 g, 3 mmol). The flask was subjected to three freeze-degas-thaw cycles. The flask was placed in an oil bath at 60°C for 24 hrs. After polymerization, the reaction mixture was dissolved in a minimal amount of N,N-dimethylformamide {DMF}. The solution was placed in cellulose dialysis tubing (2000 MW cutoff), and dialyzed against fresh methanol for 48 hrs. The polymer was precipitated from the methanol solution into a rapidly stirred, ten-fold excess of diethyl ether. The polymer was filtered and dried under vacuum. Yield 16.82 g, 28.0%. Anal. calcd. for $[C_5H_8O_2]_n$: C, 59.98, H, 8.05. Found: C, 58.1; H, 7.3. ^1H NMR (200 MHz, CD_3OD)δ: 1.05-1.20 (br, 3H), 1.95-2.40 (br, 4H). Gel permeation chromatography of the polymer was carried out as described by Schroeder and Tirrell

[56] from which $\overline{M}_n$ was determined to be 18,000 g/mol. PEAA produced by radical polymerization in bulk at 60°C has been shown to have a stereoirregular structure with 16% isotactic, 40% syndiotactic, and 44% heterotactic triads [69].

b. Poly(2-ethylacrylic acid) with 3.8 mol% pendant dansyl groups (DnsPEAA-3.8%). PEAA (1.5g, 15 mmol repeating units) was dissolved in dimethylformamide {DMF} (50 ml) and DnsEDA (0.264g, 0.9 mmol) was added. Dicyclohexylcarbodiimide {DCC} (0.204 g, 0.99 mmol) was added followed by triethylamine (0.125 ml, 0.9 mmol). The solution was stirred for 24 hrs at room temperature in the dark. The reaction was then quenched by the addition of a small amount of water. The precipitated dicyclohexylurea was filtered off and the polymer dialyzed for 24 hrs against fresh methanol. The polymer solution was concentrated on a rotary evaporator and diluted with three volumes of water. The polymer was ultrafiltered in a methanol/water solution 1:3 and freeze dried to yield 0.23 g, (15.3%) of a light yellow powder. η_{inh} (0.2% in DMF, 35°C), 0.70 dl/g. Anal. calcd. for $[C_5H_8O_2]_n$: C, 60.0; H, 8.0; N, 0.43. Found: C, 59.96; H, 7.95; N, 2.24. ^{1}H NMR (200 MHz, CD_3OD)δ: 0.55-1.10 (bs, 66H), 1.37-2.28 (bs, 77H), 2.88 (s,6H), 3.50 (m, 2H), 7.28 (d, 1H), 7.60 (m, 2H), 8.23 (d, 1H) 8.36 (d, 1H), 8.57 (d, 1H) The copolymer contains 3.8 mol% dansyl groups (based on PEAA monomer repeat unit). The concentration of dansyl groups was determined spectrophotometrically by measuring the absorbance

at 336 nm of a DnsPEAA solution of known concentration in methanol. The concentration was calculated using the Beer-Lambert law using the molar extinction coefficient of N-ε-dansyl lysine in CH_3OH, which was determined to be $4430 M^{-1}cm^{-1}$ (Lit. 4400-4500 [93,94]).

c. Poly(2-ethylacrylic acid) with 2.0 mol% pendant dansyl groups (DnsPEAA-2%). PEAA (6.493 g, 64.9 mmol repeating units) was placed in a 100 ml round bottom flask and dissolved in DMF (70 ml). DnsEDA (0.572 g, 1.95 mmol) was added and dissolved. Triethylamine (0.196 g, 1.95 mmol) was added. DCC (0.442g, 2.15 mmol) was added. The solution was stirred for 18 hours at room temperature in the dark and then isolated the same manner as DnsPEAA-3.8%. ^1H NMR (200 MHz, CD_3OD) δ: 0.63-1.22 (b, 128H), 1.61-2.30 (b, 154H), 2.88 (s, 6H), 3.53 (b, 2H), 7.28 (d, 1H), 7.60 (m, 2H), 8.23 (d, 1H), 8.36 (d, 1H), 8.57 (d, 1H).

3. Preparation of samples for optical density measurements

a. Preparation of polymer samples. The following outlines the preparation of polymer samples for optical density measurements of PEAA/lipid mixtures. PEAA (8.0 mg, 80 μmol repeating units) was placed in a 4 ml vial. The polymer was dissolved in NaOH (0.50 ml, 0.100 N) and sodium phosphate (2.0 ml, 200 mM) was added. The pH of the polymer solution was adjusted to the desired value by the addition of

0.100 N NaOH or 0.100 N HCl and the total volume was brought to 4.0 ml by the addition of doubly distilled water.

b. Preparation of multilamellar vesicles (MLVs). The following outlines the procedure for preparing MLV samples used in optical density measurements of PEAA/lipid mixtures. DPPC (36.0 mg) was placed in a 20 ml vial. Sodium phosphate (18.0 ml, 10 mM) adjusted to pH 7.4 was added. The buffer solution was heated to approximately 15°C above the phase transition for the lipid and agitated on a vortex mixer for three 30 sec intervals.

4. Optical density measurements of DPPC/cholesterol

A chloroform solution of cholesterol (0.1 mg/ml) was added to a round bottom flask followed by a chloroform solution of DPPC (2 mg/ml) such that the combined total molar amount of DPPC and cholesterol was 5.44 μmoles. The chloroform was removed under reduced pressure on a rotary evaporator to form a film. The film was hydrated with phosphate buffer (2.0 ml, 10 mM) at pH 7.4. The solution was agitated on a vortex mixer at 60°C for three 30 sec periods. A series of DPPC/cholesterol suspensions of different lipid/cholesterol ratios were prepared in this manner.

A PEAA solution was prepared at a concentration of 2.0 mg/ml in phosphate buffer (100 mM, pH 6.0). The PEAA solution (0.5 ml) and the DPPC/cholesterol suspension (0.5

ml) were equilibrated to 42.6°C ± 0.1°C and combined. The optical density at 400 nm was monitored.

5. Optical density measurements of lipid mixtures

The lipid mixture of interest was added to a small round bottom flask and dissolved in chloroform. The chloroform was removed under reduced pressure on a rotary evaporator to leave a thin lipid film on the inside of the flask. The film was hydrated with 10 mM phosphate buffer at pH 7.4 to produce a 2 mg/ml lipid concentration. The flask was heated approximately 15°C above the melting temperature of highest melting lipid of the mixture and agitated on a vortex mixer for three 30 sec periods with intermittent heating. A PEAA solution (2 mg/ml) was prepared in 100 mM phosphate buffer at pH 6.0. The two solutions were equilibrated to the desired temperature in a jacketed cell holder. The PEAA solution (1.0 ml) was added to the lipid suspension (1.0 ml) and the optical density at 400 nm was monitored.

6. Fluorescence measurements on DnsPEAA polymers

A stock solution of the polymer was prepared by dissolving 12.5 mg DnsPEAA in 1N NaOH (1.0 ml), titrating the solution to pH 7.0 and diluting the solution to 10 ml with doubly distilled water in a 10 ml volumetric flask.

Solutions were prepared by adding 0.1 ml polymer solution to a small vial via a 10-100 µl Eppendorff pipette.

Sodium phosphate (200 mM, 1.0 ml) was added and solution pH levels were adjusted with 0.1 N HCl or 0.1 N NaOH to the appropriate value. The total volume was brought to 2.0 ml by the addition of doubly distilled water.

Fluorescence emission scans (λ_{ex} = 340 nm) were recorded for each solution from 450 to 700 nm. The excitation and emission slits were each set at 5 nm.

7. Calcein release from DOPC multilamellar vesicles (MLVs)

To prepare DOPC vesicles containing entrapped calcein, 1.0 ml of a 20 mg/ml chloroform solution of DOPC solution was placed in a 10 ml round bottom flask. The chloroform was removed under vacuum on a rotary evaporator to leave a thin lipid film on the inside of the flask. Calcein (200 mM, 5.0 ml) was added to the flask. The film was hydrated by allowing the flask to stand at room temperature for 2 hrs. The flask was then vortexed three times for one minute to disperse vesicles in the solution. After transferring the solution to a centrifuge tube and diluting with approximately four volumes of NaCl (0.100 N), the solution was centrifuged at 4°C for 10 min at 12,000 rpm on a Sorval RC-2B centrifuge equipped with an SS-34 rotor. The supernatant was replaced with fresh salt solution and the process was repeated until the supernatant showed no fluorescence. On the final step, 10.0 ml of the NaCl solution was added and the vesicles were

resuspended to give a final DOPC concentration of approximately 2.0 mg/ml.

A PEAA solution was prepared at a concentration of 2.0 mg/ml in 100 mM sodium phosphate buffer at pH 7.4. The calcein-loaded DOPC suspension (1.0 ml) was added to the PEAA solution (1.0 ml) and the fluorescence of the sample was monitored at 530 nm with excitation at 490 nm. The pH of the solution was lowered by the addition of HCl (0.1 N) with stirring and the fluorescence was monitored for another 5 min. At the end of this time, the pH of the solution was recorded and Triton detergent (10%, 0.1 ml) was added to solubilize the vesicles and release any entrapped calcein. The fluorescence level of the disrupted sample was recorded.

8. Optical density measurements on DOPC multilamellar vesicles (MLVs)

A chloroform solution of DOPC (1.0 ml, 20 mg/ml) was placed in a 5 ml round bottom flask. The chloroform was removed under reduced pressure on a rotary evaporator to leave a thin film on the interior of the flask. The flask was placed on a vacuum line for 30 min to remove trace amounts of chloroform. The film was hydrated with NaCl solution (10.0 ml, 100 mM) and allowed to stand at room temperature for 2 hrs. Vesicles were suspended by vortexing three times for one minute. A PEAA solution was prepared at a concentration of 2 mg/ml in 100 mM phosphate buffer at pH

7.4. The PEAA solution (1 ml) was combined with the vesicle suspension (1 ml) in a 1 cm cuvette. The optical density (400 nm) of the solution was monitored for a few minutes. The pH of the solution was lowered by the addition of 0.1 N HCl with mixing. The optical density of the solution was monitored for one hour after addition.

9. Optical microscopy

A diagram of the microscope is shown in Figure 2.1. The transmitted light is provided by a 50 Watt tungsten-halogen bulb. The fluorescence epi-illumination system is based on a 75 Watt Hg-Xe arc lamp and a monochromator. Fluorescence excitation of the samples is at 334 nm, corresponding to a spectral line of the Hg-Xe arc. The exit port of the monochromator is directly coupled to the end of a bifurcated quartz fiber optic bundle directing the light through a computer-controlled electronic shutter and a fused silica biconvex lens to the epi-illumination port of a Zeiss IM-35 inverted microscope equipped with quartz epi-illumination optics and a Nikon 40X/1.3 NA CF Fluor UV lens. A Zeiss FT 395 dichroic mirror and a low fluorescence long-pass barrier filter with 50% cutoff at 399 nm complete the fluorescence system.

Images are detected by a charge couple device (CCD) instrumentation camera. An image is digitized to 12 bit resolution and is transmitted to the computer via a 500 kHz

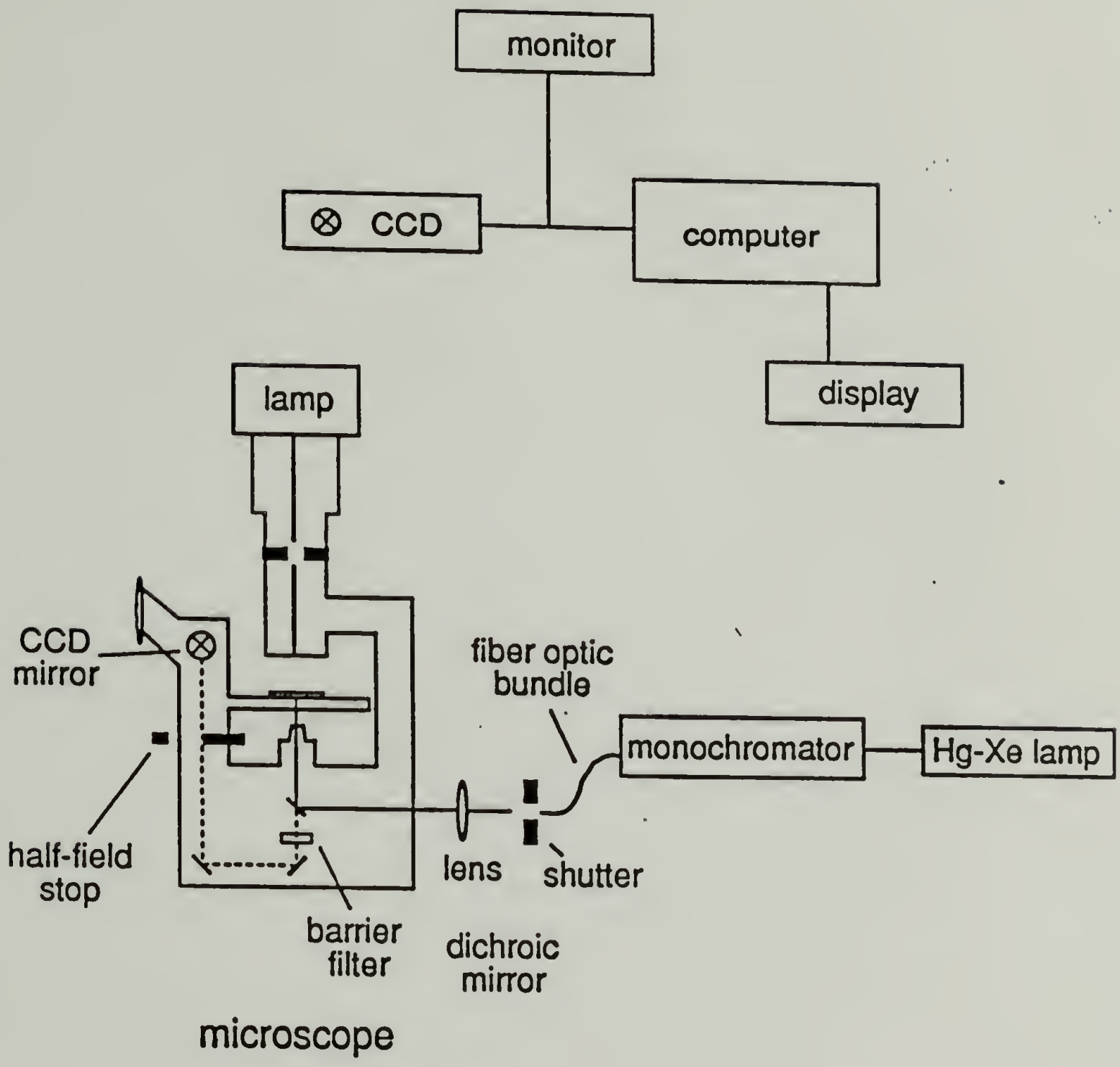

Figure 2.1 Schematic of fluorescence microscope.

IEEE-488 interface. Computer control of the illumination system (shutter opening and closing) and the CCD camera is accomplished via a Masscomp 5550 computer. A Masscomp GA-1000 graphics subsystem, which includes a pair of 1152x910 by 12 bit deep image planes and an independent graphics processor, is used for image display.

The CCD may be operated in one or more of several specialized modes, as diagrammed in Figure 2.2. For these measurements, half of the field of view is physically masked by placing a partial field stop between the specimen and the CCD in a focal plane conjugate to the image plane. A transmitted light image of the visible half of the field is collected by opening shutter 1. Typical exposure times are 2 to 20 ms. The image is binned by a factor of 2 (reduced in size by a factor of 4). After closing the shutter, the collected image is electronically shifted from the unmasked half of the CCD chip to the masked half in under 1 msec. A fluorescence image of the same half of the field is the collected by opening shutter 2 and illuminating at 334 nm. This image is also binned by a factor of 2.

DnsPEAA samples were prepared at a concentration of 2 mg/ml in 100 mM sodium phosphate buffer at pH 7.4. A chloroform solution of EYPC (0.10 ml, 100 mg/ml) was placed in a 5 ml round bottom flask. The chloroform was removed under reduced pressure on a rotary evaporator. The flask was connected to a vacuum line for 30 min to remove trace amounts of chloroform. Sodium chloride solution (5.0 ml, 100 mM) was

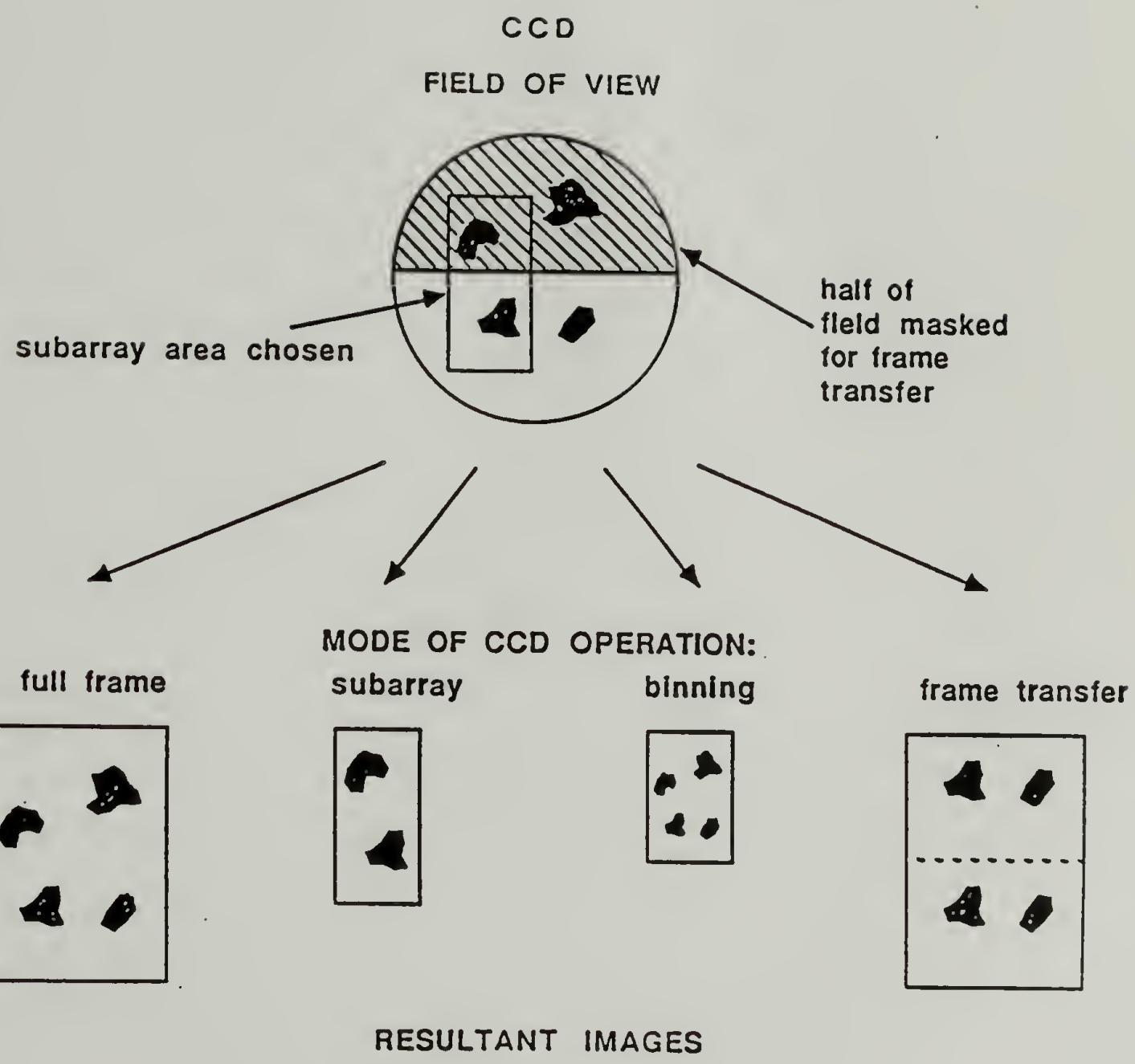

Figure 2.2 Imaging process steps.

added and the flask was allowed to stand at room temperature for 2 hours to hydrate the lipid. The flask was then gently swirled to suspend the lipid. The DnsPEAA solution (0.5 ml) was combined with the EYPC solution (0.5 ml). For low pH samples, HCl (0.05 ml, 0.100 N) was added via 100 µl syringe. One drop of the solution was placed on a precleaned microscope slide via a disposable pasteur pipette. A glass cover plate was added to the top of the sample. A small drop of non-fluorescing immersion oil was placed on top of the objective lens. The slide was mounted on the microscope and the oil on the lens was brought into contact with the slide.

10. Glucose oxidase activity assay

Dianisidine (13.2 mg, 54 µmol) was dissolved in 2 ml water. The resulting solution (1.0 ml) was placed in a 100 ml volumetric flask and diluted to 100 ml with sodium phosphate buffer (50 mM, pH 7.4). Glucose (1.0 g, 5.55 mmol) was dissolved in 10 ml water. Peroxidase (3 mg) was dissolved in 10.0 ml doubly distilled water. A glucose oxidase solution was prepared by dissolving 1.2 mg of the enzyme in 250 ml of the phosphate buffer mentioned above in a volumetric flask.

The dianisidine solution (2.40 ml), glucose solution (0.50 ml), and peroxidase solution (0.10 ml) were mixed in a 1 cm cuvette and equilibrated to 25°C in a jacketed cell holder. The glucose oxidase solution (0.10 ml) was quickly

added to the cuvette and mixed with a cuvette stirrer. The absorbance at 500 nm was monitored for several minutes. To measure the activity of the oxygen saturated enzyme, oxygen was bubbled through the dianisidine solution for 5 min immediately prior to use.

11. Determination of Michaelis constant

Glucose oxidase (10.0 mg), peroxidase (10.0 mg) and dianisidine (15.0 mg) were combined in a 4 ml vial and dissolved in 4.0 ml doubly distilled water. A PEAA solution was prepared at a concentration of 2 mg/ml in 200 mM phosphate buffer at pH 7.4. The polymer solution (1 ml) was combined with the enzyme/dianisidine solution (0.25 ml) in a 1 cm cuvette. The total volume was brought to 2.0 ml by the addition of doubly distilled water. The cuvette was placed in a jacketed cell holder and equilibrated to 25°C. Glucose (0.1 ml, 40 mg/ml) was quickly added and the absorbance at 500 nm was monitored.

12. Glucose triggered calcein release

A chloroform solution of EYPC (0.30 ml, 100 mg/ml) was placed in a 5 ml round bottom flask via a 500 µl syringe. The chloroform was removed under reduced pressure on a rotary evaporator. The flask was placed on a vacuum line for 30 min to remove trace amounts of chloroform. A calcein solution (3.0 ml, 200 mM) was added to the flask. The sample was

agitated on a vortex mixer at room temperature for 3 min and sonicated with a Branson Model 185 Cell Disruptor fitted with a 1/8 inch diameter titanium microtip at 0°C for 25 min at a power of 35 watts. The sample (1.5 ml) was placed on a Sepharose CL-2B column (1.6 X 27 cm) and eluted at 4°C with 100 mM NaCl solution at pH 7.4; 1.5 ml fractions were collected. Unilamellar vesicles with entrapped calcein were eluted in fractions 17-27 as determined by monitoring the optical density at 250 nm.

13. Measurement of pH depression by addition of glucose

The following solutions were prepared:

NaCl (100 mM)

PEAA (1 mg/ml),in 100 mM NaCl

PEAA (2 mg/ml) in 100 mM NaCl

EYPC (4 mg/ml) in 100 mM NaCl

Glucose Oxidase (GO) (2.5 mg/ml) in 100 mM NaCl

Glucose (40.0 mg/ml) in 100 mM NaCl

The PEAA, EYPC, and GO solutions were mixed in a jacketed vial equilibrated to 25°C in the amounts described in Table 2.1. A micro flea stir bar was added and the solution was stirred. The pH of the combined solutions was adjusted to 7.4 by the addition of 0.01 N NaOH and 0.01 N HCl and the final volume was brought to 2.0 ml by the addition of the NaCl solution. The jacketed vial was fitted with a pH

probe of a pH meter connected through an analog to digital converter to a Leading Edge computer. pH values were recorded at a rate of 1 sec^{-1} using the data acquisition software Acquire™. After the solution was thoroughly mixed, the glucose in the amount listed in Table 2.1 was added via an Eppendorff pipette. The pH was monitored for 30 min. Oxygen was bubbled through all solutions except for the glucose oxidase solutions for 30 min before oxygenated runs.

Table 2.1 Amounts of reagents used for pH depression measurements.

Run	PEAA #1 (ml)	PEAA #2 (ml)	GO (ml)	EYPC (ml)	O_2	Glucose (ml)
1	0.0	0.0	0.1	0.0	N	0.05
2	0.0	0.0	0.1	0.0	N	0.10
3	0.0	0.0	0.2	0.0	N	0.05
4	0.0	0.0	0.1	0.25	N	0.05
5	0.0	0.0	0.1	0.0	Y	0.05
6	1.0	0.0	0.1	0.0	N	0.05
7	1.0	0.0	0.1	0.0	N	0.10
8	0.0	1.0	0.1	0.0	N	0.05
9	1.0	0.0	0.2	0.0	N	0.05
10	1.0	0.0	0.1	0.25	N	0.05
11	1.0	0.0	0.1	0.0	Y	0.05

14. Potentiometric titrations

Samples were prepared by placing 13.1 mg of polymer in a jacketed cell maintained at 25°C and a stoichiometric amount of 0.100 ± 0.001 N sodium hydroxide was added. The solution was diluted to 7.5 ml by the addition of doubly distilled water and a stir bar flea was added. The cell was closed with a rubber septum and the solution was stirred under an

argon atmosphere until all of the polymer dissolved. The solution pH was monitored as 0.100 ± 0.001 N HCl was added via a 50 µl calibrated syringe. Stirring was maintained during HCl additions but stopped during pH measurements.

CHAPTER III

RESULTS AND DISCUSSION

A. Goals and Accomplishments

The interaction of PEAA with phosphatidylcholine vesicles has been investigated through a number of approaches. The pH dependence of the interaction and the morphological changes that accompany the interaction have been well documented. These studies showed that the vesicle suspensions clarified due to the reorganization of the membranes into PEAA/lipid mixed micelles that do not scatter light effectively due to their small size. With one exception[59], these experiments were performed under equilibrium or pseudo-equilibrium conditions and did not examine the process as it occurred.

One of the goals of the present work was to measure the rate of the PEAA induced membrane reorganization in response to a number of factors that were known or proposed to affect the process. The reorganization could be followed by measuring changes in the optical density of vesicle suspensions. The reorganization rate was found to increase with decreasing pH below a critical pH value that corresponded to the pH where the conformational transition occurs. Additionally, the reorganization was found to depend

heavily on the composition and organization of the membrane. The presence of phase defects or bilayer stabilizers was shown to affect the reorganization process. Comparison of dye release and optical density data revealed that the permeability of the membrane is increased well before structural reorganization occurs.

A second goal of the work was to follow the reorganization process through an optical microscope by photographing vesicles in a time-lapse fashion. PEAA was tagged with a fluorescent probe so that the process could be followed under a fluorescent microscope. The high fluorescence intensity from each vesicle indicated that the polymer adsorbed onto the vesicle surface at pH values that were well above the range where the conformational transition occurs. At lower pH values, reorganization was viewed as an emergence of smaller ellipsoidal particles with decreasing intensity and increasing diffusiveness of fluorescence emission.

The interaction of PEAA with vesicles has been sensitized to the stimuli of pH[67], temperature[68], and light[73]. Another goal was to sensitize the interaction to the presence of a neutral substrate. The enzyme, glucose oxidase, is known to convert glucose to gluconic acid providing a source of protons. It was shown that the reorganization of vesicles and release of entrapped solutes could be controlled systematically by the control of glucose, enzyme, PEAA and oxygen concentration in solution.

B. Interaction of Poly(2-ethylacrylic acid) with Phospholipid Vesicles

1. Potentiometric Titration of PEAA

The conformational properties of polyelectrolytes can be examined by potentiometric tiration. The ionization behavior of PEAA was studied by this technique. In Figure 3.1, the effect on pH of added HCl (0.001N) is shown. At approximately pH 6.5, there is a decrease in the slope of the pH vs. vol. of added HCl curve. This is caused by a conformational transition of the polymer.

At high degrees of ionization, PEAA exists as a random coil in aqueous solutions due to the electrostatic repulsions of the negatively charged carboxyl groups. As acid is added near the pK_a of the polymer, the acid groups of the polymer are neutralized. As the polymer becomes neutralized, the force from electrostatic repulsions is reduced to a point where intramolecular hydrophobic attractive forces overcome the repulsive forces and a coil to globule transition occurs. This is due to the hydrophobic association of the pendant ethyl groups.

The degree of ionization, α, was calculated from the electroneutrality condition [95]:

$$\alpha = \frac{C_{Na^+} + C_{H^+} + C_{Cl^-} + C_{HO^-}}{C_M} \qquad \text{(Eq. 3.1)}$$

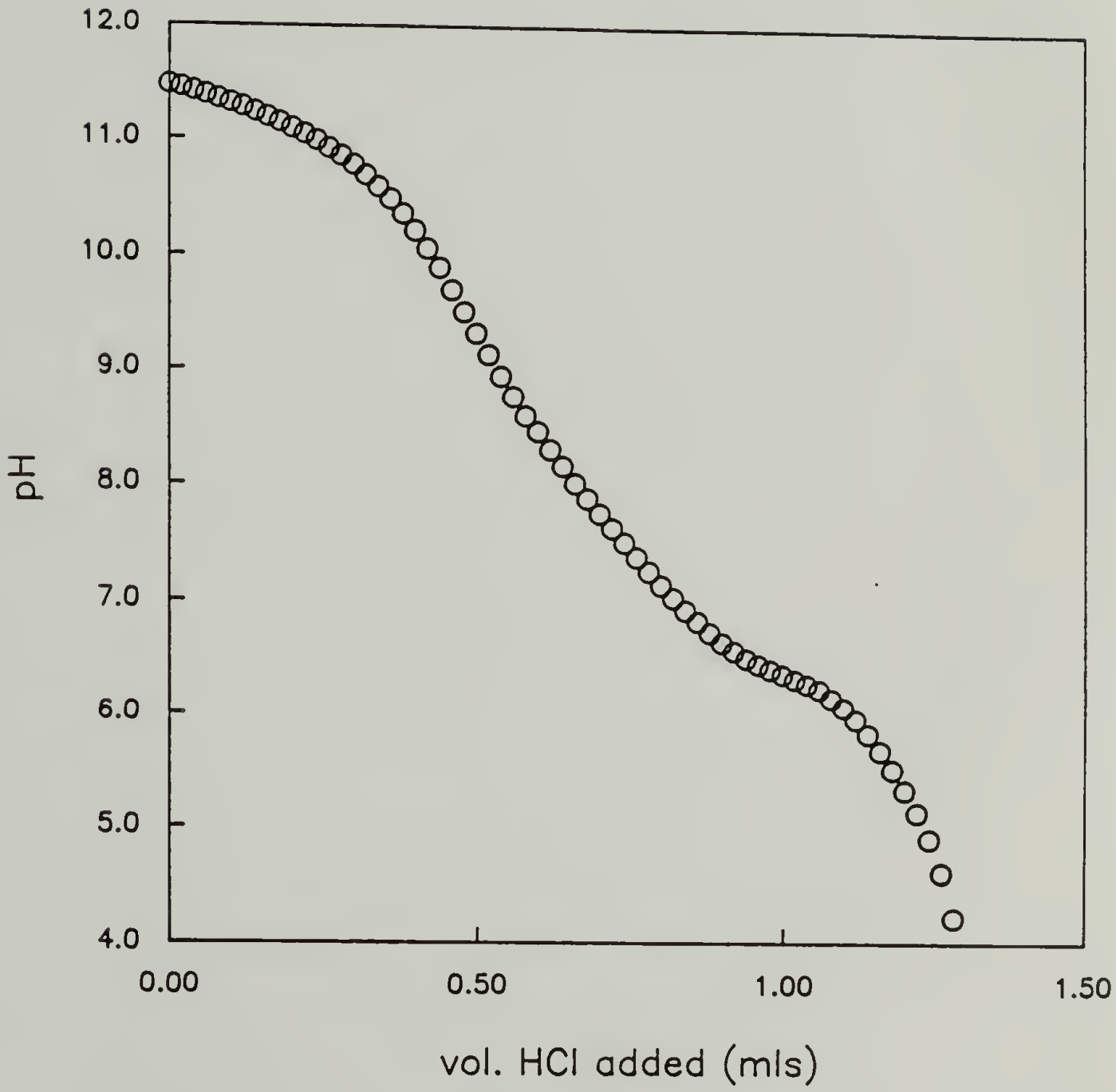

Figure 3.1 The pH of a solution of PEAA as a function of added HCl (0.100N). Measurements were recorded at 25°C.

where C_{Na^+}, C_{H^+}, C_{Cl^-}, and C_{HO^-} represent the concentrations of sodium ions, protons, chloride ions, and hydroxyl ions, respectively in solution. The ionization behavior of PEAA is shown in Figure 3.2. The degree of ionization increases almost linearly with pH until a pH value of about 6.0 where the degree of ionization increases more rapidly up to pH 6.6. There is a decrease in the slope of the curve after that point. The discontinuity in slope of the curve that occurs between α values of 0.17 and 0.30 represents the cooperative unfolding of the PEAA chain. This can be seen more easily if the pK_a of the acid groups is plotted as a function of the degree of ionization as in Figure 3.3. The apparent pK_a of the polymer was calculated from the following equation:

$$pK_a = pH + \log \frac{(1-\alpha)}{\alpha} \qquad \text{(Eq. 3.2)}$$

The pK_a of the polymer increases with degree of ionization and then remains constant at a value of 6.9 before increasing again. For poly(carboxylic acid)s, previous experiments have shown that the pK_a of the acid groups of the polymer increase with increasing pH of the solution within a certain pH range.[40,41] As ionization of a carboxylic acid groups along the polymer chain increases, further ionization becomes more difficult due to the buildup of charge making the acid groups, in effect, weaker acids.

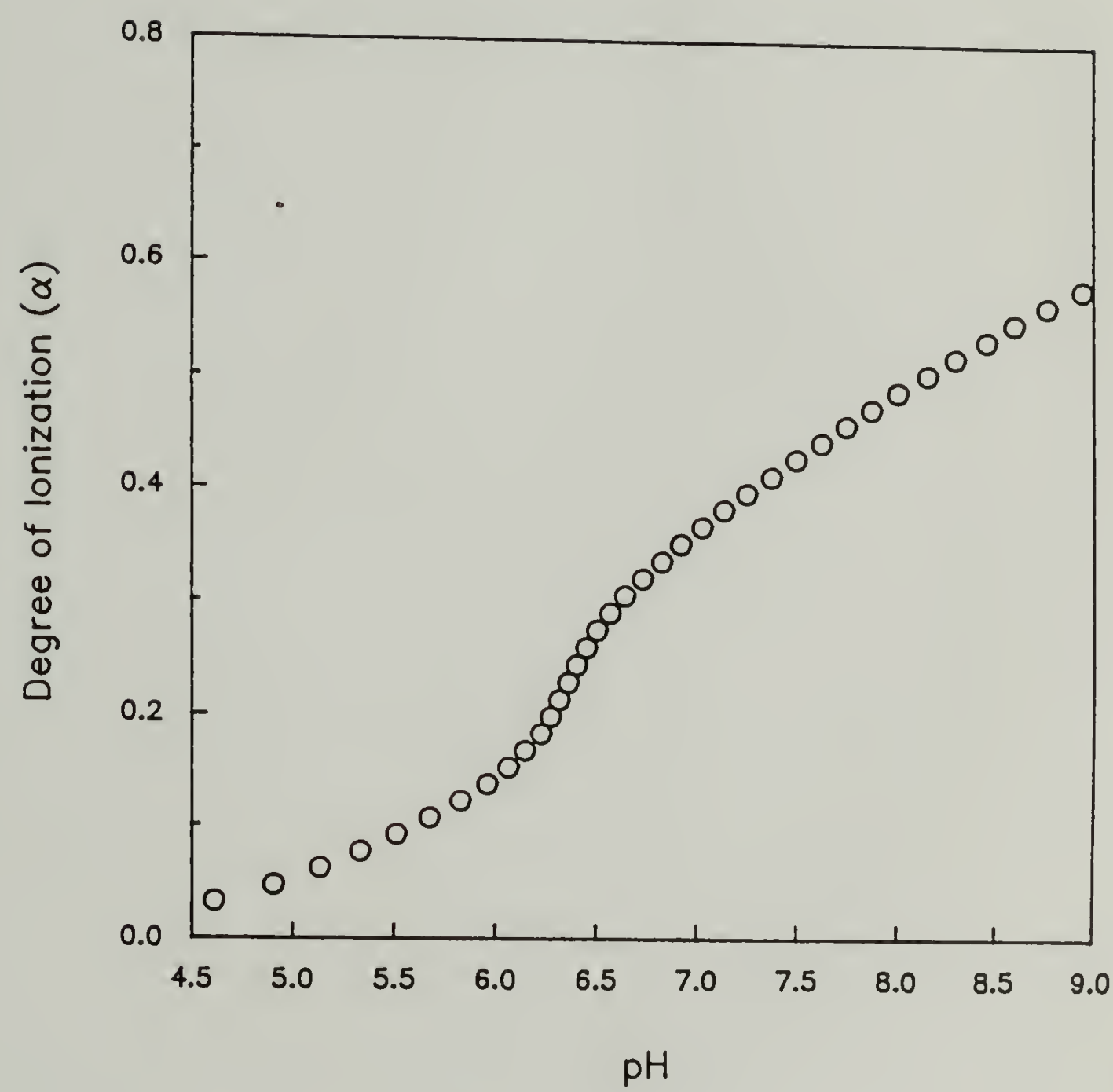

Figure 3.2 Degree of ionization of PEAA as a function of pH. Measurements were recorded at 25°C.

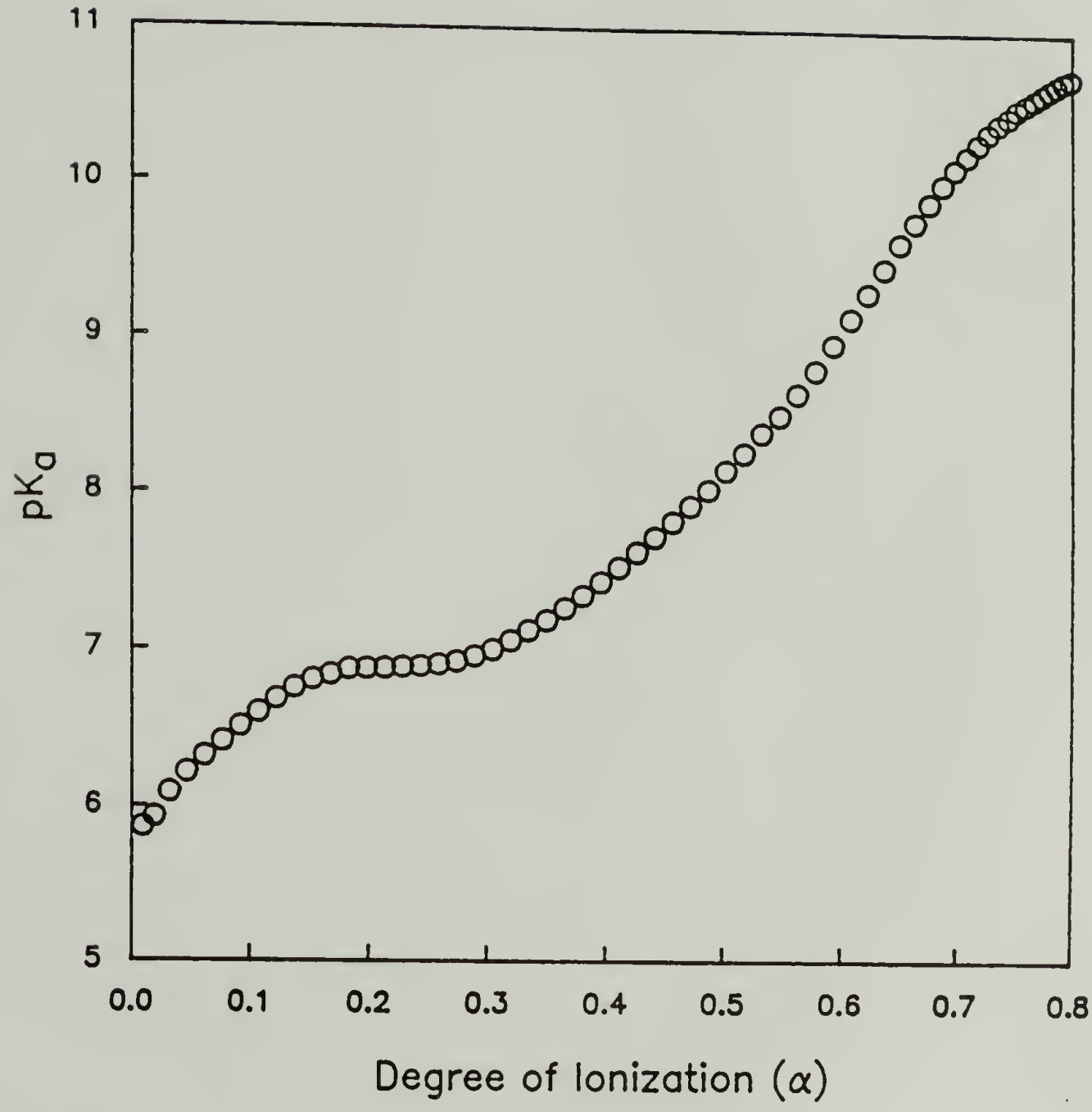

Figure 3.3 Apparent acid dissociation constant of PEAA as a function of degree of ionization. Measurements were recorded at 25°C.

Both plots show that a cooperative conformational transition for PEAA occurs over the narrow pH range of 6.0 to 6.6 in salt-free unbuffered solutions.

2. Optical density measurements

During the structural reorganization of multilamellar vesicles to mixed micelles, there are dramatic decreases in turbidity and particle size. The photograph in Figure 3.4 demonstrates this effect. All four vials contained DMPC MLV's (1 mg/ml) in 50 mM phosphate buffer. The vial on the far left was at pH 7.4 while the second vial was acidified to pH 6.0. The two vials on the right both contain PEAA (1 mg/ml). One is at pH 7.4 (second from the right) and the other was acidified to pH 6.0. All four vials were incubated at 30°C for a period of 20 minutes. The three vials on the left give a milky white appearance while the far right vial is completely clear due to the conversion of the MLV's to mixed micelles.

The change in turbidity allows kinetic study of the reorganization of vesicles by monitoring the optical density of PEAA/MLV suspensions with time. Highly buffered PEAA (2 mg/ml) solutions (100 mM phosphate) at low pH were added to weakly buffered (10 mM phosphate) vesicle suspensions (2 mg/ml) at pH 7.4. Because of the relative strengths of the two buffers, the pH of the final solution was close to the initial pH of the PEAA solution. This method of measurement

Figure 3.4 Decrease in turbidity of PEAA vesicle samples. From left to right a) DMPC MLV's pH 7.4 b) DMPC MLV's pH 6.0 c) DMPC MLV's/PEAA pH 7.4 and d) DMPC MLV's/PEAA pH 6.0. The concentrations of DMPC and PEAA (when present) were 1 mg/ml.

was preferred to direct acidification of a PEAA/vesicle mixture because of complications caused by the local precipitation of PEAA at the solution/acid interface causing a temporary inhomogeneity of the optical density. Possible disruptive osmotic forces created by the difference in ionic strengths was of concern. However, no difference was noticed in the optical density behavior using the two methods.

Previous studies indicated that the interaction of PEAA with phosphatidylcholine vesicles was not sufficient to cause structural reorganization below the melting transition of the lipid. Below T_m, the lipid molecules pack into a crystalline array with the polymethylene chains in an all-trans conformation. Upon heating above T_m, there is a gel to liquid crystalline transition and a loss of crystallinity.

The response of the rate of the reorganization to temperature was studied. Figure 3.5 shows the loss in optical density of a DMPC/PEAA mixture at various temperatures when acidified to pH 6.4. The T_m of DMPC is reported to be 23.7°C.[30] At 20.5°C, there is negligible loss of optical density. At this temperature, the bilayer is in the crystalline state. As the temperature is increased to T_m, the rate of optical density loss increases up to a maximal rate at the T_m. Above T_m, the rate begins to decrease again. Similar behavior is seen for DPPC MLV's in PEAA solutions under the same conditions except at higher temperature (see Figure 3.6). At 39.4°C, 2° below the reported phase transition temperature of 41.4°C, there is no

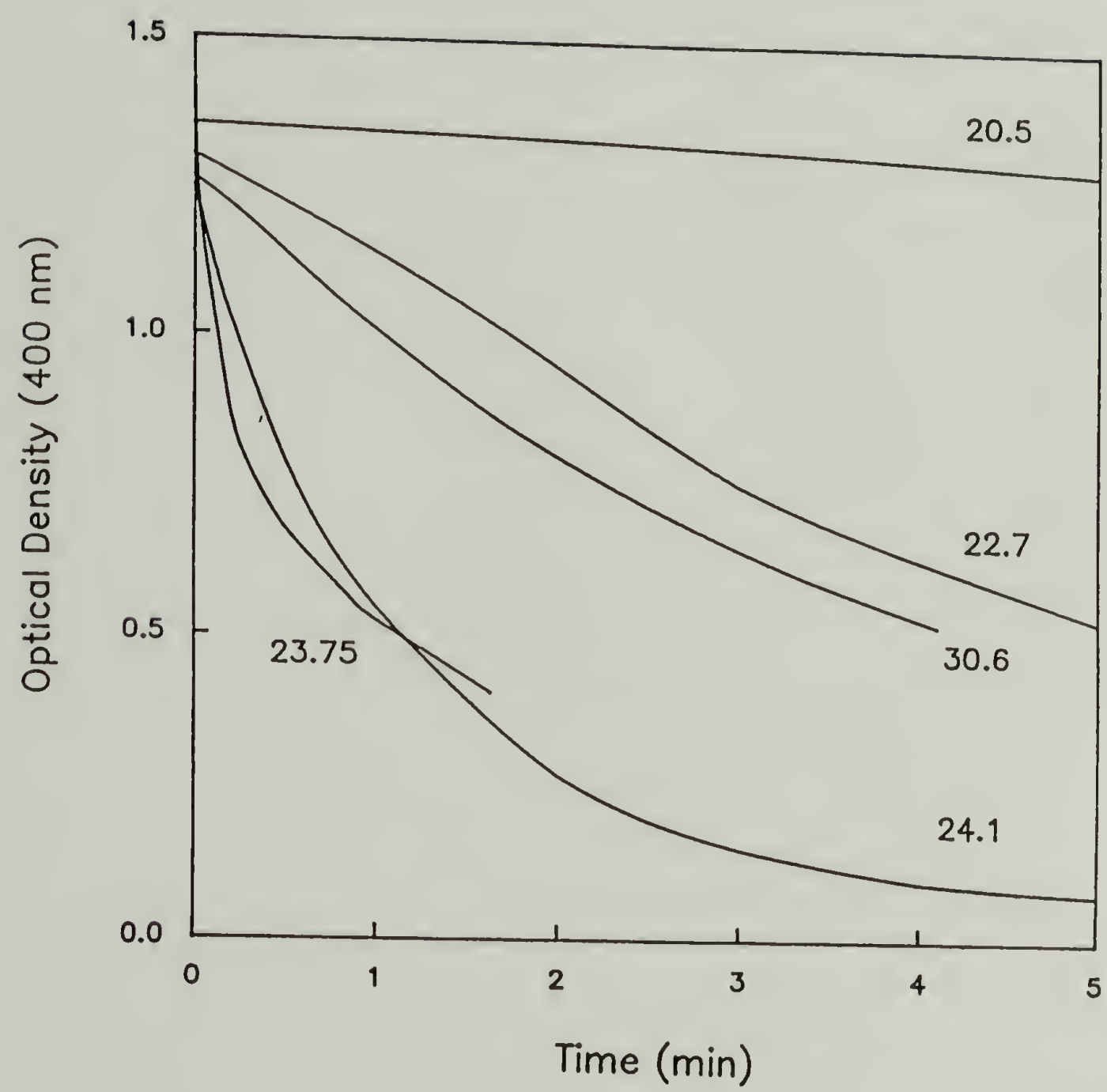

Figure 3.5 Effect of temperature on the decrease in the optical density of a DMPC MLV (1 ml, 2 mg/ml) suspension in 10 mM phosphate buffer at pH 7.4 upon addition of PEAA (1 ml, 2 mg/ml) in 100 mM phosphate buffer at pH 6.4. The final pH was 6.45.

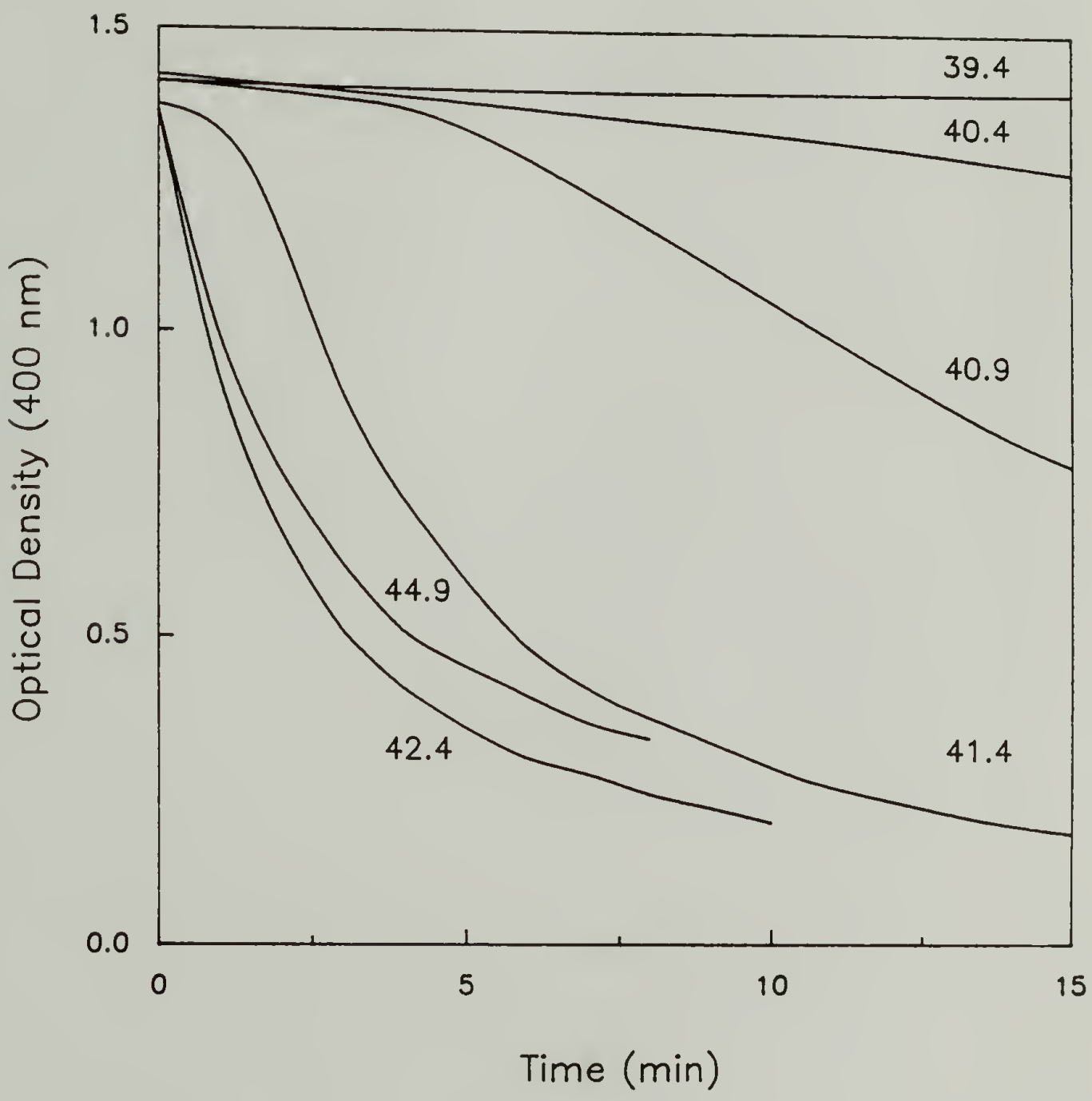

Figure 3.6 Effect of temperature on the decrease in the optical density of a DPPC MLV (1 ml, 2 mg/ml) suspension in 10 mM phosphate buffer at pH 7.4 upon addition of PEAA (1 ml, 2 mg/ml) in 100 mM phosphate buffer at pH 6.4. The final pH was 6.45.

change in optical density over the course of 15 minutes. As the temperature is raised, the rate of the reorganization process goes through a maximum at a temperature slightly above the T_m for DPPC and then decreases again. Because the maximal rate for DPPC clarification was observed at a higher temperature than T_m, the temperature calibration was checked. The light scattering properties of phosphatidylcholine vesicles are known to change slightly upon going through the melting transition.[96] This fact was used to calibrate the temperature (see Figure 3.7) The optical density was measured for a suspension of DPPC MLV's (1 mg/ml) at different temperatures. There is a sharp decrease in the optical density centered at 41.0°C which agrees with the literature value of T_m. The discrepancy in temperature may be due to a cooling of the PEAA sample as it was transferred to the vesicle solution. Examination of DSPC MLV's under identical conditions showed an increase in the rate at T_m but no maximal rate (see Figure 3.8). Under these conditions, DSPC MLV's reorganize very slowly. To check that PEAA does effect a complete reorganization of DSPC vesicles, a suspension was acidified to pH 5.8 at 58.5°C (see Figure 3.9). Under these conditions, the reorganization is complete in less than 5 minutes.

Analysis of the optical density curves revealed that the data did not fit first order kinetics. Vesicles are polydisperse and the total light scattering intensity from these mixtures represents different contributions from each

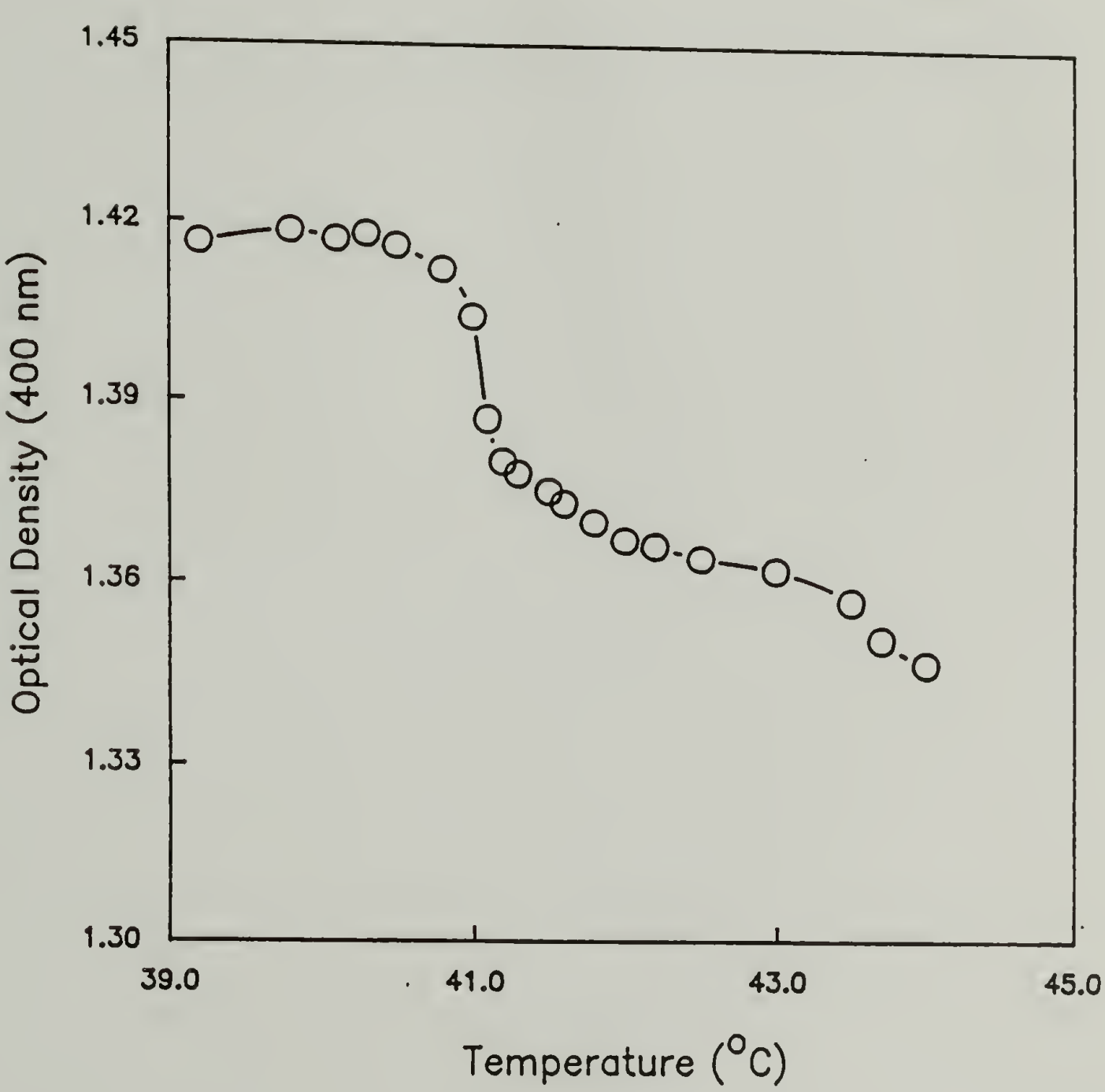

Figure 3.7 Calibration of temperature for optical density experiments by the change in O.D. of DPPC MLV's (1 mg/ml) at T_m of the lipid.

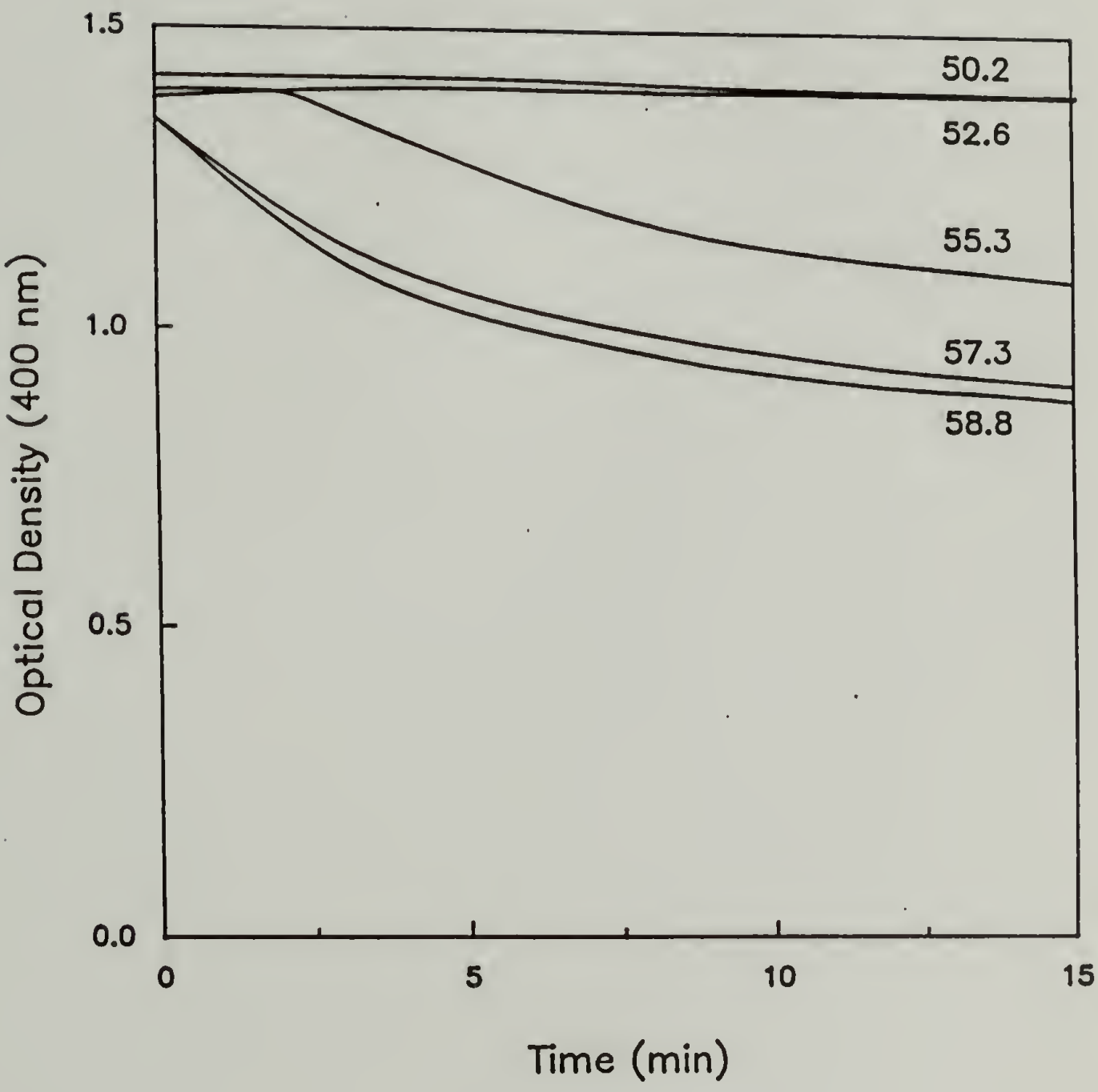

Figure 3.8 Effect of temperature on the decrease in the optical density of a DSPC MLV (1 ml, 2 mg/ml) suspension in 10 mM phosphate buffer at pH 7.4 upon addition of PEAA (1 ml, 2 mg/ml) in 100 mM phosphate buffer at pH 6.4. The final pH was 6.45.

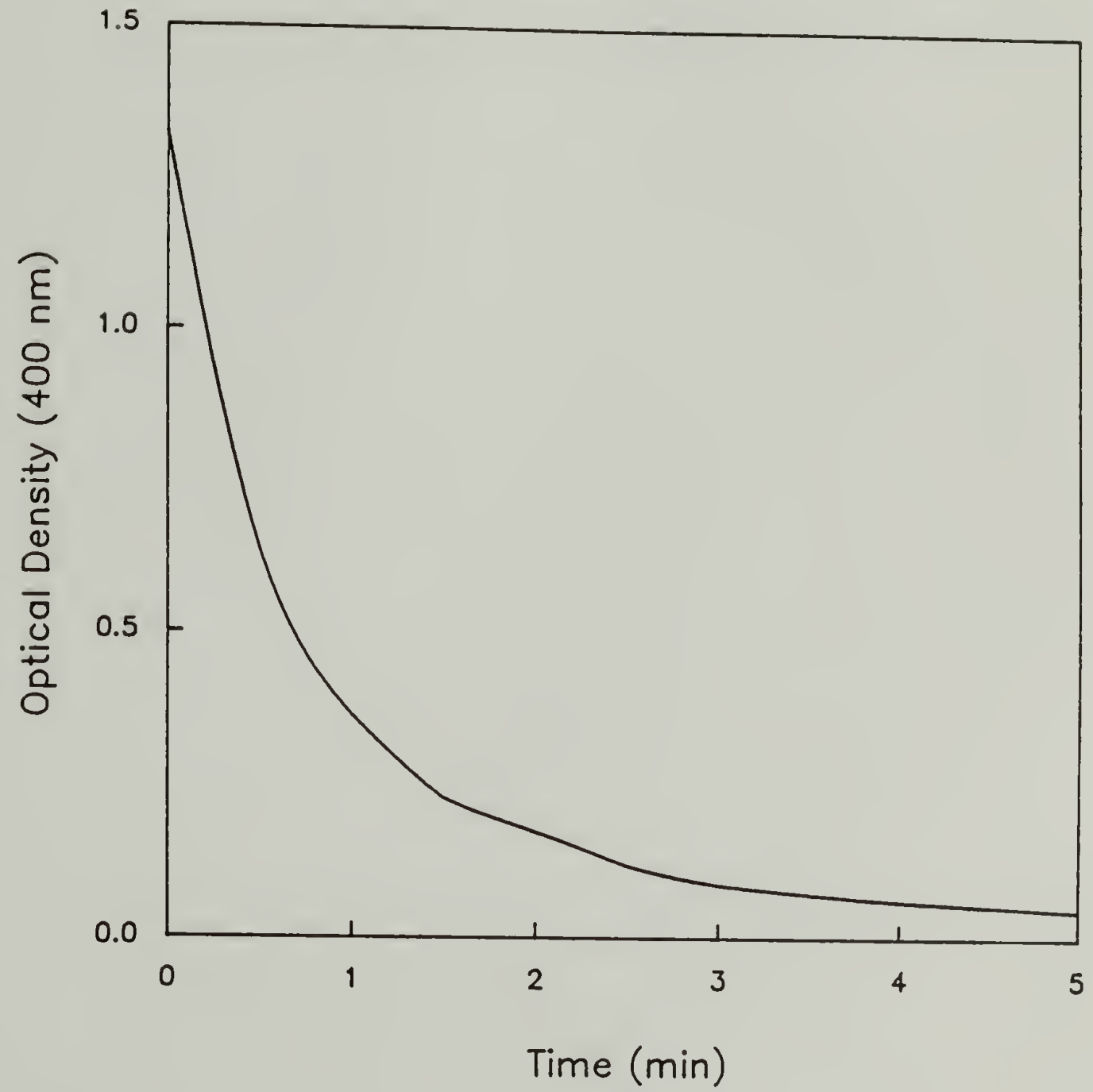

Figure 3.9 The decrease in the optical density of a DSPC MLV (1 ml, 2 mg/ml) suspension in 10 mM phosphate buffer at pH 7.4 upon addition of PEAA (1 ml, 2 mg/ml) in 100 mM phosphate buffer at pH 5.8. The final pH was 5.85.

size vesicle weighted according to their relative abundance. The relationship between liposome size and light scattering cross section is nonlinear so that changes in light scattering intensity with time would not be expected to be exponential even for a first order reaction.

Therefore, a convenient rate parameter to choose is the reciprocal of the time it takes for the optical density to decrease halfway to that of a completely reorganized suspension at equilibrium ($t_{1/2}^{-1}$). Plotting $t_{1/2}^{-1}$ as a function of temperature gives a better view of the temperature behavior (see Figure 3.10). A sharp maximum occurs at the phase transition of DMPC. This behavior has been seen before in the interaction of DMPC MLV's with lipoproteins.[97] Apolipoprotein A-I (apoA-I) undergoes a helix to random coil transition upon heating[98,99] and with pH shifts[99,100]. It has been shown to interact via a hydrophobic effect with certain phosphatidylcholines.[101] Electron microscopy of lipid/apoA-I complexes revealed discs that were 55Å thick and 64-148Å in diameter depending on the lipid/apoA-I ratio.[70] The micrographs of the discs are almost identical in appearance to those published by Borden of DPPC/PEAA complexes.[57]

Pownall studied the kinetics of the interaction of vesicles of DMPC and DPPC with apoA-I. In a similar optical density experiment with DMPC and apoA-I, there was a large rate maximum at T_m for DMPC.[97] The rate maximum at T_m was proposed to be due to holes or channel defects at the borders

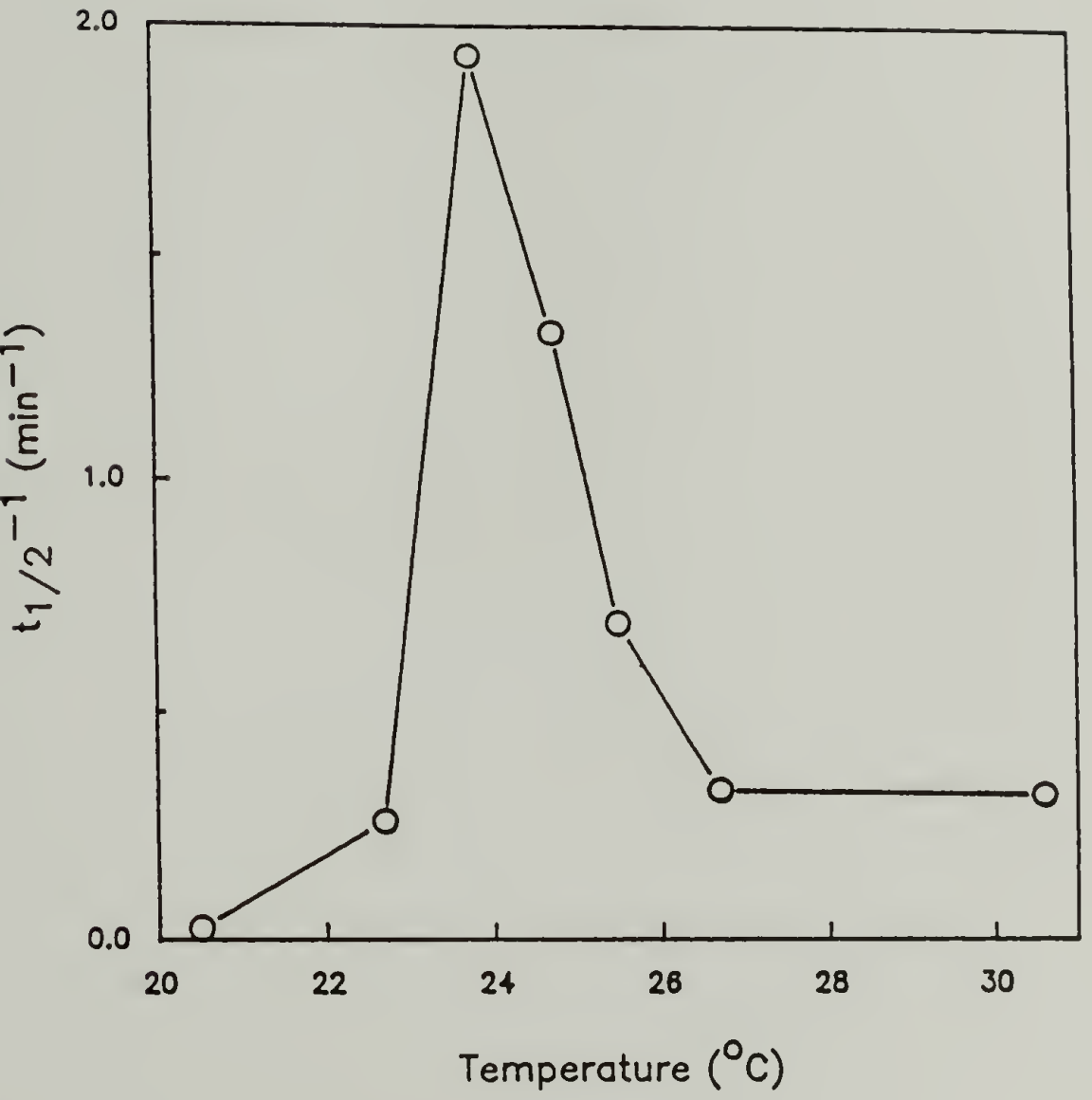

Figure 3.10 Effect of temperature on the the rate of decrease in the optical density ($t_{1/2}^{-1}$) of DMPC MLV (1 ml, 2 mg/ml) suspensions in 10 mM phosphate buffer at pH 7.4 upon addition of PEAA (1 ml, 2 mg/ml) in 100 mM phosphate buffer at pH 6.4. The final pH was 6.45.

of coexisting gel and liquid crystalline phases. Marsh suggested that the latter is the site of selective passive transport of Tempo-choline out of DMPC vesicles at T_m.[102]

Comparison of the optical density behavior of DMPC with that of other phosphatidylcholines reveals some interesting trends (see Figure 3.11). For DPPC at the same pH and ionic strength, there is a maximum in the rate of reorganization near the T_m of DPPC. The maximum is less pronounced and maximum rate is less than for DMPC. The same behavior was seen by Pownall in the interaction of DPPC with apoA-I. The trend continues with DSPC. As the alkyl chain length increases, the rate of reorganization decreases due to the increase in the hydrophobic association between lipid molecules of the bilayer. Thus, it seems as if there is competition between hydrophobic sites on the polymer and on neighboring lipids. When the hydrophobicity of the polymer is increased by lowering the pH, the lipid organization is disrupted more easily as was seen for DSPC.

A decreased level of ionization of the PEAA chain should yield a tighter more hydrophobic species that would be expected to interact more strongly with vesicle bilayers. Figure 3.12 shows the rates of reorganization of mixtures of DPPC MLV's (1 mg/ml) and PEAA (1 mg/ml) at various pH values. Above pH 6.55, the rate of reorganization is very slow. The reorganization does occur to a significant extent below an approximate pH of 6.9 (dependent on the ionic strength of the solution) as displayed in Figure 1.5 and the rate of the

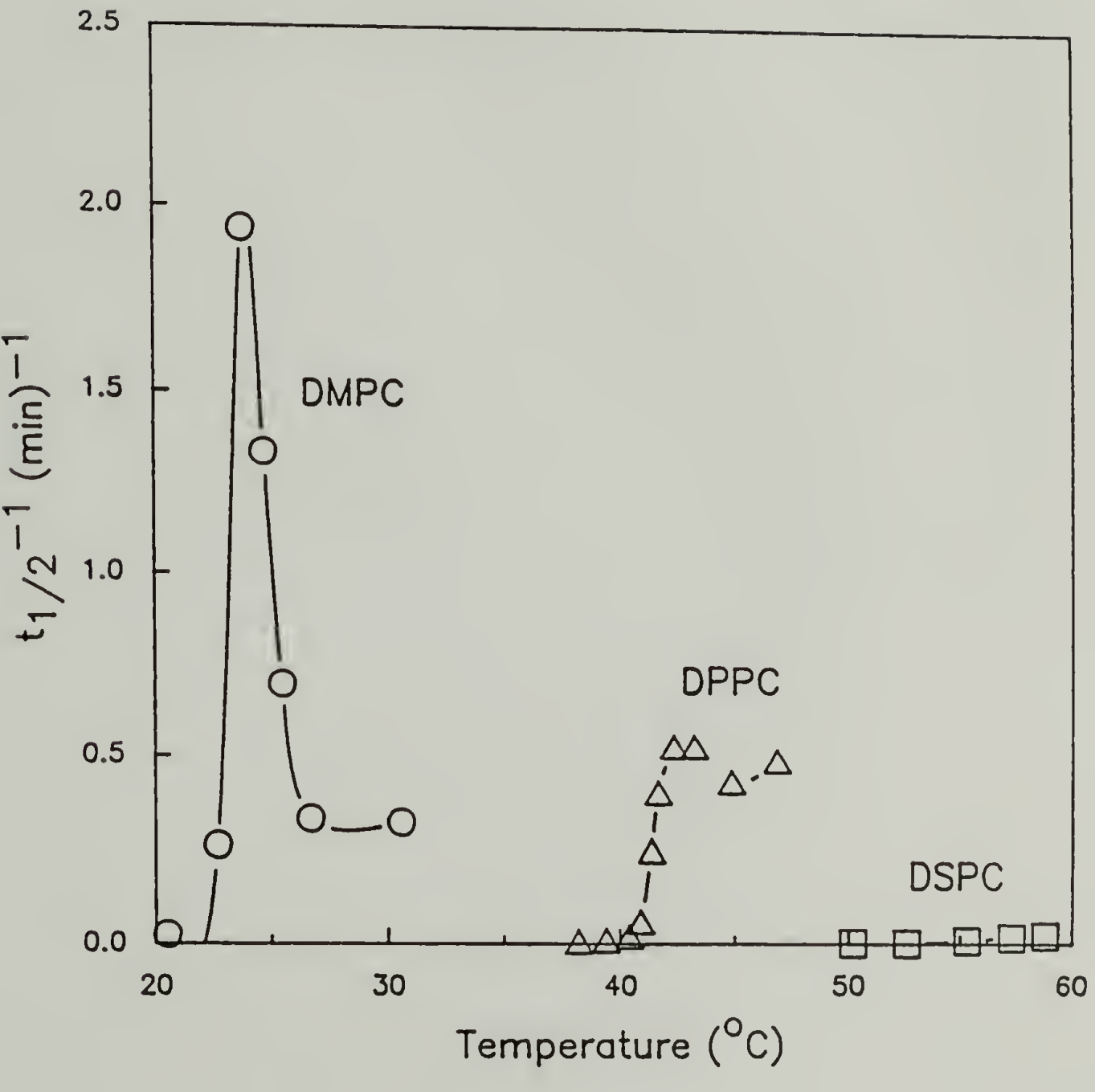

Figure 3.11 Comparison of the temperature effects on the rate of optical density decrease for DMPC, DPPC, and DSPC (1 mg/ml) upon acidification to pH 6.45 in the presence of PEAA (1 mg/ml).

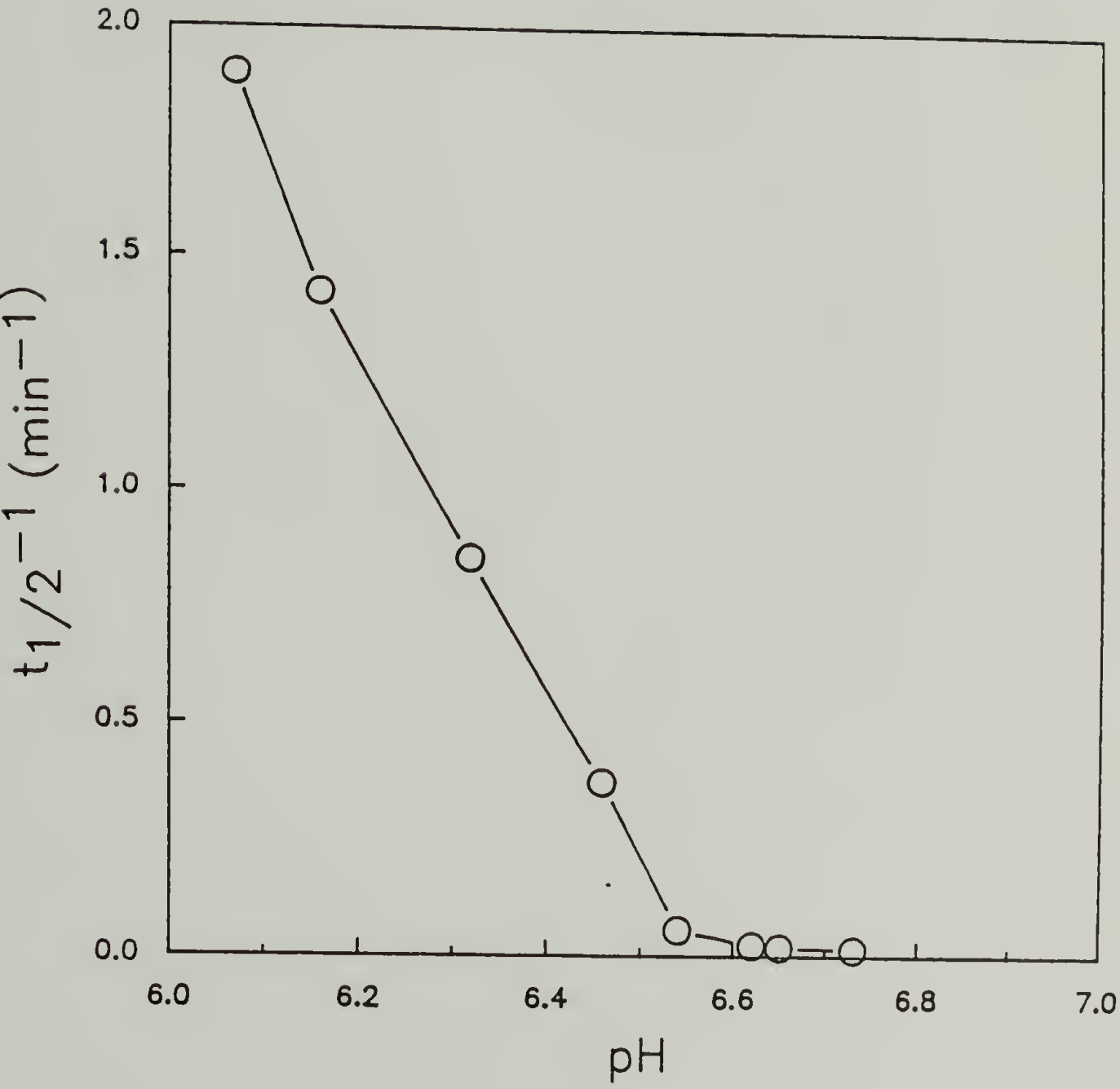

Figure 3.12 Effect of pH on the rate of optical density decrease for DPPC MLV's (1 mg/ml) upon acidification in the presence of PEAA (1 mg/ml).

process increases with decreasing pH to pH 6.55. Below 6.55, the process accelerates linearly with decrease in pH at a much greater rate. Examination of the potentiometric titration transition of PEAA (see Figure 3.1 and 3.2) shows that the onset of the conformational transition begins at about pH 6.55-6.60 in unbuffered solutions. In 55 mM phosphate buffer, the conformational behavior of PEAA should be shifted to lower pH values from that of the unbuffered polymer due to the increased screening of charge repulsions by the solvent stabilizing the expanded coil form of the polymer. It appears as though PEAA interacts with the vesicles considerably in the expanded form and perturbs vesicular structures but interacts much more strongly during the conformational transition of PEAA. As the extent of ionization is decreased, the rate of reorganization is accelerated.

The interaction with phosphatidylglycerol(PG) vesicles behaves somewhat differently. Phosphatidylglycerols contain a glycerol headgroup which imparts an overall negative charge to the molecule and thus to the bilayer. This differs from PC's which are zwitterionic with no net charge. The interaction of PEAA with dipalmitoyl phosphatidylglycerol (DPPG) vesicles as a function of pH displays the same qualitative behavior as was observed for DPPC (see Figure 3.13) There is a negligible rate of reorganization above a 'critical' pH and a nearly linear increase in rate with a decrease in pH below this value. The behavior differs

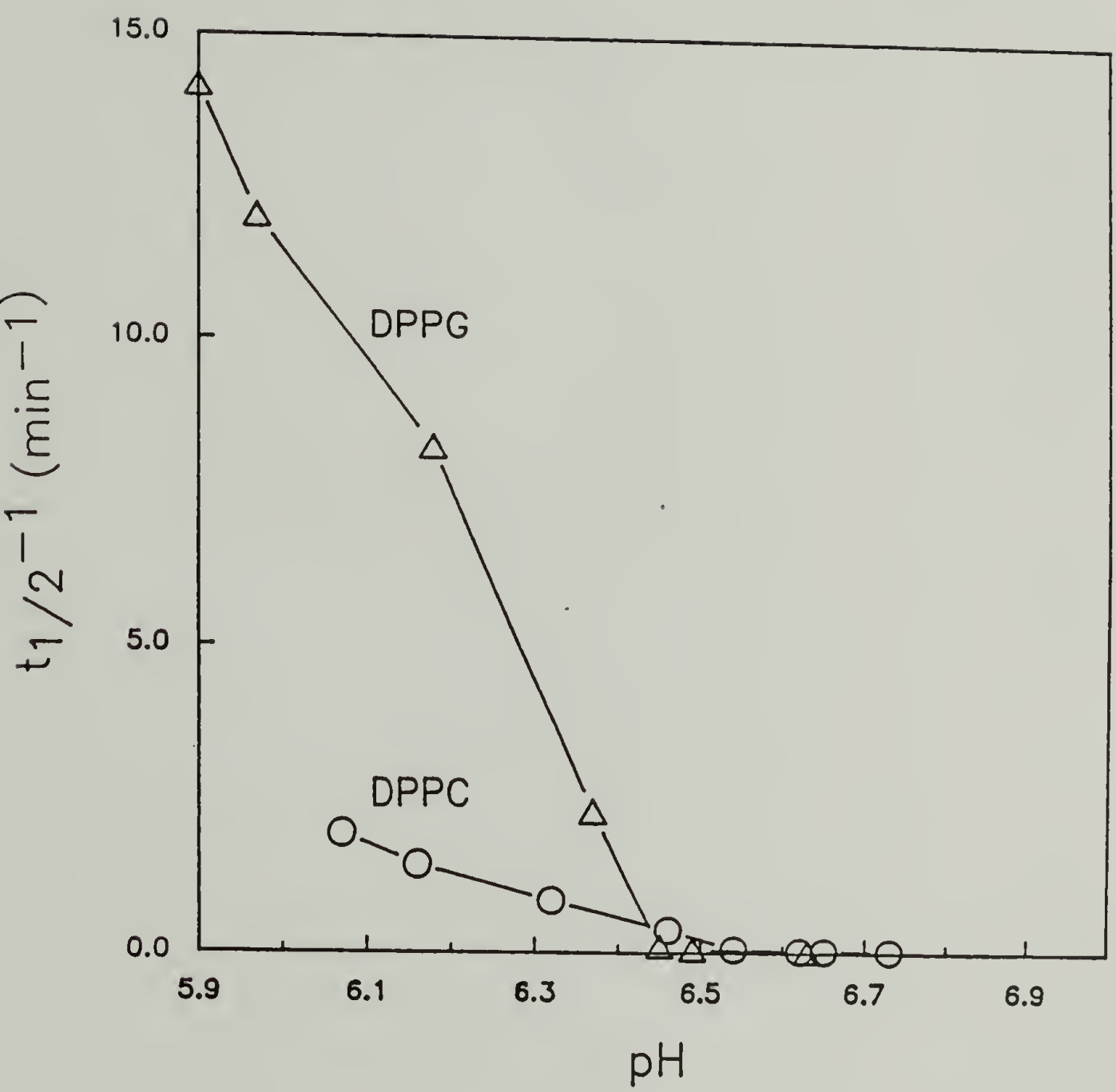

Figure 3.13 Comparison of the effect of pH on the rate of optical density decrease for DPPC MLV's (1 mg/ml) and DPPG MLV's upon acidification in the presence of PEAA (1 mg/ml).

significantly in two aspects though. First, the reorganization is enhanced at low pH for DPPG. The repulsion of negative headgroup of neighboring DPPG molecules in the bilayer destabilizes the vesicle to some extent. However, it can not be ruled out that some contribution to the rate enhancement might come from a different population of MLV's that might form for DPPG vesicles in terms of average size and number of bilayers per vesicle. A different size distribution would affect the scattering behavior of the solution affecting the measurements. A decrease in the average number of bilayers per vesicle might speed the conversion to mixed micelles. Second, the 'critical' pH is shifted about 0.1 pH units to 6.45 for DPPG. The negative surface charge of DPPG vesicles results in an electrostatic repulsion of the negatively charged polymer. Evidently, the extent of ionization of PEAA must be decreased to a greater degree until hydrophobic attractive forces overcome the repulsive forces.

3. Lipid mixtures

The accelerated rate of reorganization at the T_m of phosphatidylcholines is postulated to be due to the presence of phase boundaries between regions of melted lipid and lipid in the gel phase. It follows that introduction of defects by alternative means should produce a similar enhancement in the rate of reorganization. Certain phospholipid mixtures are

known to contain defects. Lyso-PC's, found in cell membranes at 1-4% of total phospholipid [103] differ from PC's in that lyso-PC's contain only one hydrocarbon chain instead of two. The cross-sectional areas of the two lipid head groups are identical, but the cross-sectional areas of lyso-PC alkyl chains are one half that of the PC's. This imparts a wedge-shaped geometry to the molecule imposing many implications for the stability of cell membrane interfaces.[104] Increased lyso content creates conditions for cell fusion.[36,105] In PC vesicles containing 15% lyso-PC, the lyso content in the outer monolayer was determined to be 4.9 times greater than that in the inner leaflet, imparting a higher degree of curvature to the vesicle.[106] Increasing the lyso content in phosphatidylcholine vesicles has been shown to result in a decreasing bilayer thickness until vesicle formation is no longer warranted.[107,108] Additionally, permeability to cations is found to increase sharply above 40% lyso content.[109]

Introduction of 10 mol% lyso-palmitoyl PC enhances considerably the rate of reorganization of DPPC vesicles by PEAA (1 mg/ml) (see Figure 3.14). The $t_{1/2}^{-1}$ value for lyso-PC containing vesicles (1 mg/ml) is 0.049 sec^{-1} compared to 0.014 for the pure DPPC vesicles (1 mg/ml). The rate is so rapid that it was difficult to measure accurately with the experimental setup used.

Cholesterol incorporation has the opposite effect. The cholesterol molecule has a reverse wedge shape with a small

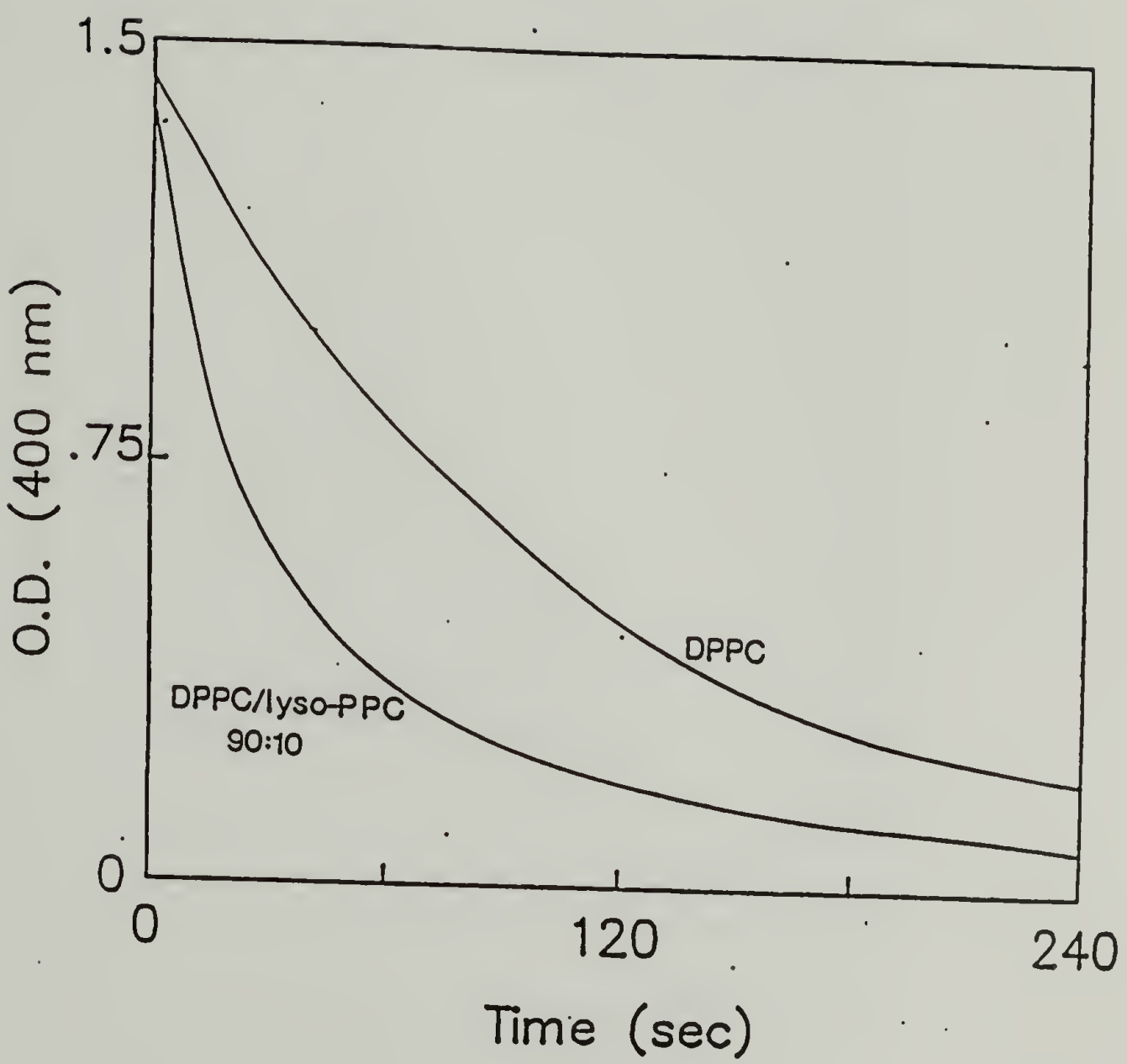

Figure 3.14 Decrease in optical density of a 90:10 DPPC/lyso-PPC mixture (2 mg/ml) in 10 mM phoshate buffer at pH 7.4 upon addition of PEAA (2mg/ml, 1 ml) in 100 mM phosphate buffer at pH 6.4 at 41.6°C.

polar head group and a larger hydrophobic cross section. The different geometry of the cholesterol molecule is demonstrated by the fact that mixtures of cholesterol and lysophosphatidylcholine exhibit a stable lamellar phase at a 1:1 molar ratio.[110] Above a cholesterol incorporation of 5 mol% into PC vesicles, two phases are detected by DSC.[37] DSC traces show a narrow peak at the transition temperature of the pure lipid, superimposed on a broader peak. As the percentage of cholesterol in the bilayer is increased, the narrow peak decreases in size and the broad peak moves to higher temperature until, at an incorporation of 50 mol% cholesterol, no phase transition is observed. Spin label studies indicate the existance of two phases up to 20 mol% cholesterol.[111,112] Despite much work, there is still considerable uncertainty about the nature of lipid/cholesterol mixtures.

Study of the interaction of PEAA (1 mg/ml) with DPPC/cholesterol (1 mg/ml) mixtures reveals interesting behavior as a function of the precentage cholesterol incorporation (see Figure 3.15). Up to 10 mol% cholesterol incorporation, the optical density curves fall on top of one another indicating that the presence of cholesterol has little effect on the structural integrity of the bilayer. As 20 mol% cholesterol incorporation is approached, there is a trend toward a rapid initial drop in optical density followed by an increase in optical density. The reason for this is not clear. The vesicles may reorganize into a transitional

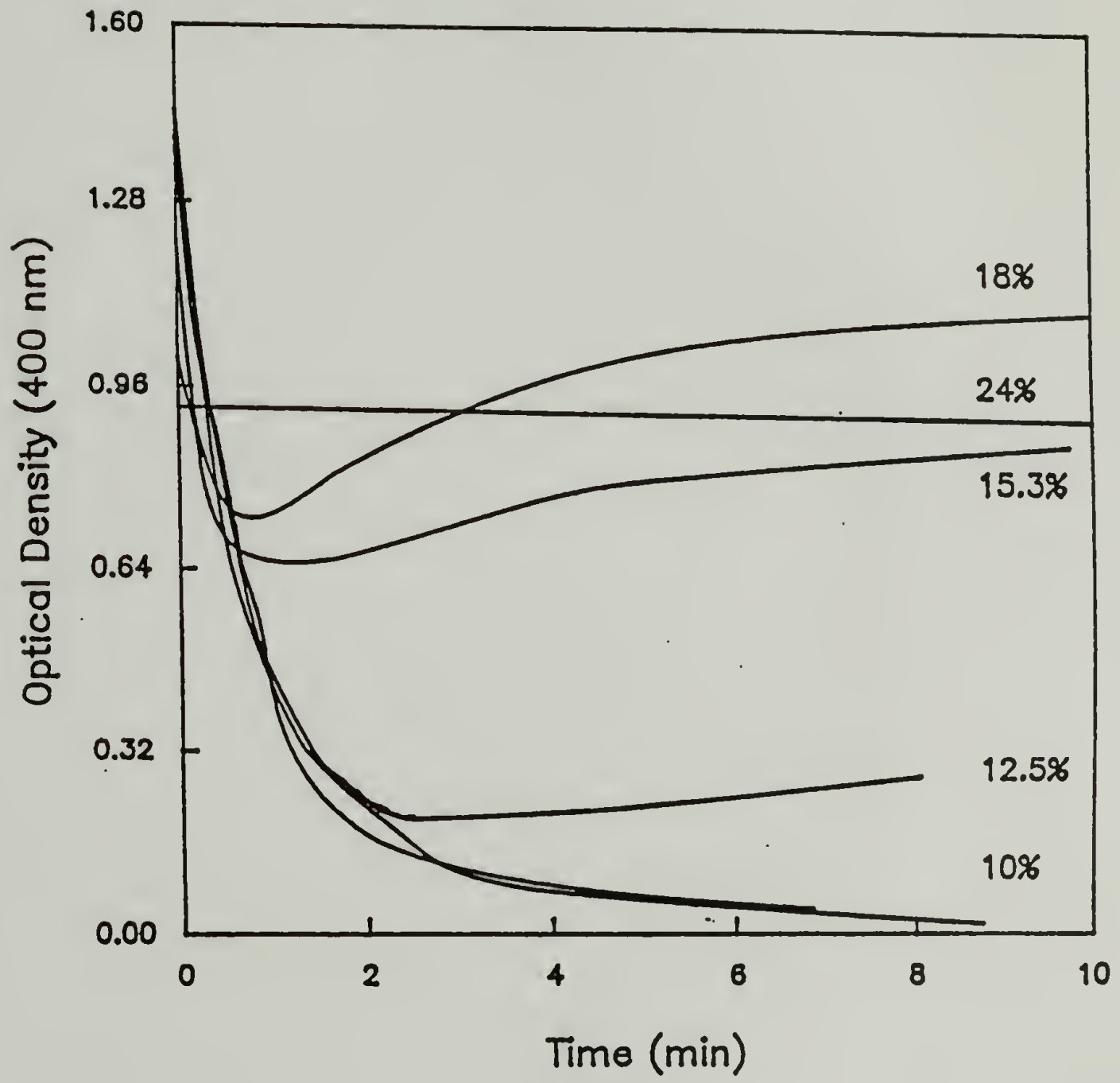

Figure 3.15 Effect of cholesterol incorporation on the optical density behavior of DPPC MLV's in the presence of PEAA (1 mg/ml) upon acidification to pH 6.4.

structure that does not scatter light as effectively as the equilibrium structure. At 24 mol% cholesterol, there is no change in the optical density indicating that no structural reorganization is occurring.

Very similar behavior has been seen in studies of the interaction of apoA-I and DMPC vesicles. Addition of up to 12 mol% cholesterol actually stimulates the rate of DMPC association with apoA-I.[97] Between 12 and 20 mol% cholesterol, the rate of association between the lipoprotein and vesicles decreases. Above 20 mol%, the interaction does not go to completion as measured by optical density. A decrease in the cholesterol content of DMPC/apoA-I complexes formed from vesicles containing higher than 18 mol% cholesterol suggests that cholesterol and apoA-I compete for sites on the phospholipid surface.[97] Cholesterol has a higher affinity for lipid (more hydrophobic) and excludes apoA-I at high cholesterol content. Pownall asserted that the inability of apoA-I to associate with phospholipid containing a high mole% of cholesterol is thermodynamically rather than kinetically controlled.[113]

Binary mixtures of phosphatidylcholines exhibit complex phase behavior. Calorimetric data show that a DLPC-DSPC mixture exhibits monotectic phase behavior (see Figure 1.3).[30,114] The peak for DLPC remains at constant temperature over the entire concentration range while the peak for DSPC is broadened and moves down in temperature with increasing DLPC content. This indicates that melted DLPC is

somewhat soluble in crystalline domains of DSPC, but not vice-versa. The reorganization behavior of a 1:1 DLPC/DSPC mixture is complex (see Figure 3.16). At 28.5°C, there is a rapid initial drop in optical density followed by a very slow decrease in optical density. The initial drop may be due to the interaction of PEAA with pure DLPC phases in the membrane. The slow drop in O.D. is due to the interaction of a DSPC mixture. Under these conditions, DLPC membranes reorganize quickly and DSPC does not reorganize at all. As the temperature is increased through the broad melting phase of the mixture, the optical density decreases to lower values. At 45.1°C, the reorganization is very fast (complete in less than 3 min). This may be a result of the two lipids possibly being immiscible in the fluid phase. In this case, there should exist many phase boundaries that gives rise to the enhanced rate of reorganization.

Not all lipid mixtures change the level of interaction of the vesicle with PEAA significantly from that of the pure lipid. Incorporation of up to 20% dipalmitoyl phosphatidic acid has little effect on the optical density behavior of DPPC/PEAA mixtures (see Figure 3.17). DPPA differs from DPPC in that the choline portion of the head group is not present. This places a negative charge on the molecule. The slight increase in the optical density loss may be due to the increase in headgroup repulsions similar to that with vesicles of DPPG.

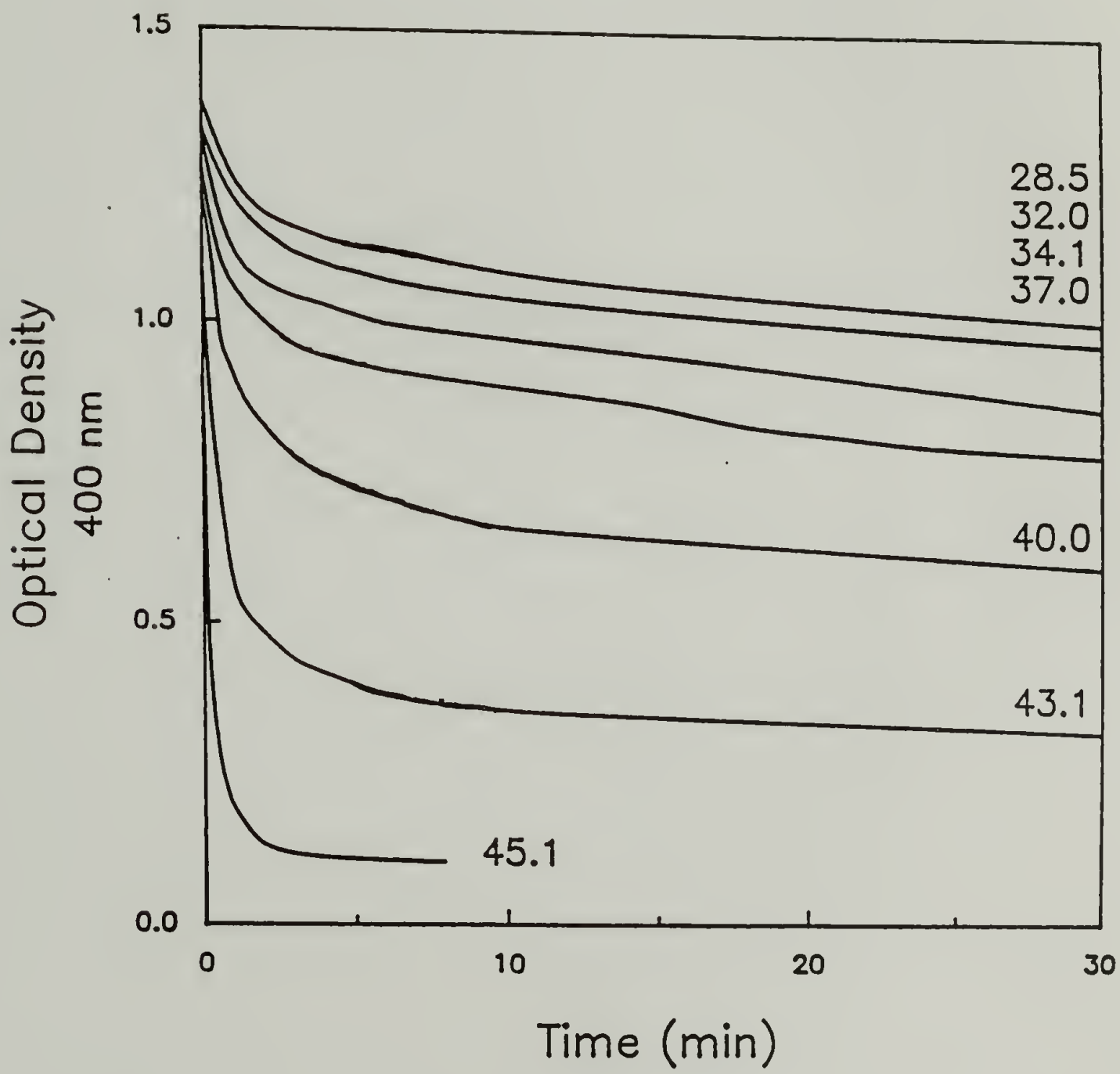

Figure 3.16 The effect of temperature on the decrease in the optical density of a 1:1 DLPC/DPPA MLV (1 ml, 2 mg/ml) suspension in 10 mM phosphate buffer at pH 7.4 upon addition of PEAA (1 ml, 2 mg/ml) in 100 mM phosphate buffer at pH 6.4. The final pH was 6.45.

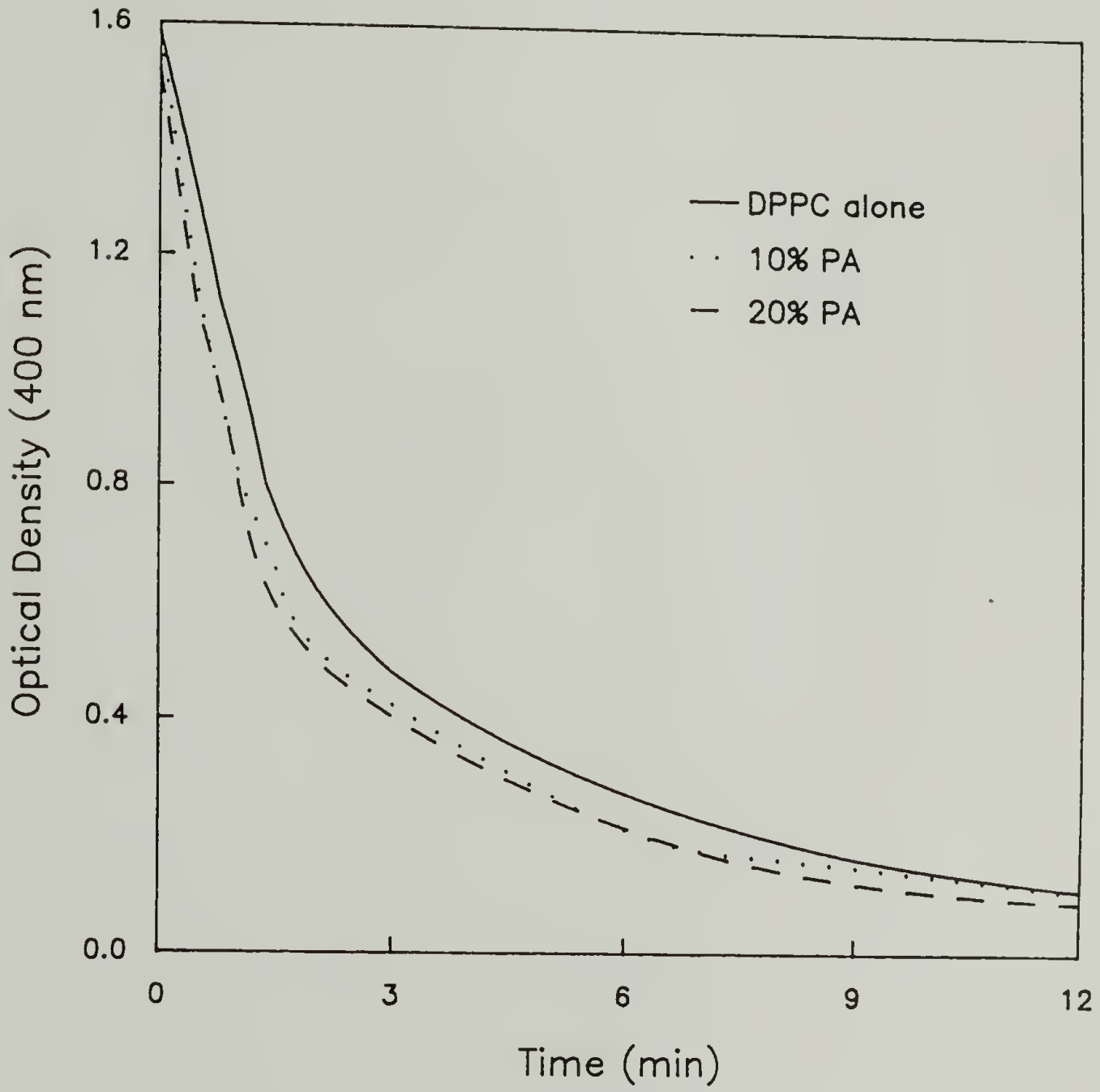

Figure 3.17 The decrease in the optical density of a DPPC/DPPA MLV (1 ml, 2 mg/ml) suspensions in 10 mM phosphate buffer at pH 7.4 upon addition of PEAA (1 ml, 2 mg/ml) in 100 mM phosphate buffer at pH 6.4. The final pH was 6.45.

4. Comparison of dye release and reorganization kinetics

One of the interesting properties of vesicles is the ability to entrap solutes within the aqueous core. It was demonstrated that the fluorescent dye, 6-carboxyfluorescein, could be entrapped in EYPC SUV's in the presence of PEAA and released completely and rapidly in response to a change in pH (see Figure 1.7). It seems likely that loss of membrane integrity should precede complete reorganization, but the relationship between the two processes is not clear. To examine the relationship, it was necessary to compare the optical density dye release behavior of DOPC MLV's. MLV's were used because SUV's do not scatter light effectively due to their small size making optical density measurements difficult. DOPC was chosen as the lipid because previous results indicated that vesicles of EYPC do not clarify completely when interacted with PEAA. Other phosphatidylcholines were ruled out because their T_m values were at or above room temperature. Preparation of these samples would involve bringing the suspensions through the transition temperature which destabilizes the retention of the marker.

Figure 3.18 shows the optical density of DOPC MLV's (1 mg/ml) acidified to different pH in the presence of PEAA (1 mg/ml). The behavior is similar to that seen for other phosphatidylcholines. At pH 6.58, the reorganization is very

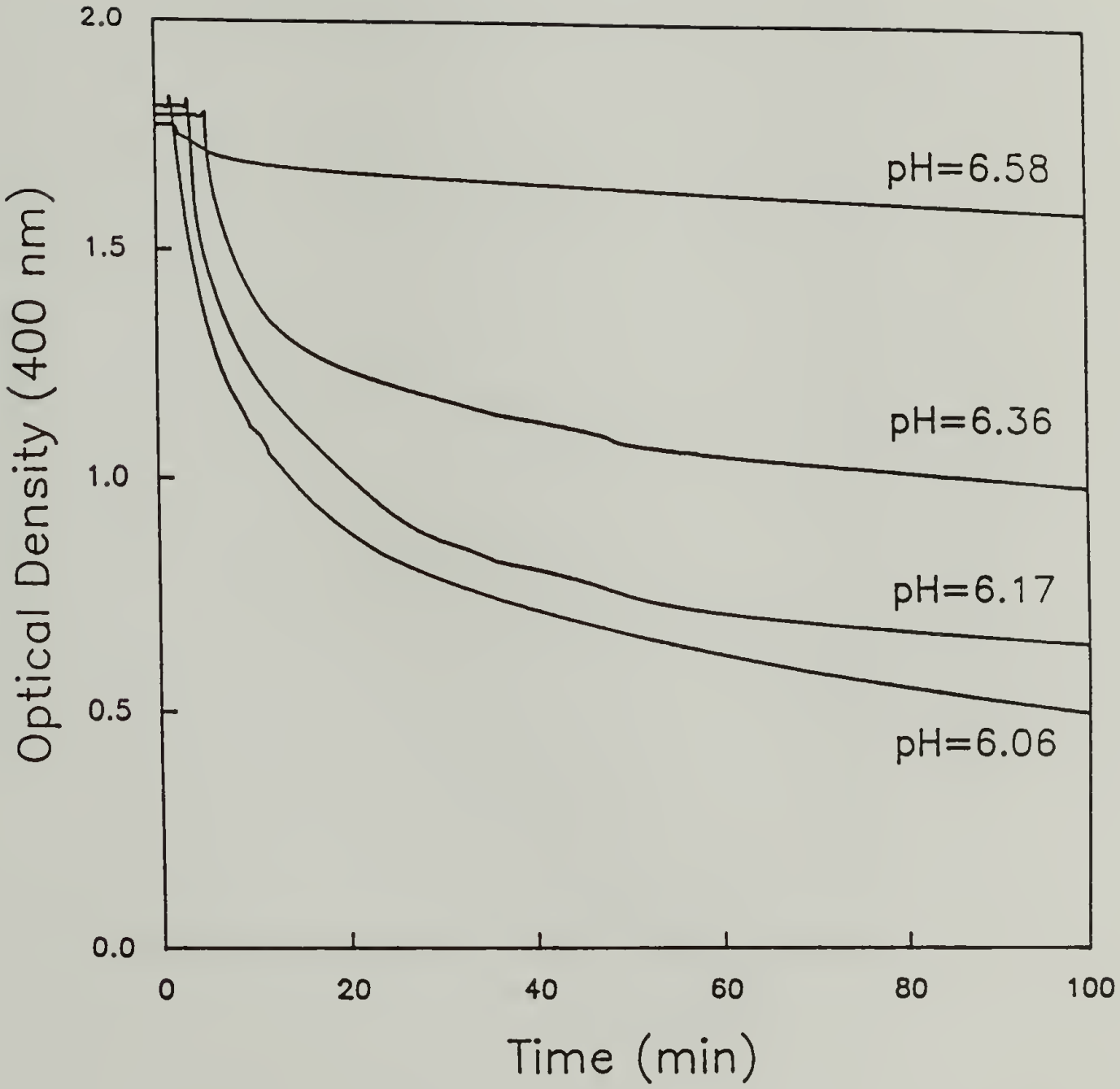

Figure 3.18 The effect of pH on the decrease in the optical density of a DOPC MLV (1 mg/ml) suspensions in the presence of PEAA (1 mg/ml) in 100 mM phosphate buffer. Measurements were performed at 25°C.

slow but speeds up with decreasing pH. For DOPC, reorganization occurs much slower than for DMPC and DPPC (incomplete clarification after 100 min.). DOPC possesses two acyl chains 18 carbons in length just as in DSPC, but DOPC contains unsaturation in the acyl chains (see Figure 1.2). The slow rate is similar albeit still much slower than that for DSPC. The reason for this has been proposed to be due to a reluctance of the unsaturated DOPC lipid (larger cross-sectional area of the unsaturated acyl chains) to adopt the higher degree of surface curvature characteristic of micellar organization.[59]

For the permeability measurements, calcein was entrapped in DOPC MLV's. The use of calcein as a fluorescent marker has distinct advantages over 6-carboxyfluorescein. In the physiological pH range, the fluorescence of calcein is relatively pH independent. Also, the calcein carries a net negative charge of -2 in that pH range and would therefore be expected to show high latency in vesicles.

Preparations of calcein-loaded EYPC SUV's are stable to leakage of the dye for several hours, so it was expected that DOPC MLV's should be able to entrap the dye effectively. At a concentration of 200 mM, calcein solutions do not fluoresce.[115] When calcein is entrapped at this concentration in vesicles and the unentrapped dye is removed, the vesicle suspensions appear light brown due to the color of the calcein. When the dye is released, the self quenching condition is relieved due to the dilution of the dye and a

green fluorescence is observed. This change can be quite striking as depicted in Figure 3.19. The vial on the left shows calcein entrapped in EYPC SUV's in the presence of PEAA (1 mg/ml) at pH 7.4. The vial on the right was acidified to pH 6.0 with 0.1N HCl and shows the greenish fluorescent emission of the calcein.

In the preparation of samples, calcein containing DOPC MLV's were subjected to many steps of centrifugation and washing with 100 mM NaCl solution to separate free from entrapped calcein. This method of preparation was necessary because suitable gel filtration media of sufficient pore size as to allow passage of the larger MLV's were not available. The pelleted vesicles were washed with salt solution because the vesicles were less dense than a 100 mM sodium phosphate solution and could not be sedimented in the buffer solution.

The permeability of DOPC MLV's (1 mg/ml) at a range of pH values in the presence of PEAA (1 mg/ml) is shown in Figure 3.20. The fraction of calcein released was determined by assuming the fluorescence intensity in the absence of PEAA corresponded to 0% released calcein and that addition of the detergent, Triton X-100 (0.1 ml, 10%), released any remaining dye. The addition of detergent solubilizes any remaining vesicles. The PEAA/DOPC mixtures were acidified from pH 7.4 by the addition of 0.1N HCl. At pH 7.4, there is no noticeable release of calcein. Significant release (10%) was observed at pH 7.04. There is a fast initial release of dye followed by a gradual release. Both of these features

Figure 3.19 Calcein-containing EYPC SUV's in the presence of PEAA (1 mg/ml) in 100 mM phosphate buffer. Vial on the left is at pH 7.4. Vial on the right was acidified to pH 6.0.

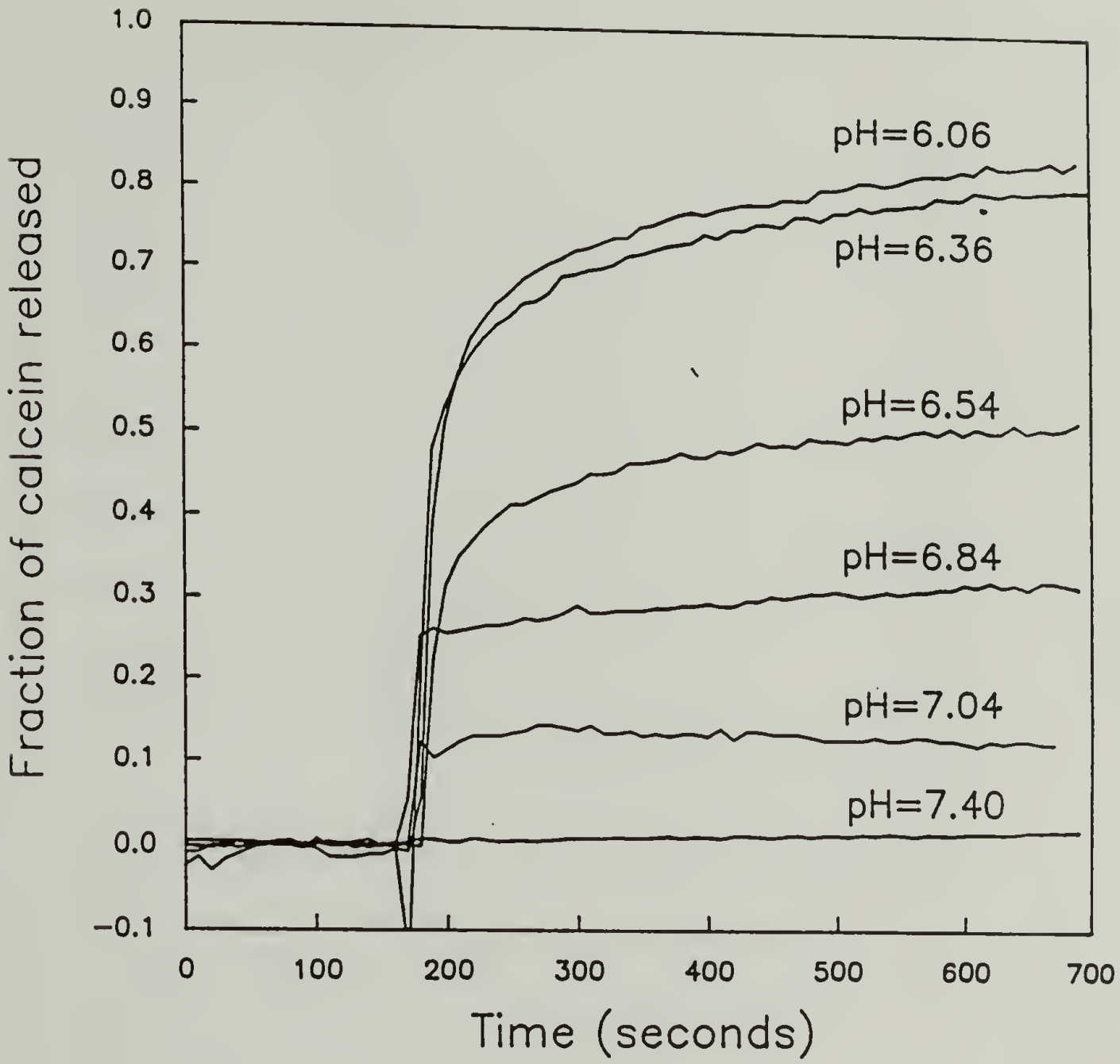

Figure 3.20 Fraction of calcein released from DOPC MLV's (1 mg/ml) at 25°C in the presence of PEAA (1 mg/ml) in 100 mM phosphate buffer as a function of the degree of acidification.

increase with decreasing pH. The increase in the amount of dye release in going from pH 6.54 to 6.36 is very large (30%) due the conformational transition of PEAA occurring in this range. At pH 6.06, over 80% of the entrapped dye was released in less than 350 seconds. Release experiments performed with EYPC SUV's mixed with PEAA show an instantaneous quantitative release upon acidification (see Figure 1.7) which is quite different from the behavior displayed by MLV's.

MLV's contain approximately 6 to 9 concentrically arranged bilayers per vesicle. The majority of entrapped material resides in the central core of the vesicle, but there is a significant amount of material dissolved in the aqueous layers between adjacent bilayers. The vesicles were formed in the absence of PEAA which precludes the possibility of a PEAA chain traversing several bilayers of a vesicle. Hence, the release of dye should be gradual as the 'layers of the onion' are successively peeled away or made permeable. The fast initial release may be due to the interaction of imperfectly formed or unstable vesicles with PEAA.

Comparison of the time frames of the optical density (Figure 3.19) and release (Figure 3.20) experiments reveals the fact that the increase in permeability occurs over an order of magnitude faster than does the structural reorganization of DOPC MLV's. At pH 6.06, 80% of the calcein is released in about 550 seconds while the optical density change is a little less than 80% complete in 6000 seconds under the same conditions.

C. Interaction with DnsPEAA

1. Synthesis

The goal of this phase of the work from the outset was to develop a fluorescently labeled PEAA that would allow observation of the PEAA-vesicle interaction under the fluorescent microscope. There were two properties that were examined for selection of the probe. First, the amount of incorporation of the probe had to be controllable. The presence of the probe could not significantly disturb the conformational properties of the polymer so the degree of functionalization had to be kept low. Yet, there had to be sufficient functionalization to allow visual detection. Second, it was thought that a probe whose fluorescence emission intensity increased greatly in a nonpolar medium was needed. The association of PEAA onto vesicles is of a hydrophobic nature therefore, a hydrophobic probe attached to an adsorbed chain would partition into the bilayer. The probe in the bilayer would fluoresce more intensely than on an unassociated chain 'lighting up' the vesicle under a fluorescence microscope.

There has been a considerable amount of work done on fluorescently labeling polymers. Two probes that have been used frequently are pyrene and the 1-dimethylamino-naphthalene-5-sulfonyl (dansyl, Dns) group. Either probe

could have been chosen since both fluoresce strongly in a nonpolar medium and there are examples of successful incorporation of each chromophore on poly(carboxylic acid)s in the literature.[51,116,117]. The dansyl group was chosen over pyrene, because it was felt that there was greater control over the amount of probe placed on PEAA. Previous attempts to place pyrene on PEAA had resulted in only 0.002-0.04 mol% pyrene incorporation.[55]

The polymers were synthesized according to the scheme outlined in Figure 3.21. N-Dansyl ethylenediamine was placed on PEAA via a coupling reaction with dicyclohexyl-carbodiimide. Extensive purification of the polymer was necessary to remove trace amounts of unreacted dansyl groups. For this purpose, ultrafiltration of the polymer was carried out until free probe could no longer be detected by thin layer chromatography. The limit of detection was determined to be approximately 0.005% of the amount of incorporated Dns groups . The percent incorporation of Dns was determined to be 3.8% by UV spectroscopy. This value agreed with ^{1}H NMR data. A second polymer was synthesized by decreasing the amount of dansyl ethylenediamine in the DCC coupling by a factor of two. Analysis of the polymer by UV and ^{1}H NMR showed 2.0% incorporation of the dansyl moiety.

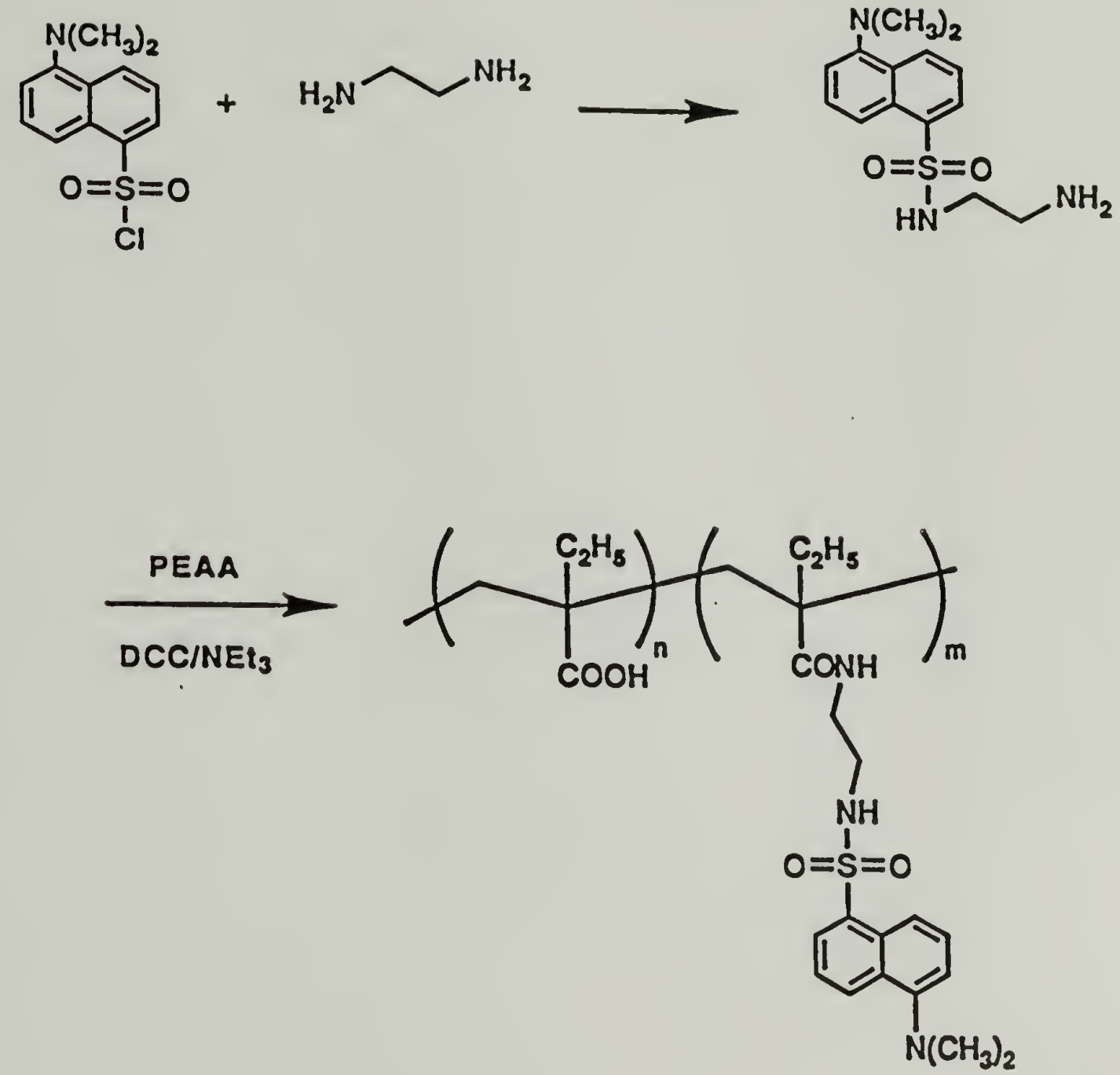

Figure 3.21 Scheme for synthesis of DnsPEAA.

2. Fluorescence behavior of aqueous DnsPEAA solutions

Figure 3.22 shows the fluorescence spectrum of DnsPEAA-2% in methanol. The spectrum exhibits a maximum at 525 nm. The position and intensity of this maximum are very sensitive to solvent polarity but relatively insensitive to oxygen.[118] When DnsPEAA is dissolved in water, the fluorescence emission behavior of the polymer is dependent on the pH of the solution. The response of the fluorescence maximum and intensity (λ_{ex} = 340 nm) to the pH of the solution for DnsPEAA-2% is shown in Figure 3.23. At pH 6.5 to 8.0, the fluorescence intensity is low and exhibits a maximum at approximately 580 nm. The position of the maximum at these pH values is similar to the fluorescence maximum of N-ε-dansyl-lysine in distilled water which was measured at 571 nm. This indicates that the attached probe on PEAA in solution, above a pH of 6.5, experiences an environment similar to that of the free probe in water. In this pH range, PEAA exists as an extended coil exposing the probe to contacts with water molecules. As the pH is lowered below 6.5, there is an increase in the fluorescence emission and a blue shift in the emission maximum that one would expect with decreasing solvent polarity.[119] This change in the emission of the Dns groups is due to the conformational collapse of PEAA that provides a nonpolar environment for the probe shielding it from water contacts. The midpoint for this transition is approximately pH 6.3, agreeing with the

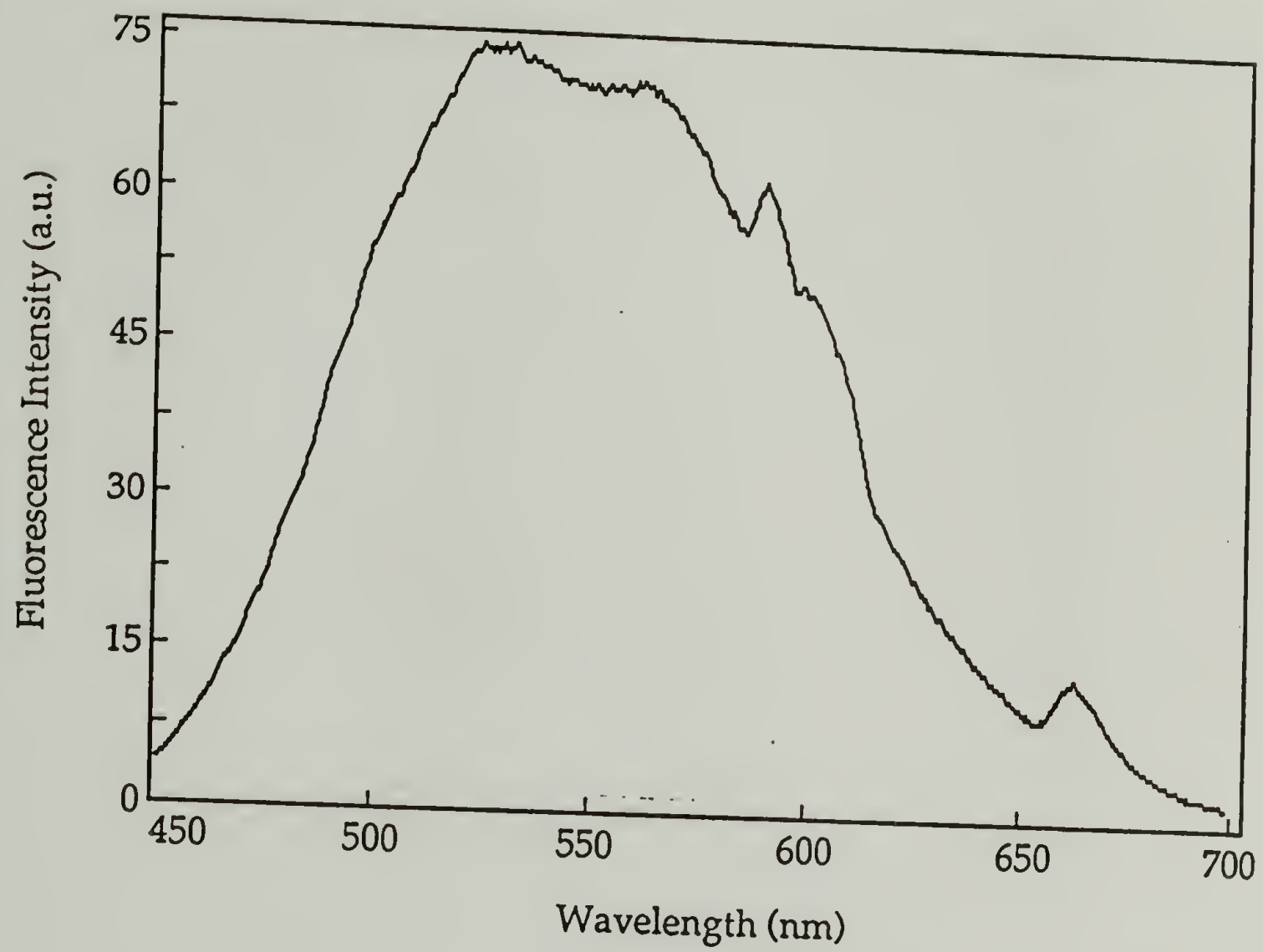

Figure 3.22 Fluorescence emission spectrum (λ_{ex}=340 nm) of DnsPEAA-2% in methanol.

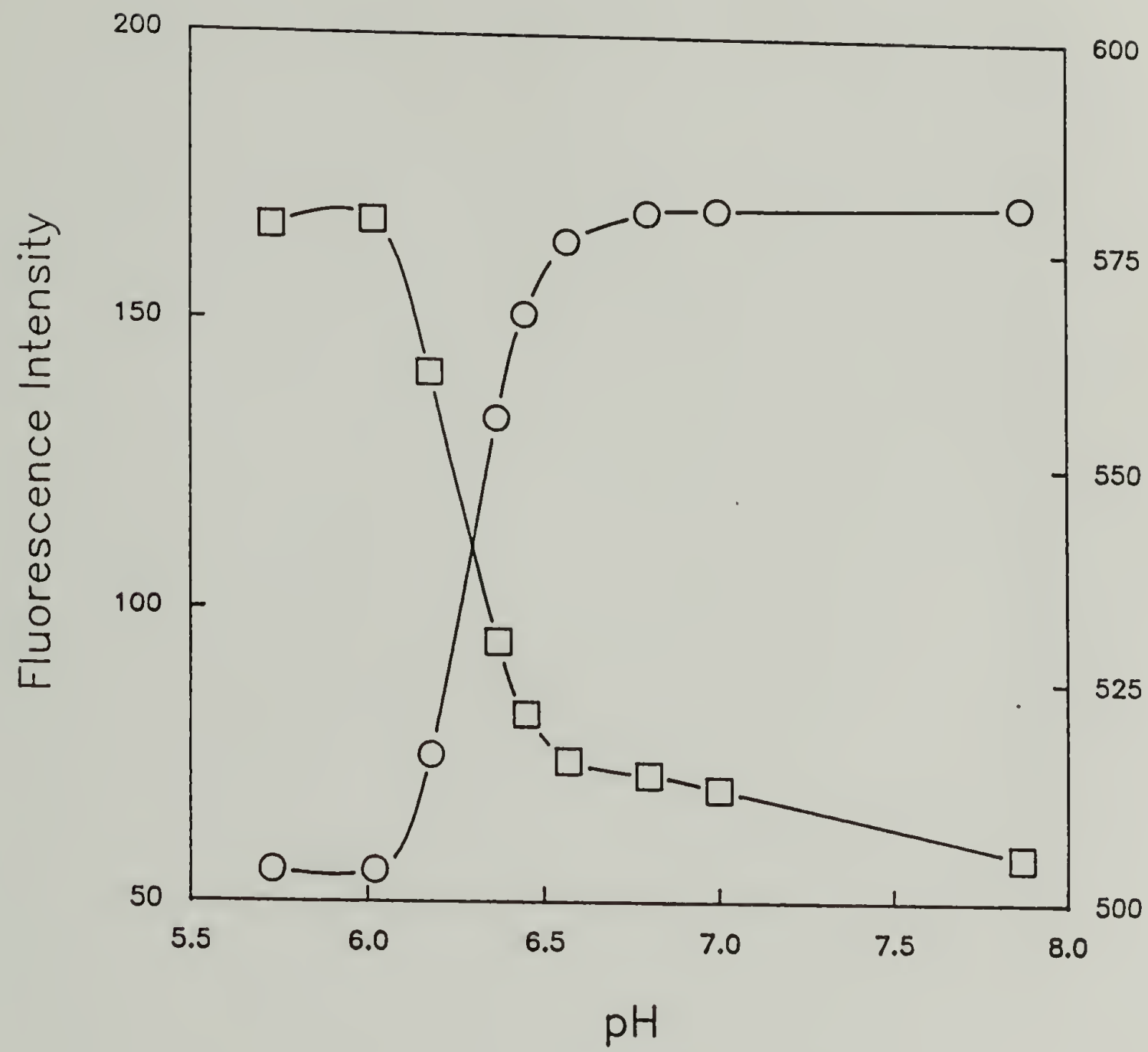

Figure 3.23 Fluorescence emission intensity (□, λ_{ex}=340 nm) and wavelength of maximum emission (○) for aqueous DnsPEAA-2% solutions as a function of pH.

data obtained by Borden with pyrene labeled PEAA[55]. The same experiment performed with DnsPEAA-3.8% provides a similar picture except that the midpoint of the conformational transition is shifted upward in pH (see Figure 3.24). The presence of extra dansyl moieties on the polymer results in a decreased number of polar acid groups on the chain and increased number of hydrophobic groups increasing the average hydrophobicity of the chain. This increases the pK_a of the acid groups in the same manner that increasing the alkyl chain length in the series PAA, PMAA and PEAA increases the respective pK_a of those polymers.

The fluorescence behavior of the DnsPEAA-2% changes significantly in the presence of EYPC SUV's (see Figure 3.25). The polymer in the presence of vesicles shows an increased fluorescence emission intensity over the entire pH range displayed. The fluorescence increases with decreasing pH and then gradually decreases after passing through a maximum. The increased fluorescence at pH 8 indicates that there is considerable adsorption of the polymer on to the vesicles at this pH. There is an increasing association of PEAA with the vesicles down to pH 6.9. As the ionization of the polymer decreases, PEAA becomes more tightly associated with the vesicle surface providing a means for the Dns groups to find a more nonpolar environment. A hydrophobic medium is provided by the lipid bilayer that helps solubilize the hydrophobic Dns group. PEAA begins to solubilize lipid bilayers at about pH 6.9 corresponding to the maximum. As

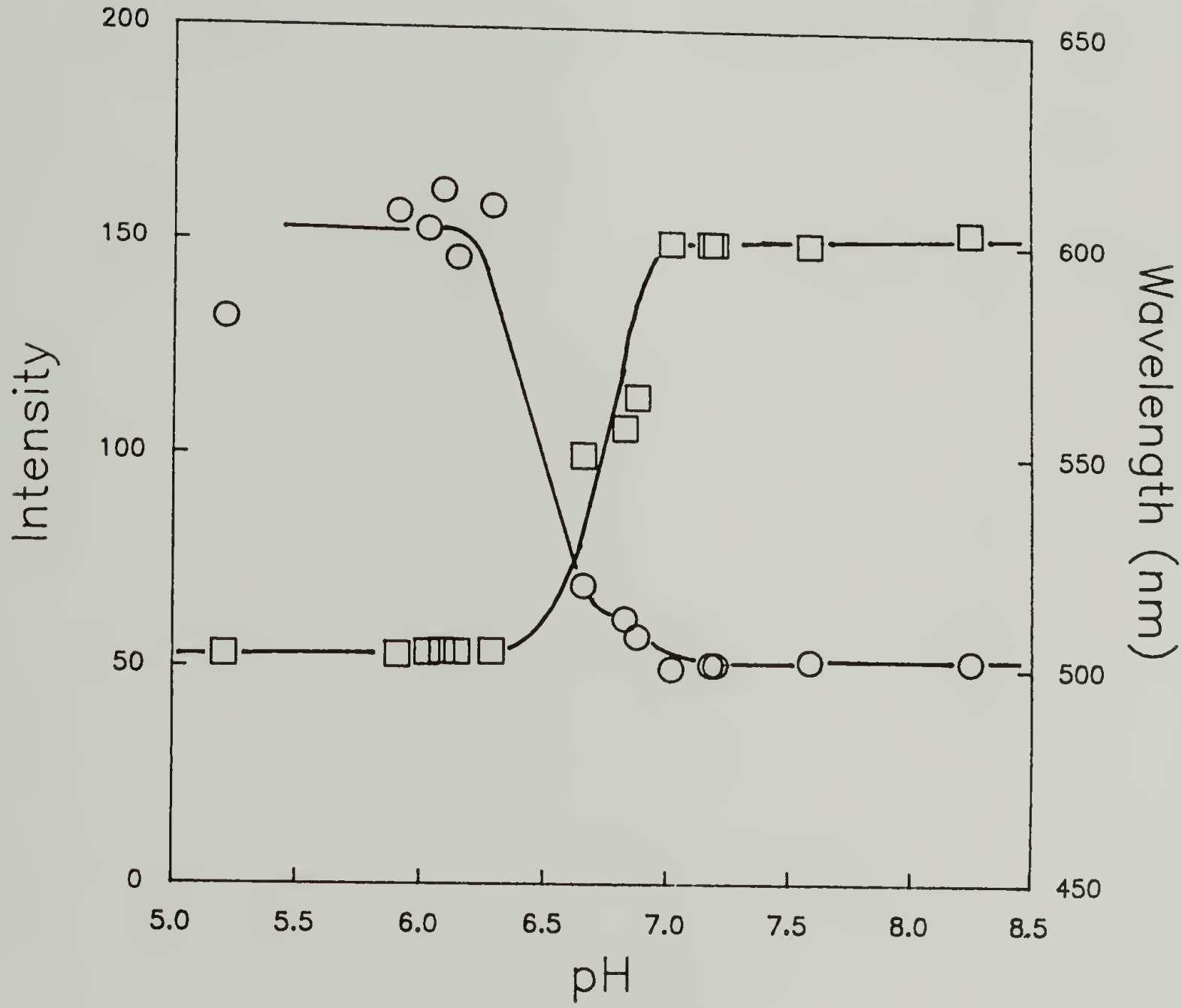

Figure 3.24 Fluorescence emission intensity (□, λ_{ex}=340 nm) and wavelength of maximum emission (○) for aqueous DnsPEAA-3.8% solutions as a function of pH.

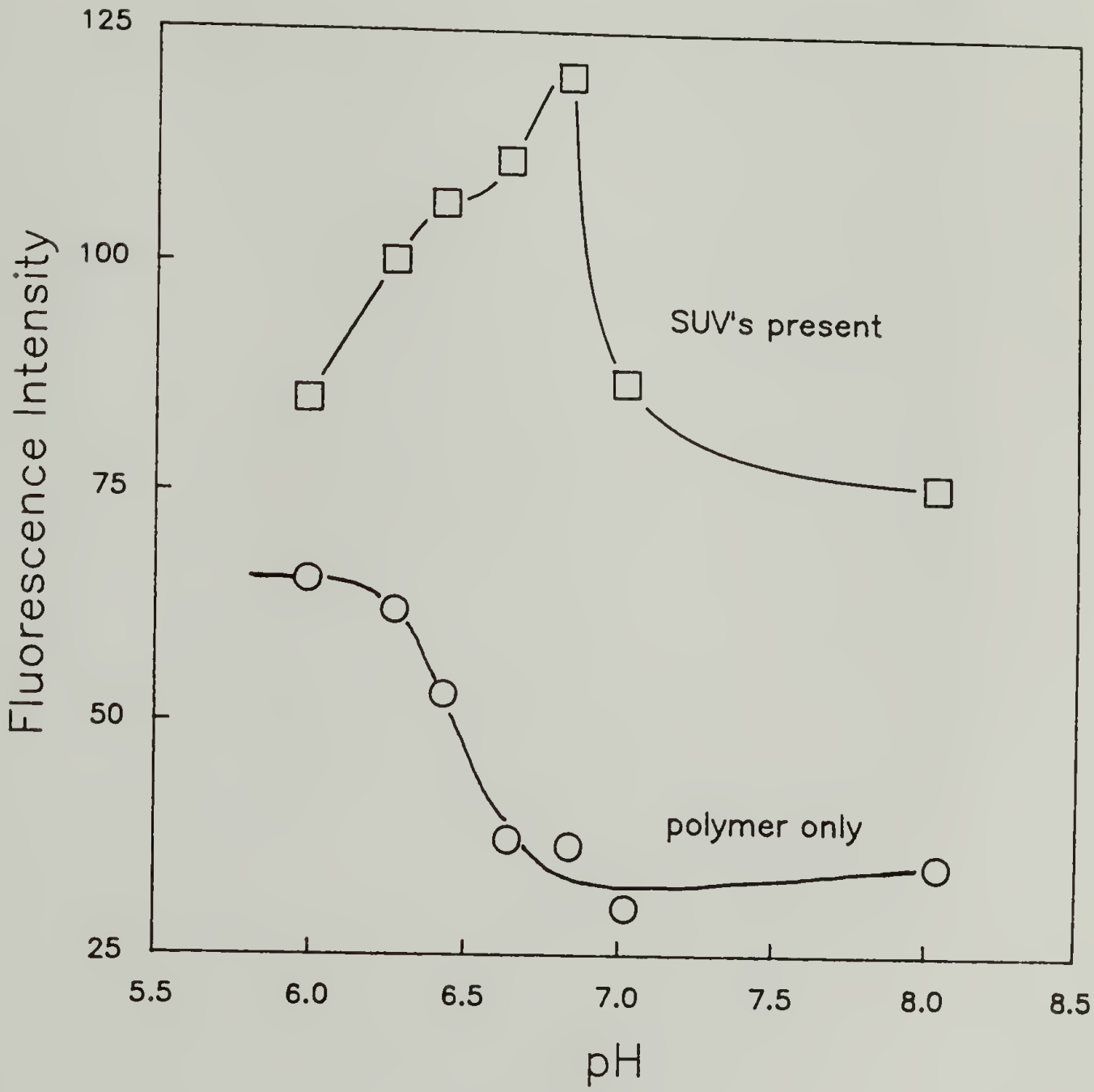

Figure 3.25 Fluorescence emission intensity (λ_{ex}=340 nm) for aqueous DnsPEAA-2% solutions as a function of pH in the presence (□) and absence (○) of EYPC SUV's.

the polymer begins to solubilize the vesicle, there is a preferred association of the polymer and lipid. The Dns group may become the more polar group in this arrangement and be turned to the outside of the mixed micelle, exposing it somewhat to the polar solvent. A similarly shaped curve was observed by Borden in fluorescence polarization experiments with diphenylhexatriene-containing DPPC MLV's in the presence of PEAA.[55] The polarization increased to a maximum at pH 6.9 and then fell sharply with decreasing pH. The behavior was assigned to a rigidification of the bilayer upon interacting with PEAA, and the decreasing size of the vesicles caused a change in the correlation time of the probe.

3. Potentiometric titrations of DnsPEAA

Potentiometric titration is another means of probing the conformational properties of the polymers. Plots of the pK_a of DnsPEAA-2% and DnsPEAA-3.8% as a function of the degree of dissociation show interesting behavior (see Figures 3.26 and 3.27). Both polymers exhibit an elevated pK_a relative to PEAA for a given α. This may be due to the extra hydrophobicity of the polymers as explained earlier. Also, there may exist hydrogen bonding between the dimethylamino group on the dansyl moieties and acid groups on the polymer making the chain more compact which would elevate the pK_a by intensifying the charge repulsions of ionized carboxyl

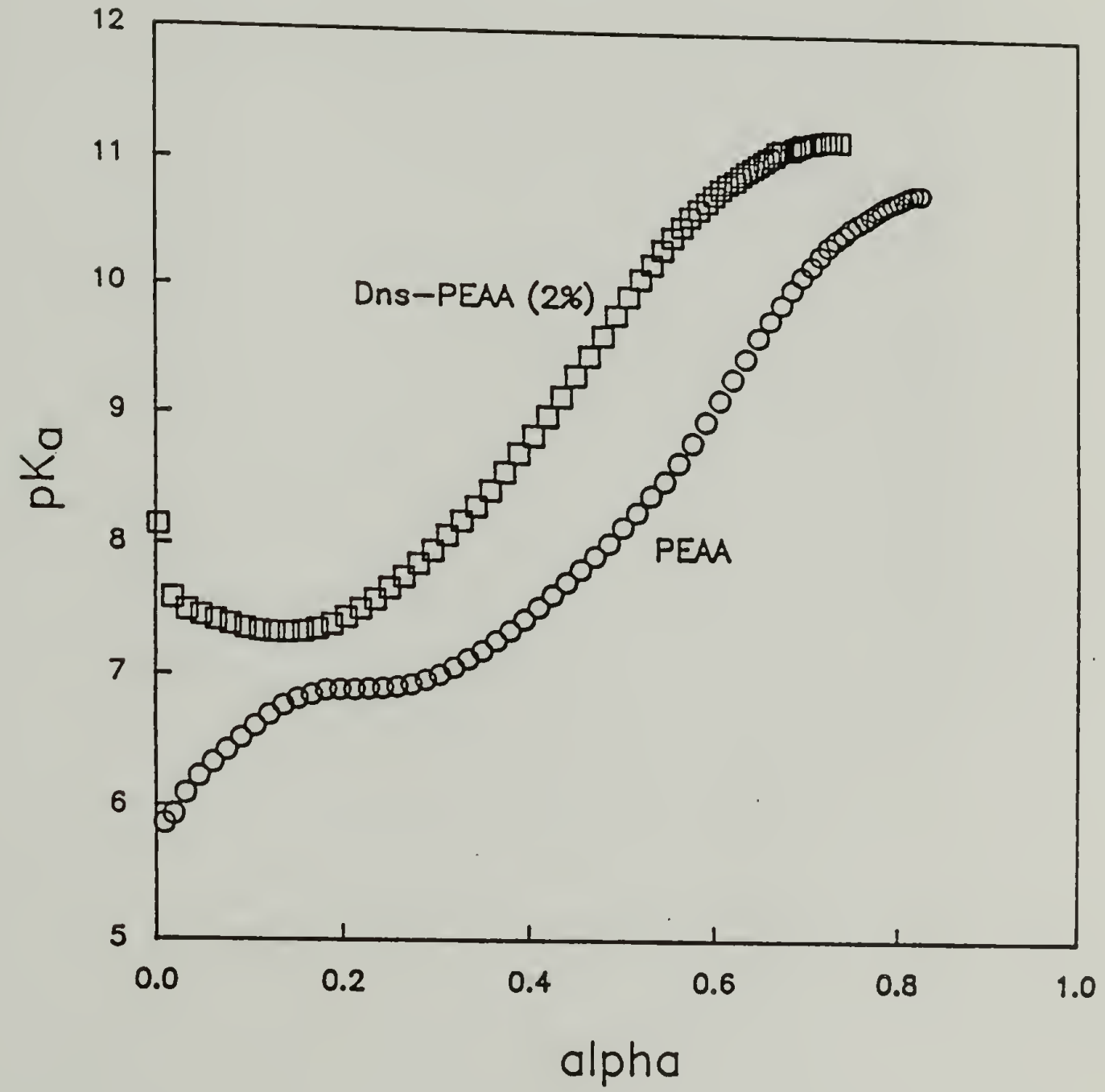

Figure 3.26 Apparent acid dissociation constant of DnsPEAA-2% as a function of degree of ionization.

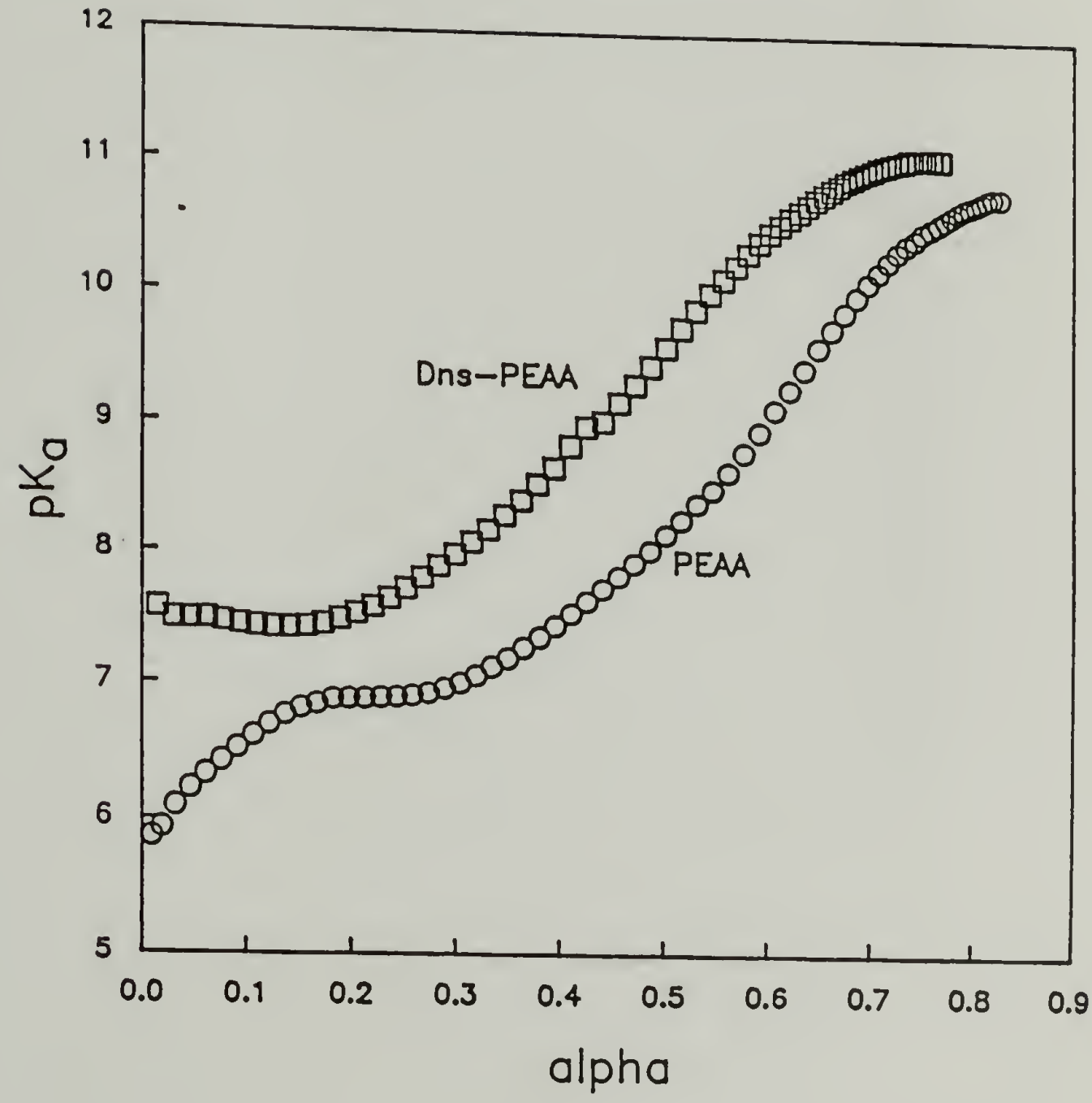

Figure 3.27 Apparent acid dissociation constant of DnsPEAA-3.8% as a function of degree of ionization.

groups. At low extents of ionization, the titration behavior deviates significantly from that of the unlabeled polymer. According to Strauss and Vesnaver, the pK_a of the dansyl group is approximately four.[120] The dansyl group is fully protonated at pH 1 and fully deprotonated at pH 6. It is reasonable to assume that below pH 6, the dansyl groups become protonated ionizing the PEAA chain and causing subsequent elevation of the pK_a of the acid groups.

4. Microscopy of DnsPEAA/EYPC vesicle mixtures

The purpose of synthesizing the DnsPEAA samples was to enable the visualization of the reorganization process. Electron microscopy has provided a wealth of information about the morphological changes that accompany the interaction. However, electron microscopy suffers from the fact that samples need to be dried down in their preparation. This often leads to artifacts, preventing one from viewing a changing sample in real time. Using an optical microscope, one can view and film processes as they occur without having to dry down samples. Fluorescence microscopy is a valuable tool for visualizing fluorescent labeled structures that might not be visible using a conventional transmitted light microscope. The combination of the two types of optical microscopy is ideal for visualizing the PEAA-induced reorganization of vesicles. MLV's are of sufficient size to

see via transmitted light microscopy and DnsPEAA can be viewed via its fluorescence.

The microscope system used was equipped for both fluorescence and transmitted light visualization. Images are recorded digitally via a charge couple device (CCD). Because exposure times for recording images are typically 2-50 msec, the system can switch between modes and record fluorescent and transmitted light images almost simultaneously.

When the images are recorded, they are converted to digital images and then binned by a factor of two (Four pixels are averaged and then recorded as one pixel in order to reduce the disk storage space required for the graphic image files). The digitizing and binning of the image results in a small loss of resolution. The intensity of the each pixel is mapped into one of 256 gray levels. The fluorescent images are processed in the same manner except that pixel intensities are mapped into a 256 level color scheme.

Figure 3.28 shows fluorescent and transmitted light images of EYPC MLV's (1 mg/ml) mixed with DnsPEAA-3.8% (1 mg/ml) at pH 7.4. The transmitted light images (top) show two elliptically shaped vesicles about 10 μm in diameter. Because the images are recorded by a CCD camera, the magification of the image is not easily determined. The calibration of the magnification is recorded in a program that places the size bar on the image (lower right hand corner). The fluorescent images of the vesicles appear as

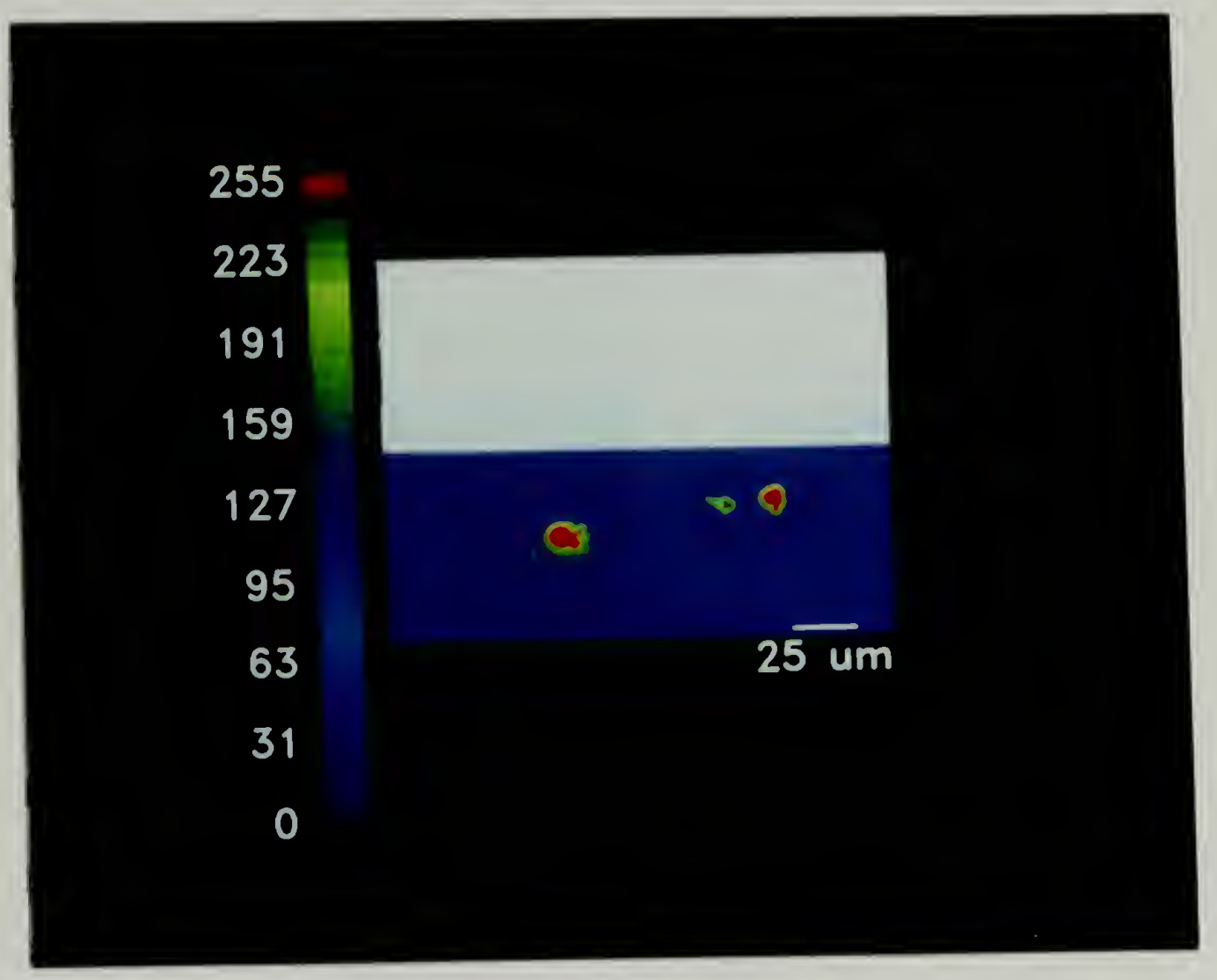

Figure 3.28 Transmitted light and fluorescence images of EYPC MLV's (1 mg/ml) in the presence of DnsPEAA-3.8% (1 mg/ml) in 50 mM phosphate, 50 mM NaCl at pH 7.4.

brightly colored ellipsoids on a blue background with the corresponding intensity scale shown to the side. Adsorption of the polymer onto the vesicle surface causes the dansyl groups to fluoresce strongly giving rise to the green and red colors. Care must be taken not to assume that the fluorescence intensity in the center of the vesicles is much greater than that on the outer edges. Because of the colors chosen for the intensity map, a small difference in fluorescence intensity can result in completely different colors.

When the EYPC MLV's are mixed with DnsPEAA-2% under identical conditions, similar images are obtained (see Figure 3.29). The fluorescence intensity actually appears slightly greater for this sample even though DnsPEAA-2% contains a smaller concentration of chromophores. Exposure times for the DnsPEAA-2% samples were 10 msec compared to only 4 msec for DnsPEAA-3.8% accounting for the difference. The vesicles were seen to fluoresce strongly in the presence of both DnsPEAA samples up to pH 10. This indicates significant association of the polymer with the lipid bilayers at this pH. Data from energy transfer measurements of pyrene labeled PEAA and DPPC vesicles labeled with tryptophan residues support this conclusion.[55]

When the pH is lowered to 6.4, the reorganization was found to occur at a convenient rate for photographing. Figure 3.30 shows the different stages of the reoganization of EYPC MLV's by DnsPEAA 3.8%. The photographs are taken at

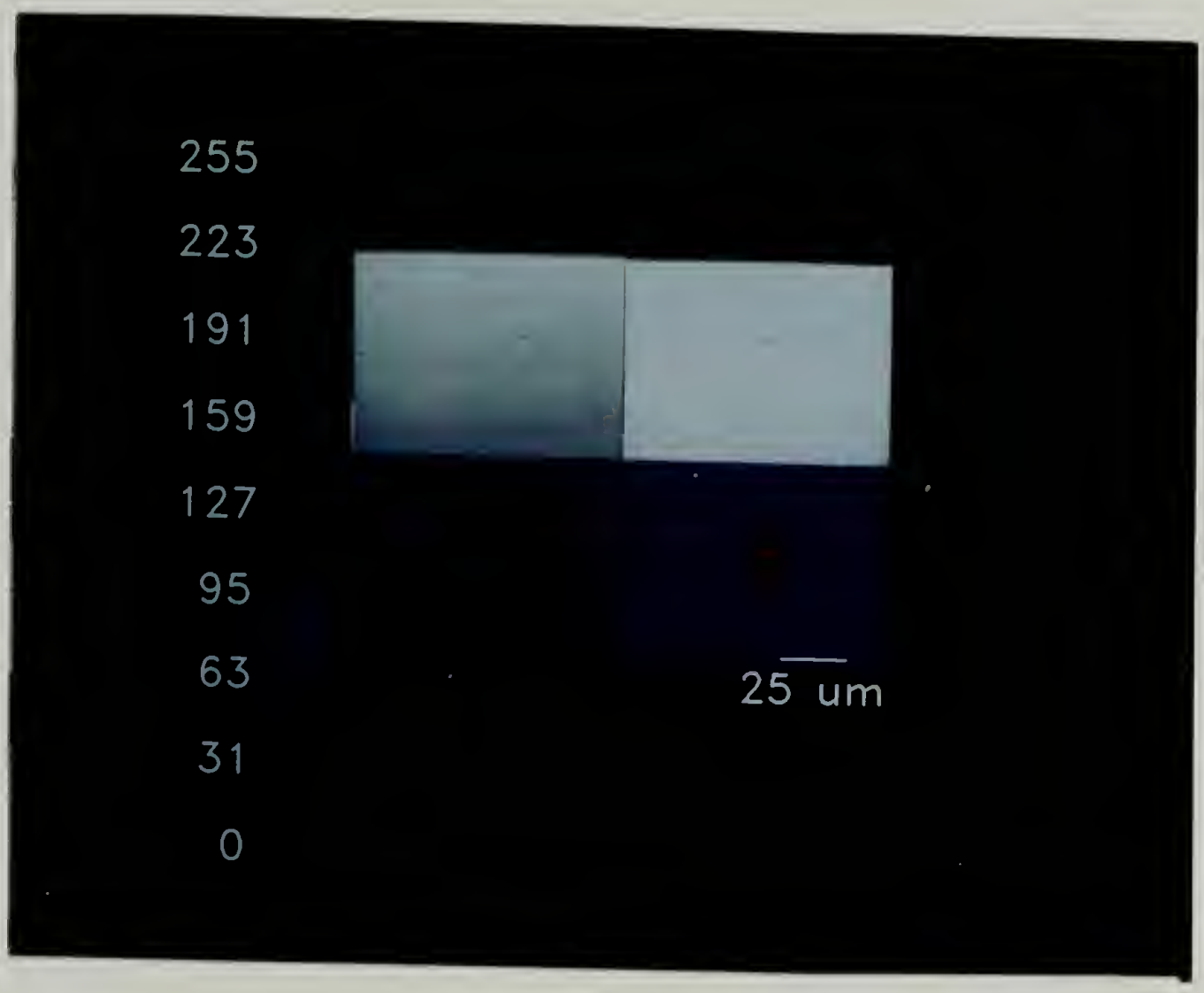

Figure 3.29 Transmitted light and fluorescence images of EYPC MLV's (1 mg/ml) in the presence of DnsPEAA-2% (1 mg/ml) in 50 mM phosphate, 50 mM NaCl at pH 7.4.

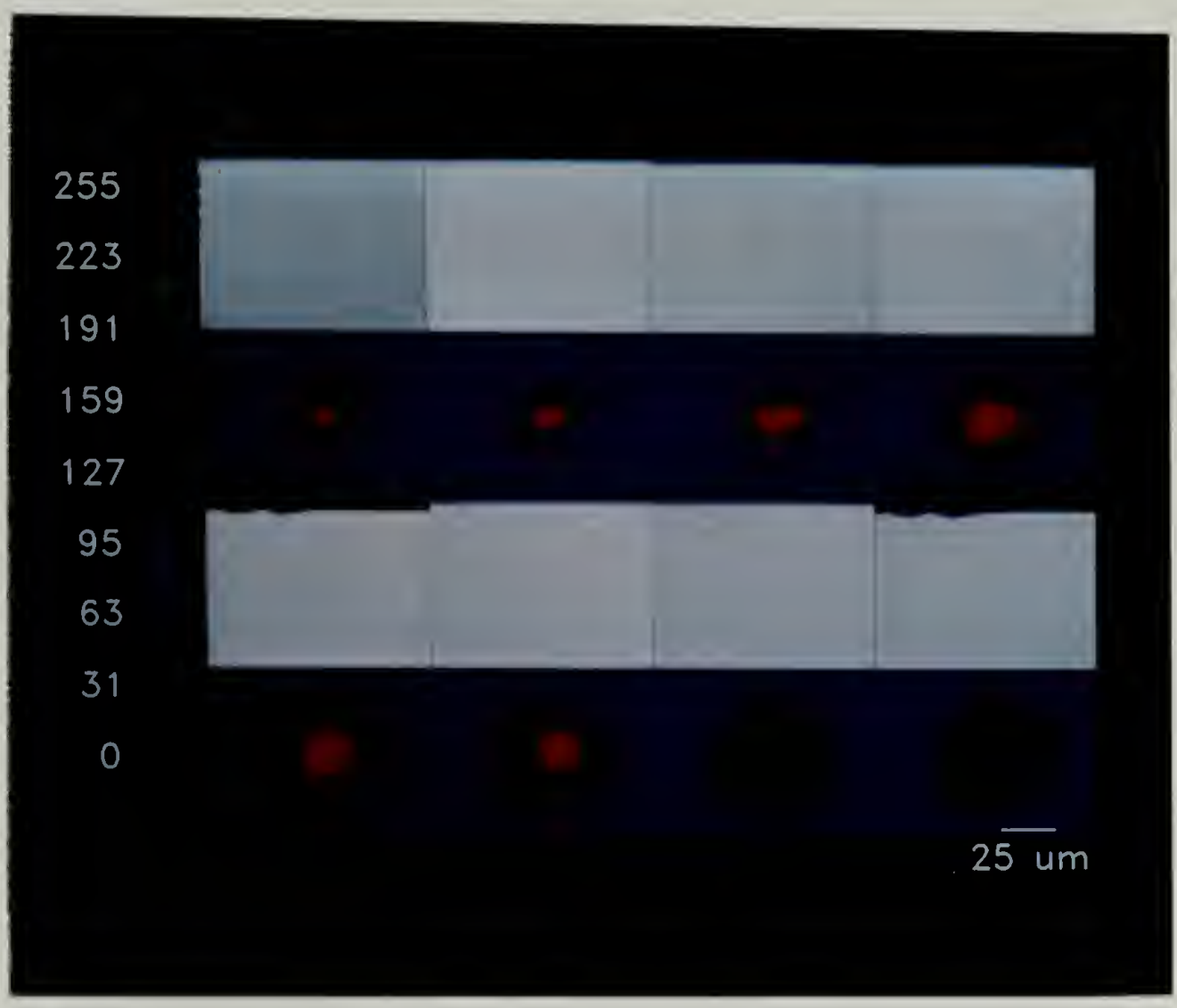

Figure 3.30 Transmitted light and fluorescence images of EYPC MLV's (1 mg/ml) in the presence of DnsPEAA-3.8% (1 mg/ml) in 50 mM phosphate, 50 mM NaCl at pH 7.4 upon acidification to pH 6.4. Images were recorded at (from left to right, top to bottom) 4.5, 5.5, 7.5, 10.5, 13.5, 15.5, 16.5, and 19.5 minutes after acidification.

(from left to right, top to bottom) 4.5, 5.5, 7.5, 10.5, 13.5, 15.5, 16.5, and 19.5 minutes respectively from the time at which acidification occurred. The vesicle that was focused on was one of the largest of the vesicle population. At 4.5 minutes, a large highly fluorescent vesicle is observed that is similar in appearance to vesicles at pH 7.4. At later stages, small particles are seen emerging from the vesicle surface. The fluorescent images show an increase in the surface area of the vesicle with no noticeable increase in the fluorescence intensity. At the 13.5 minute mark (lower right hand corner), the transmitted light images show a large increase in the number of smaller particles on the outside of the vesicle. This is accompanied by the beginning of the increase in diffusiveness of the fluorescence. At the end of the series, the transmitted light images become very faint and the fluorescent images show a lower level diffuse fluorescence.

The same behavior is seen during the interaction of DnsPEAA-2% (1 mg/ml) with EYPC vesicles (1 mg/ml) (see Figure 3.31). The photograph shows a single vesicle at 3.5, 5.5, 7.5, 9.5, 11.5, 12.5, 13.5, 15.5 (left to right, top to bottom) minutes after acidification from pH 7.4 to 6.4. There is an increase in surface area during the early stages of the reorganization with little change in fluorescence intensity followed by a period of large structural changes and diffusiveness of the fluorescence. The diffusiveness of fluorescence is more noticeable with the DnsPEAA-2% sample.

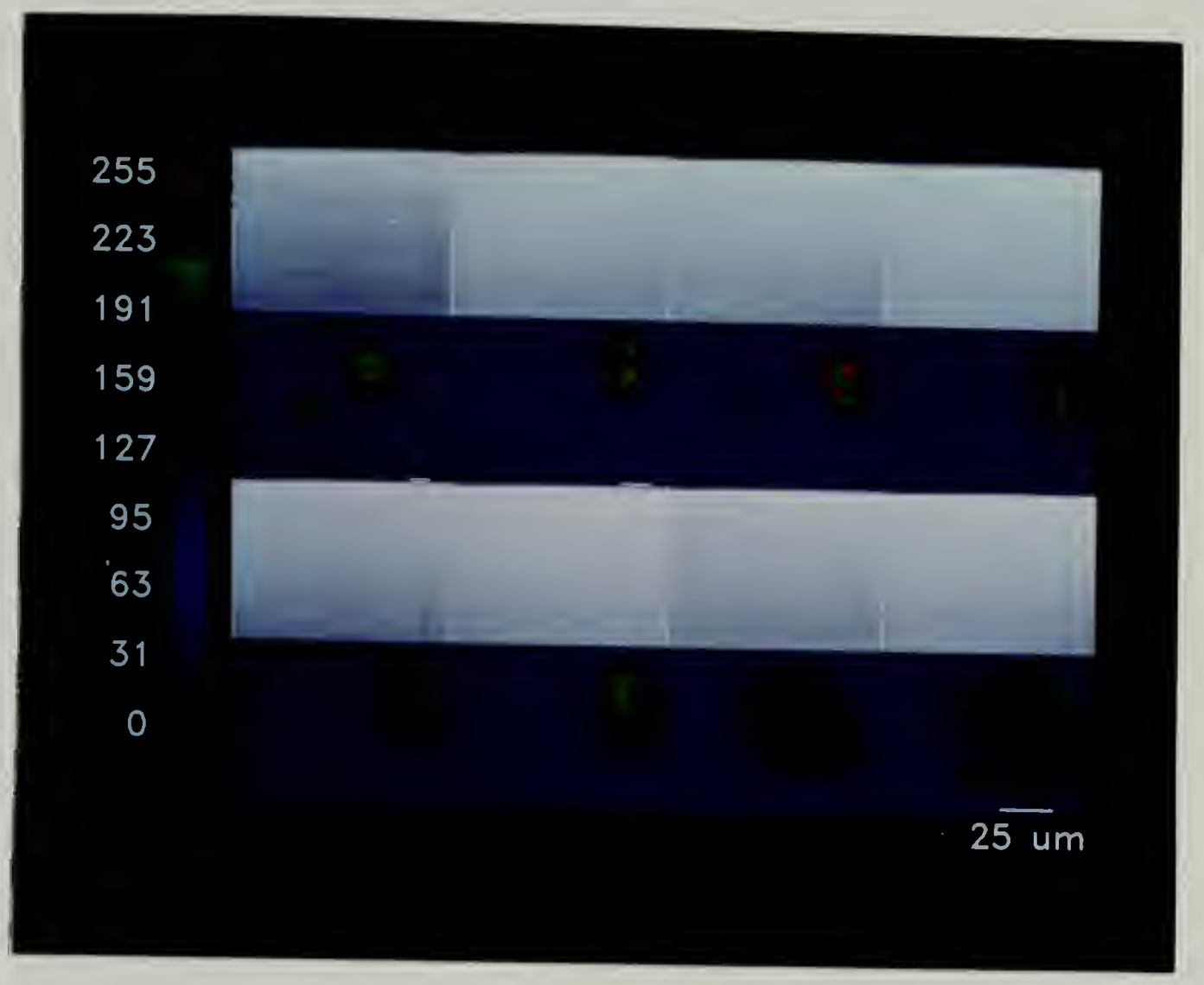

Figure 3.31 Transmitted light and fluorescence images of EYPC MLV's (1 mg/ml) in the presence of DnsPEAA-2% (1 mg/ml) in 50 mM phosphate, 50 mM NaCl at pH 7.4 upon acidification to pH 6.4. Images were recorded at (from left to right, top to bottom) 3.5, 5.5, 7.5, 9.5, 11.5, 12.5, 13.5, and 15.5 minutes after acidification.

With both samples, the major structural changes begin to occur at approximately 13 min.

The change in vesicle fluorescence agrees with the fluorescence measurements of DnsPEAA-2% in the presence of EYPC SUV's (see Figure 3.25). The fluorescence intensity of the probe increases during the association of the polymer with the vesicle and then begins to decrease as reorganization occurs.

D. Glucose-Sensitive Membrane Reorganization

1. Determination of enzyme activity

The reaction of glucose oxidase (GO) with glucose produces gluconic acid. In unbuffered or weakly buffered solutions, the gluconic acid can serve as a source of protons that will drive the conformational change of the polymer. The rate of production of gluconic acid is determined by a number of factors including the concentration and activity of the enzyme. The activity of the enzyme was determined by a modification of a colorimetric assay procedure.[121] The assay is based on the following reactions:

$$\text{Glucose} + O_2 + H_2O \xrightarrow{GO} \text{Gluconic acid} + H_2O_2$$

$$H_2O_2 + \underset{(reduced)}{\text{o-Dianisidine}} \xrightarrow{POD} \underset{(oxidized)}{\text{o-Dianisidine}} + H_2O$$

In the reaction, the enzyme peroxidase (POD) reacts with H_2O_2 in the presence of dianisidine to produce an oxidized dianisidine and water. The reduced form of dianisidine is colorless in solution while the oxidized form produces a red color. From the slope of the absorbance (500 nm) change with time, the oxidation rate of dianisidine is determined . The rate of this reaction is determined by the rate of H_2O_2 production since it is fast relative to the glucose oxidase reaction. From the data obtained, the activity of the GO can be determined. The activity of the enzyme used was calculated to be 157 units/mg (245 units/mg in oxygen saturated solutions). A unit, in this case, is defined as the activity needed to oxidize 1.0 micromole of glucose to gluconic acid in one minute at 25°C at pH 7.4.

2. Determination of Michaelis constants

For the kinetic study of the enzymatic depression of pH, it was necessary to determine whether the presence of PEAA affected the enzymatic production of gluconic acid. The Michaelis constant, equal to the substrate concentration at which the initial reaction velocity is half maximal, is fundamental to the mathematic description of enzyme kinetics. If PEAA altered the kinetic parameters of the GO reaction, the Michaelis constant should reflect those changes. The constant for GO in the presence and absence of PEAA was

determined by analyzing the initial reaction velocities of the assay reaction for the enzyme. Algebraic transformation of the Michaelis-Menten relationship can lead to more useful ways to plot experimental relationship. One transformation leads to the Lineweaver-Burk equation:

$$\frac{1}{v_o} = \frac{K_m}{V_{max}} \frac{1}{[S]} + \frac{1}{V_{max}} \qquad \text{(Eq. 3.4)}$$

where v_o, V_{max}, and [S] are the reaction velocity, maximum velocity and substrate concentration respectively. The Michaelis constant is determined readily from the x-intercept of a plot of this equation. A Lineweaver-Burk plot for the enzyme in the presence and the absence of PEAA (1 mg/ml) is displayed in Figure 3.32. The lines are coincident within experimental error. The intercepts correspond to values of K_m of 0.125M and 0.092M for the enzyme in the absence and presence of PEAA respectively. This value agrees with the K_m for GO obtained by Gibson of 0.11M. [122] From this result it follows that PEAA does not affect the reactivity of the enzyme.

3. Kinetics of enzymatic pH depression

In unbuffered solutions, the pH of solutions containing both glucose and GO will drop due to the production of gluconic acid. The rate of production of gluconic acid will depend upon the temperature, concentration of glucose,

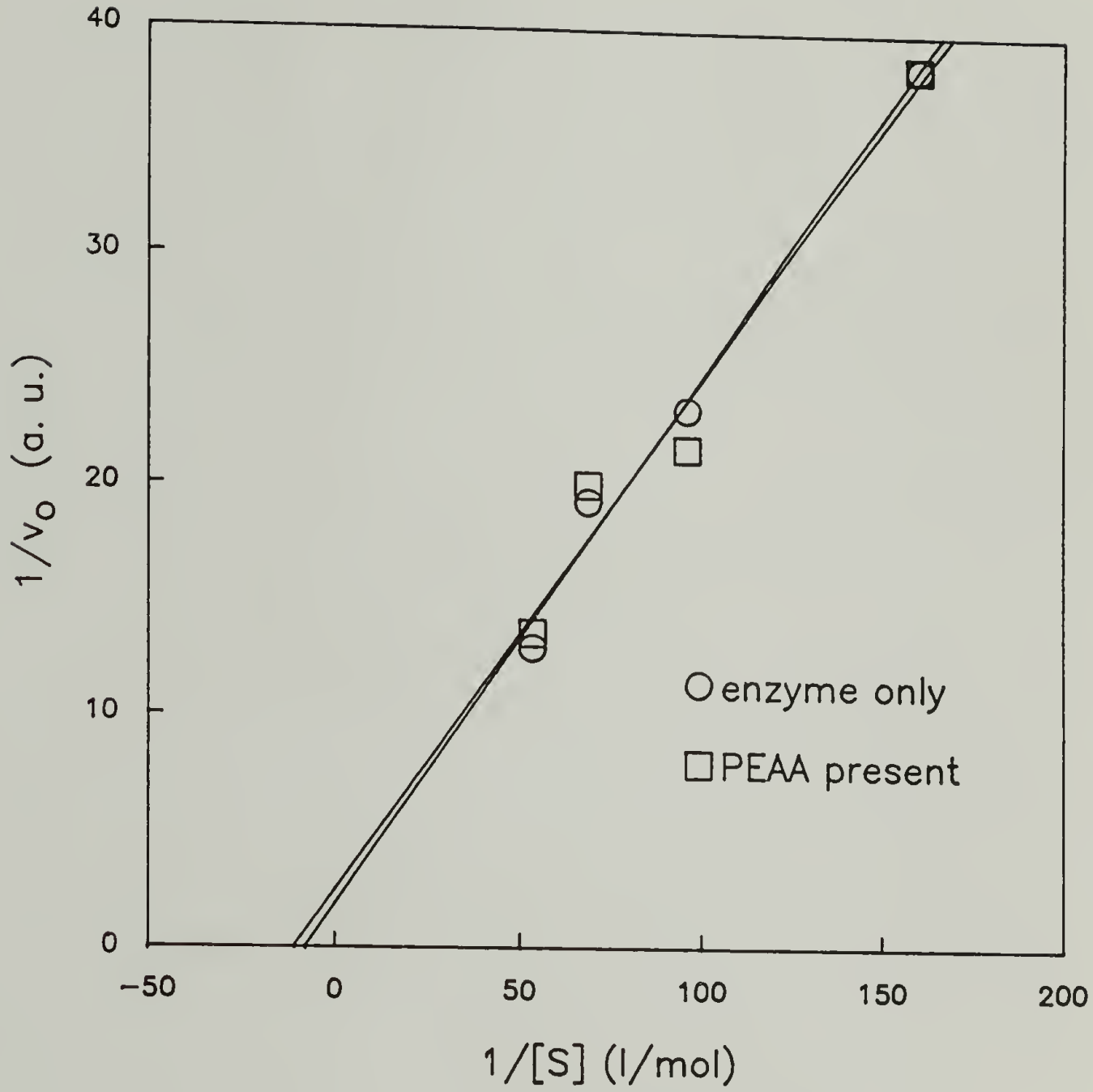

Figure 3.32 Determination of Michaelis constant for GO in the presence (□) and absence (O) of PEAA (1 mg/ml). Measurements were performed at 25°C in phosphate buffer (100 mM) at pH 7.4.

concentration of GO, pH of the solution, and the concentration of oxygen. The effects of some of these parameters were examined by systematic variation. The effect of glucose concentration and oxygen concentration can be seen in Figure 3.33. Addition of glucose at a concentration of 100 mg% (1 mg/ml, 5.6 mM) to a solution of GO (0.125 mg/ml) results in a smooth decrease in the pH of the solution. This concentration of glucose was chosen because it represents the normal concentration of glucose found in the blood of non-diabetic humans.[123] Doubling the glucose concentration to 200 mg% while keeping the concentration of GO at 0.125 mg/ml results in only a small increase in the rate of pH depression due to the logarithmic dependence of pH on the concentration of protons. However, oxygenation of the solution (30 min) results in a significant increase in the rate. From the pH equation in Eq.3.5, one can determine the rate of

$$pH = -\log[H^+] \qquad \text{(Eq. 3.5)}$$

proton production. Figure 3.34 shows the results of that calculation for the data in Figure 3.33. In the cases of 100 mg% glucose and 200 mg% glucose, the rates of the proton production were 1.13×10^{-10} and 1.52×10^{-10} mol/min respectively. This is surprising because the glucose concentrations (5.6 mM and 11.1 mM) are at or below the K_m for the enzyme. The rate of glucose turnover in this concentration range should be linear with concentration so

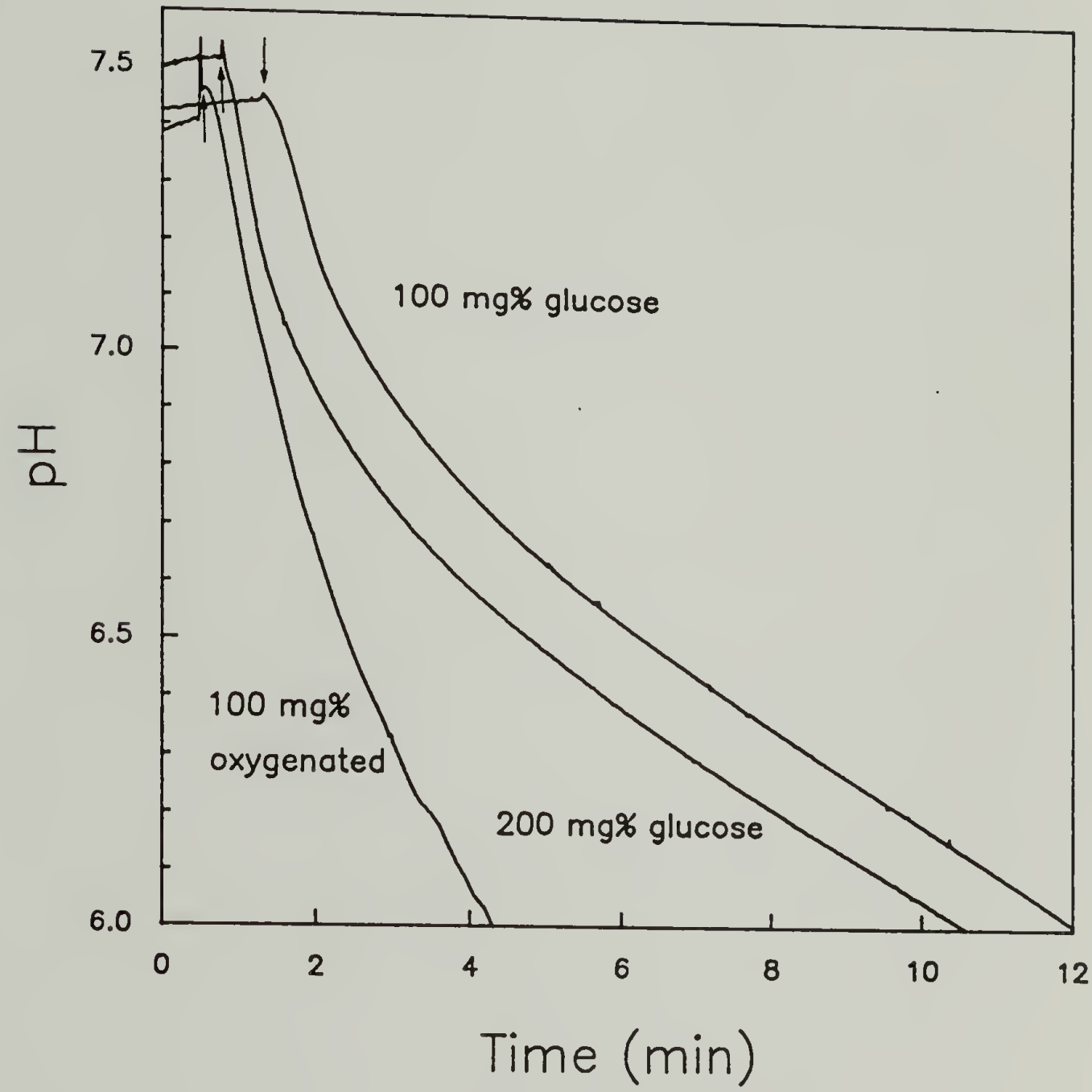

Figure 3.33 Change in pH of GO solutions (0.125 mg/ml) in 100 mM NaCl upon addition of glucose (indicated by arrows) at the concentrations indicated. Oxygen was passed through the oxygenated sample for 30 min prior to glucose addition.

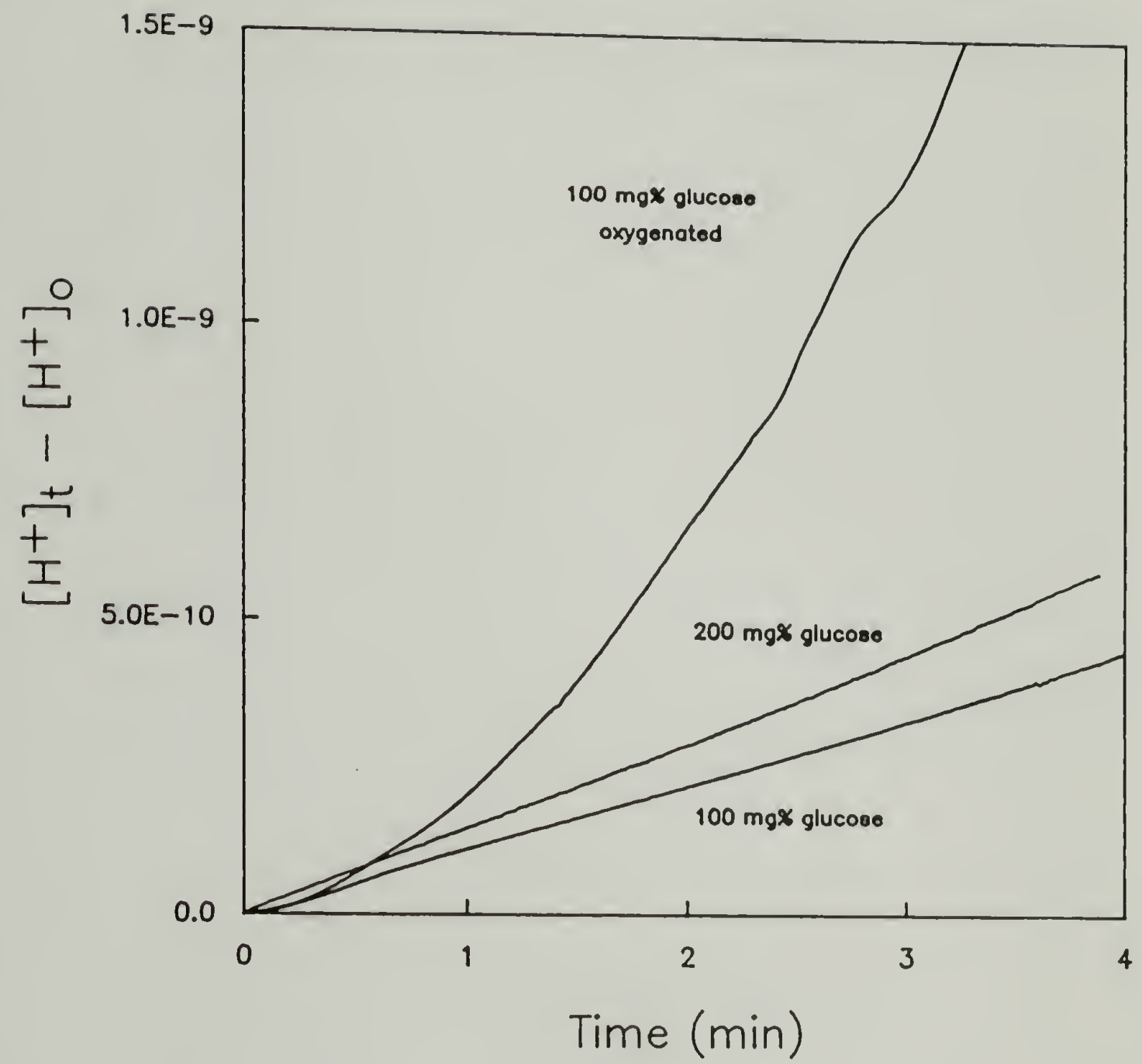

Figure 3.34 Increase in the concentration of protons of GO solutions (0.125 mg/ml) in 100 mM phosphate upon addition of glucose at the concentrations indicated. Oxygen was passed through the oxygenated sample for 30 min prior to glucose addition.

doubling the amount of glucose should double the rate of output of protons. Instead, the concentration of glucose appears to be higher than K_m or closer to the saturation point. It has been argued that the Michaelis treatment of enzyme kinetics is not valid for glucose oxidase except at high oxygen tensions since the treatment assumes the enzyme acts on one substrate[124,125]. Glucose oxidase reacts with two substrates, glucose and oxygen. Thus, the enzyme may be saturated at these glucose concentrations. Saturation of the solution with oxygen results in a large increase in the rate of proton production. The average slope of the line is 4.77×10^{-10} mol/min corresponding to a 4.2 fold increase over that of the non-oxygenated sample. Closer examination of the line reveals that the slope increases with time, consistent with the fact that the rate of glucose oxidation increases with decreasing pH down to pH 5.1 for GO.[126]

Figure 3.35 shows the effect of increasing the GO concentration from 0.125 mg/ml to 0.250 mg/ml and keeping the glucose concentration at 100 mg%. Analysis of the data shows the rate of proton production to be 1.3×10^{-10} mol/min for this system. The near doubling of the rate is to be expected since twice as many reactive sites were present.

The presence of vesicles should not affect the rate of pH drop since vesicles should not interfere with the turnover of the enzyme and the lipids should not absorb any protons produced in this pH range. There appears to indeed be no effect until lower pH values(see Figure 3.36).

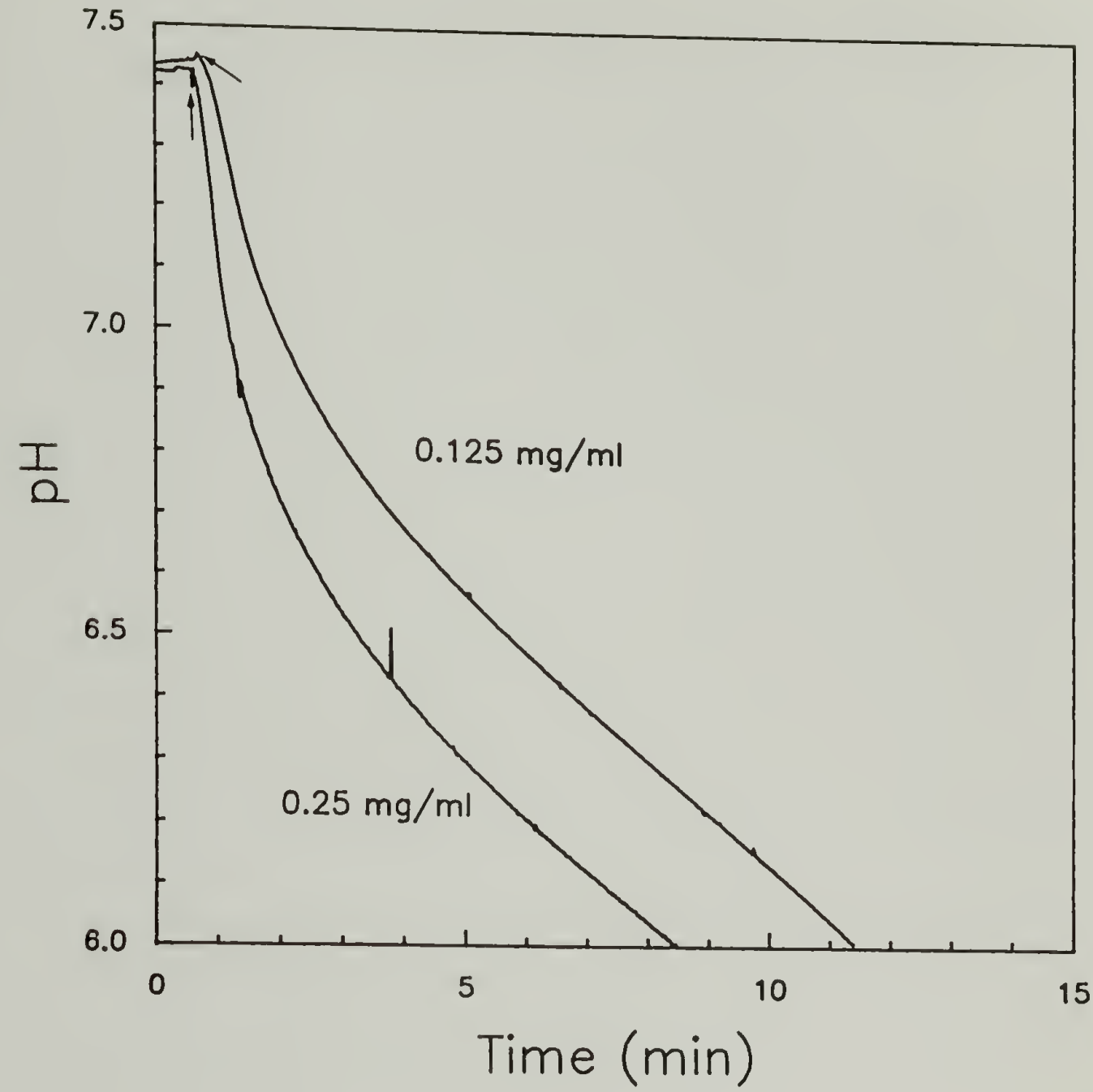

Figure 3.35 Effect of GO concentration on the decrease of pH in 100 mM NaCl upon addition of glucose (indicated by arrows) at a concentration of 100 mg%.

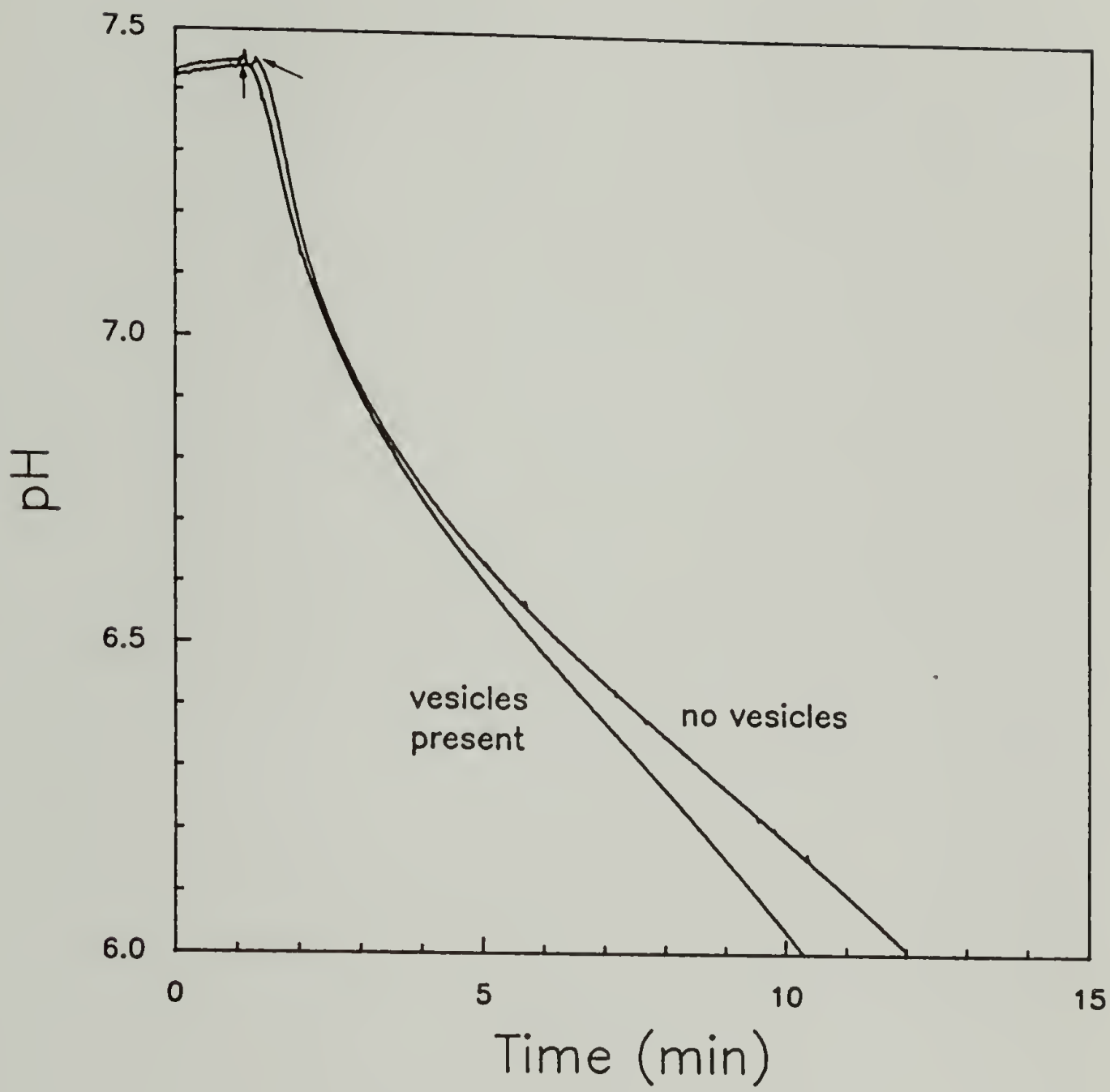

Figure 3.36 Effect of EYPC MLV's on the decrease of pH in GO solutions (0.125 mg/ml) in 100 mM NaCl upon addition of glucose (indicated by arrows) at a concentration of 100 mg%.

Addition of PEAA does not affect the reactivity of the enzyme as was shown earlier. However, the polymer does absorb protons in this pH range as shown by potentiometric titration and therfore, acts as a buffer. The effect of adding PEAA (1 mg/ml) is shown in Figure 3.37. There is a significant decrease in the rate of pH drop by the addition of PEAA. The rate of production of protons that are not absorbed by PEAA was calculated to be 4.6×10^{-12} mol/min. Comparison of this rate with that obtained in the absence of the polymer (1.13×10^{-10}) indicates that PEAA absorbs a large majority of the protons produced. Doubling the glucose concentration results in a modest increase in rate of pH depression. Decreasing the PEAA concentration by a factor of two to (0.5 mg/ml) decreases the buffering capacity which expedites the rate of pH drop (see Figure 3.38). The rate of 'free' proton production was calculated to be 1.2×10^{-11} mol/min. Increasing the enzyme concentration and oxygen concentration in the presence of PEAA produces a similar effect as with the absence of PEAA (see Figure 3.39 and Figure 3.40). The presence of EYPC vesicles does not affect the pH depression as expected (see Figure 3.41).

4. Kinetics of dye release

The acidification of calcein-loaded EYPC SUV's in the presence of PEAA was shown to produce a rapid and quantitative release of the dye. Using glucose and GO, it

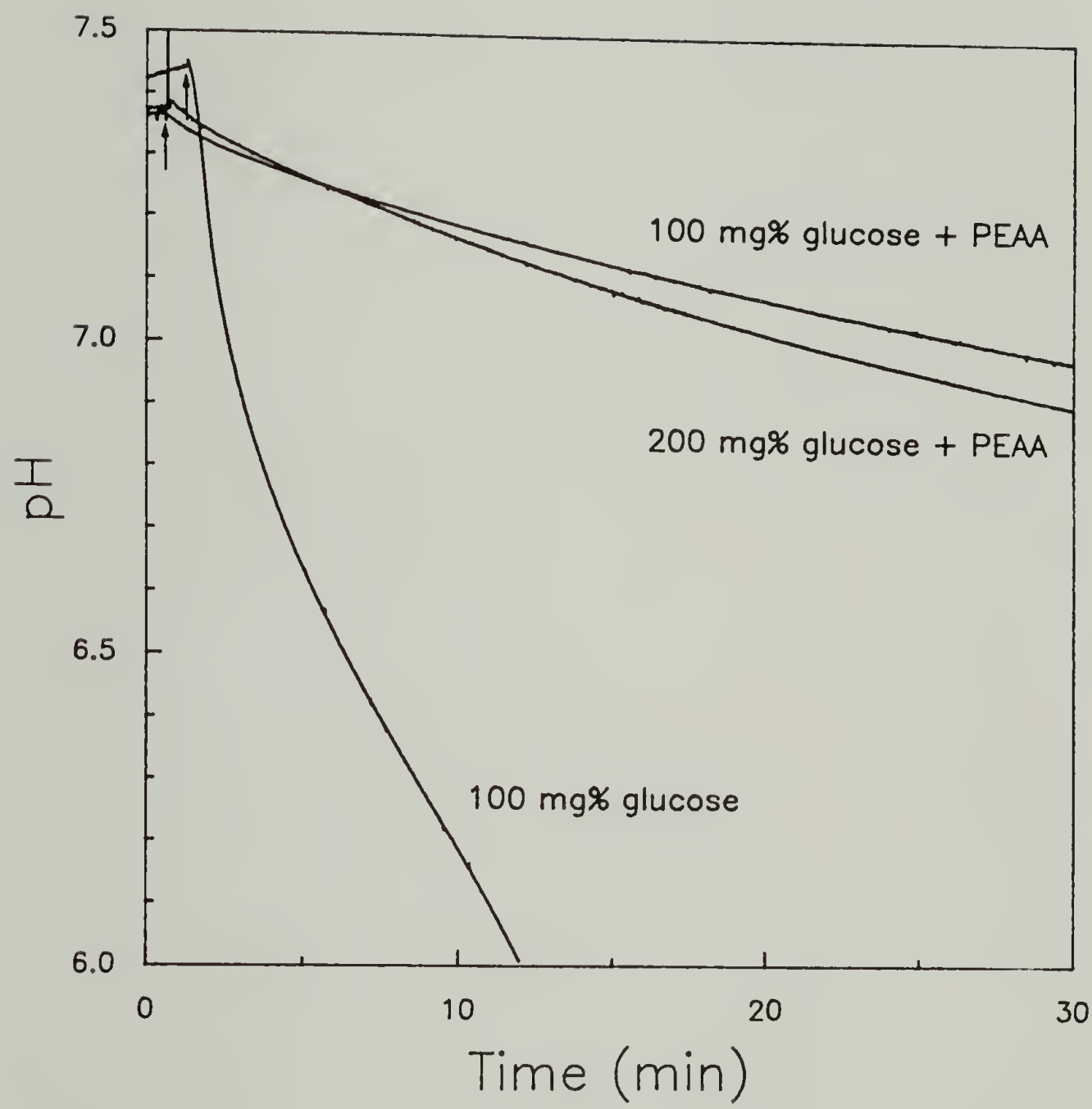

Figure 3.37 Effect of PEAA (1 mg/ml) on the decrease of pH of GO solutions (0.125 mg/ml) in 100 mM NaCl upon addition of glucose (indicated by arrows) at the concentration indicated.

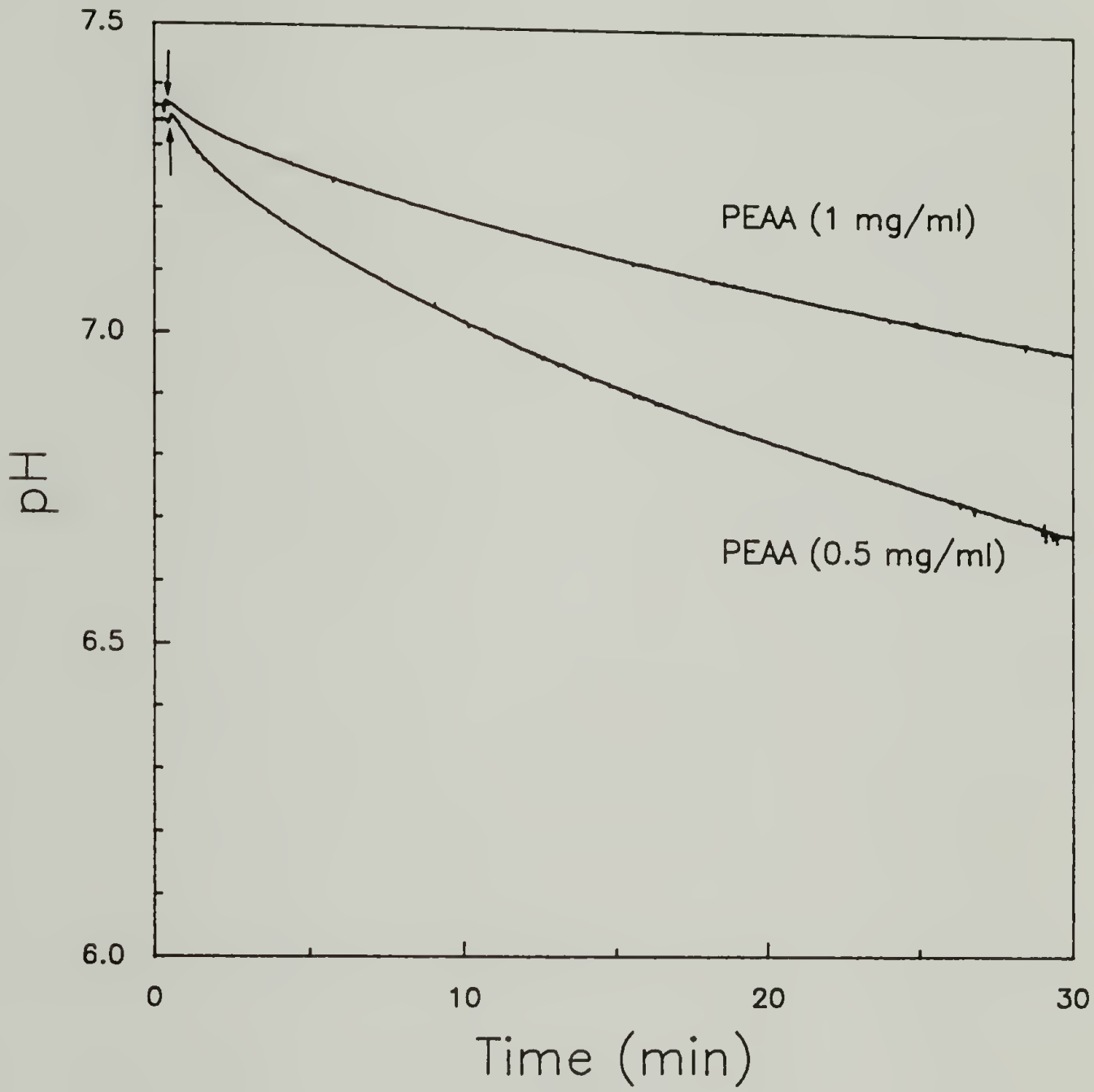

Figure 3.38 Effect of PEAA concentration on the decrease of pH of GO solutions (0.125 mg/ml) in 100 mM NaCl upon addition of glucose (indicated by arrows) at the concentration of 100 mg%.

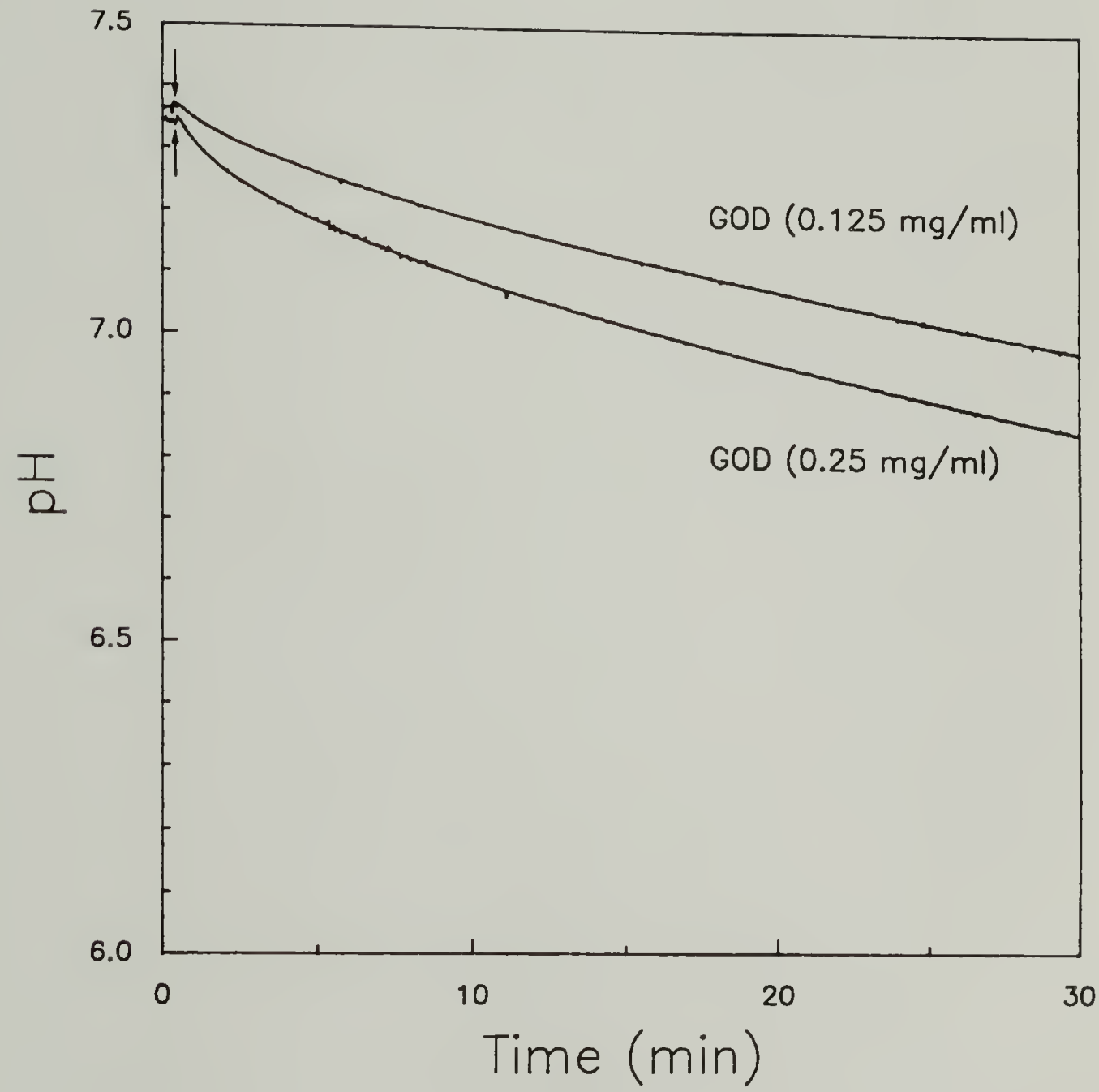

Figure 3.39 Effect of GO concentration on the decrease of pH of PEAA solutions (1 mg/ml) in 100 mM NaCl upon addition of glucose (indicated by arrows) at the concentration of 100 mg%.

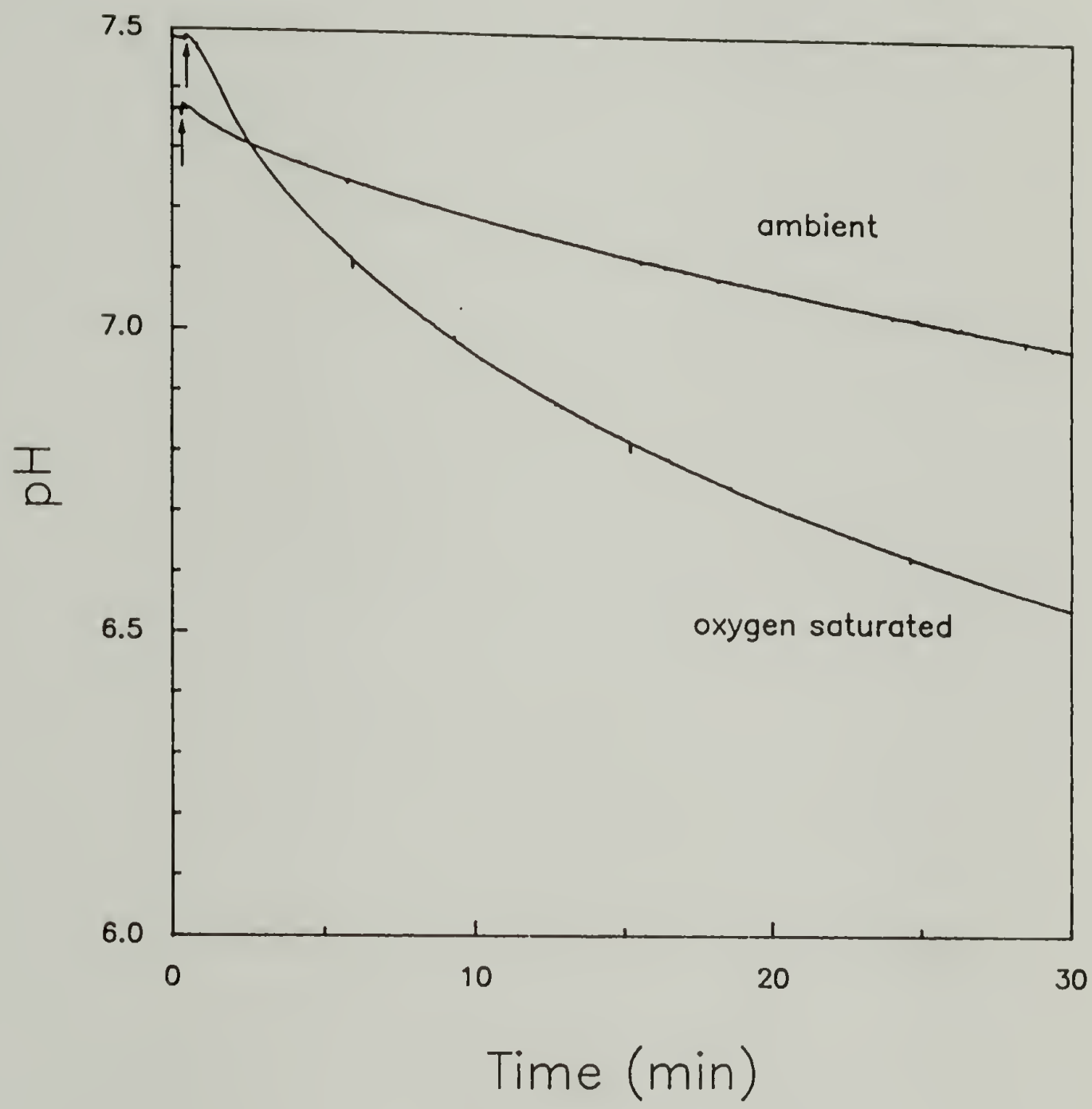

Figure 3.40 Effect of oxygen concentration on the decrease of pH of GO solutions (0.125 mg/ml) in the presence of PEAA (1 mg/ml) in 100 mM NaCl upon addition of glucose (indicated by arrows) at the concentration of 100 mg%.

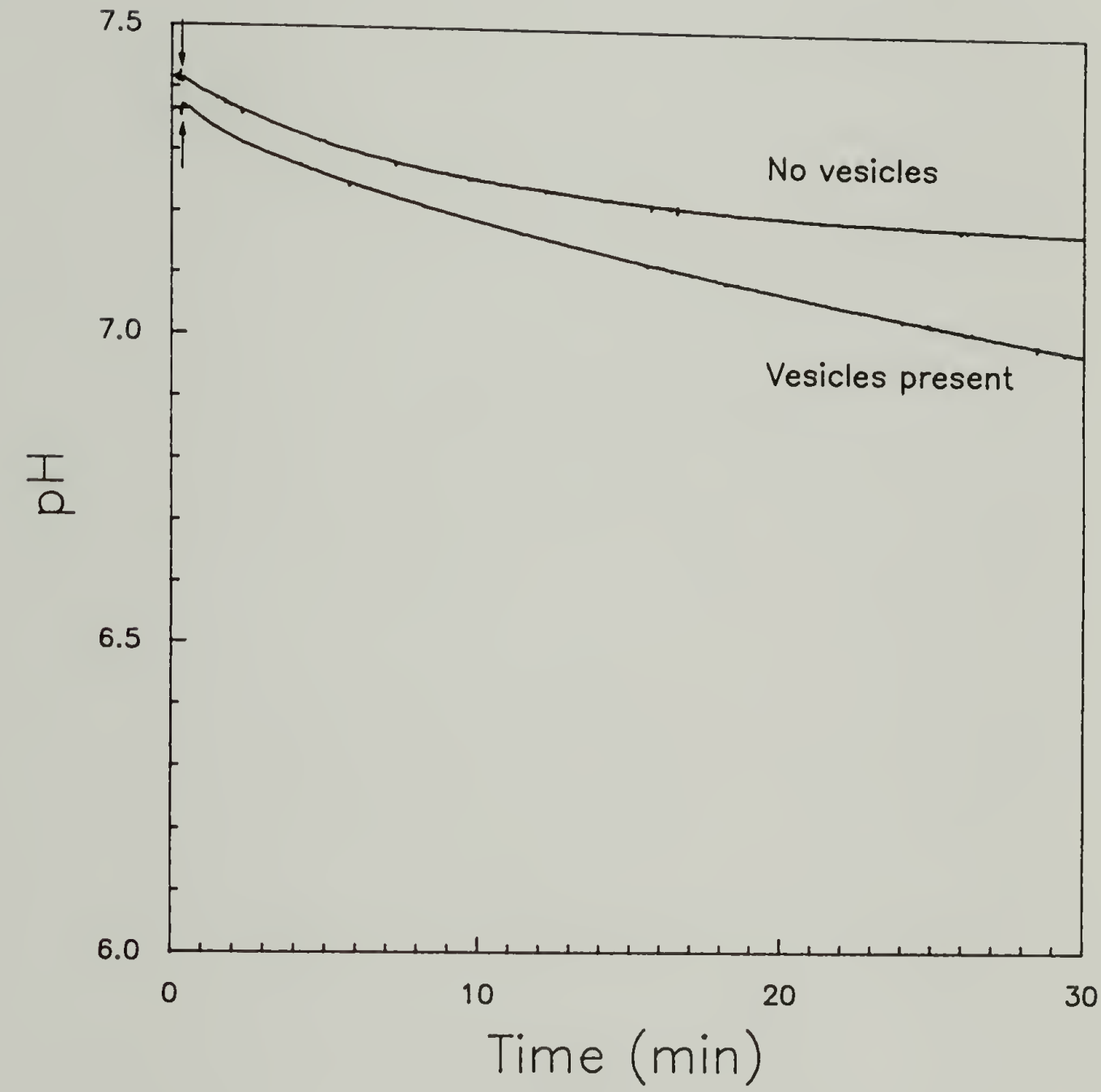

Figure 3.41 Effect of EYPC MLV's on the decrease of pH of GO solutions (0.125 mg/ml) in the presence of PEAA (1 mg/ml) in 100 mM NaCl upon addition of glucose (indicated by arrows) at the concentration of 100 mg%.

should be possible to produce a similar release of calcein. Additionally, the enzyme system provides a means to lower the pH in a slow continuous manner. Examining the dye release in this way should provide additional information on the response of the permeability of the membrane. In Figures 3.42 through 3.46, the release behavior of EYPC SUV's with entrapped calcein in the presence of PEAA is compared to the pH behavior of the GO/glucose systems just discussed. In each case, the membrane starts to become permeable as the pH drops to approximately 7.15. The increased permeability at this pH may result from using SUV's. SUV's, being smaller than MLV's, possess a higher radius of curvature that makes them less stable than MLV's. As the pH decreases further, the fluorescence intensity rises more rapidly. The rate of increase in fluorescence due to the release of calcein increases rapidly at approximately pH 7.0 which coincides closely to the critical pH for structural reorganization. From the data, it can be seen that a large degree of temporal control of dye release can be obtained through changes in the concentrations of glucose, GO, PEAA and oxygen in solution.

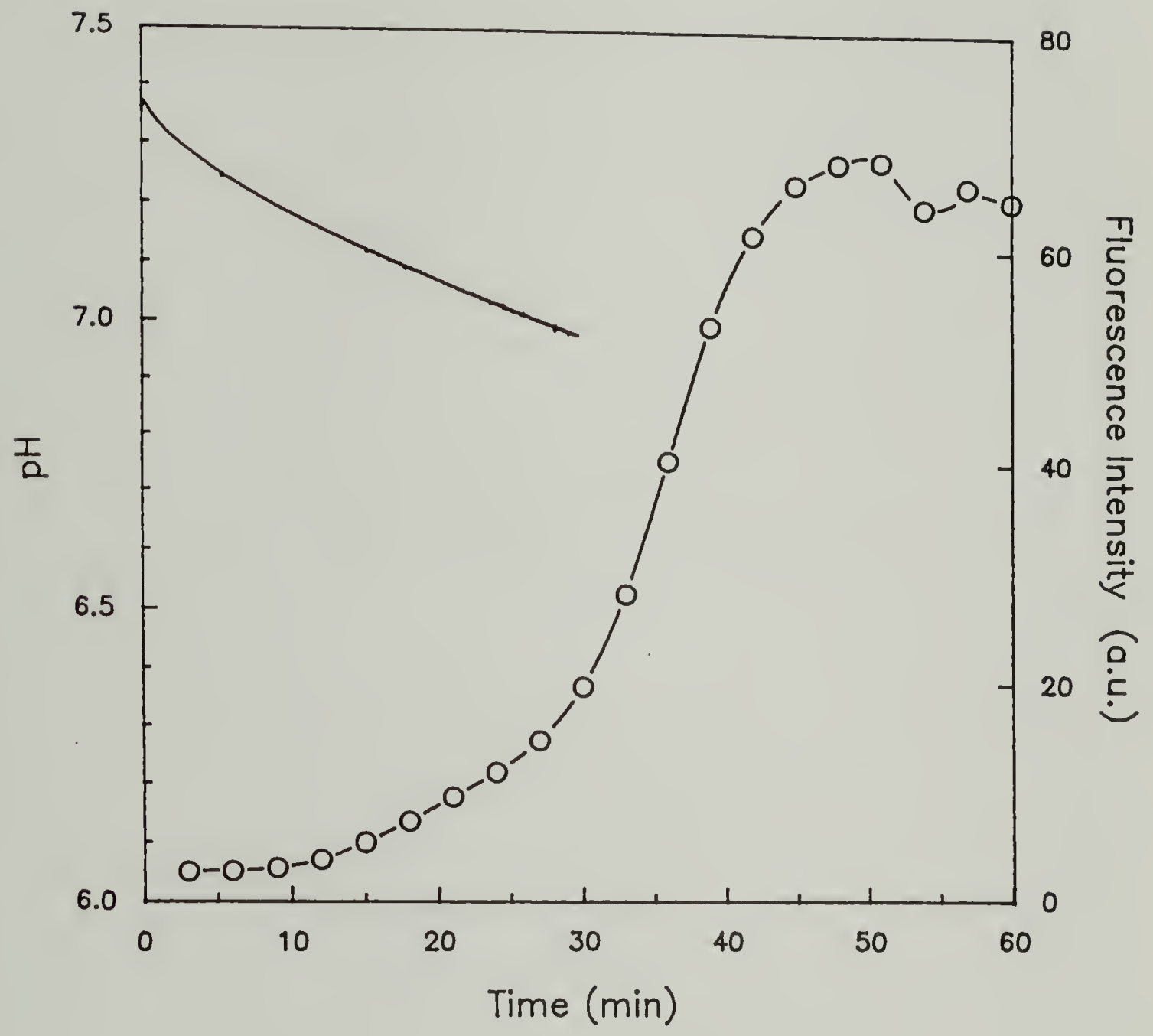

Figure 3.42 Comparison of the decrease in pH (solid line) with the dye release (O) in GO solutions (0.125 mg/ml) in the presence of PEAA (1 mg/ml) upon addition of glucose at a concentration of 100 mg%. Dye release experiments were performed with calcein loaded EYPC SUV's..

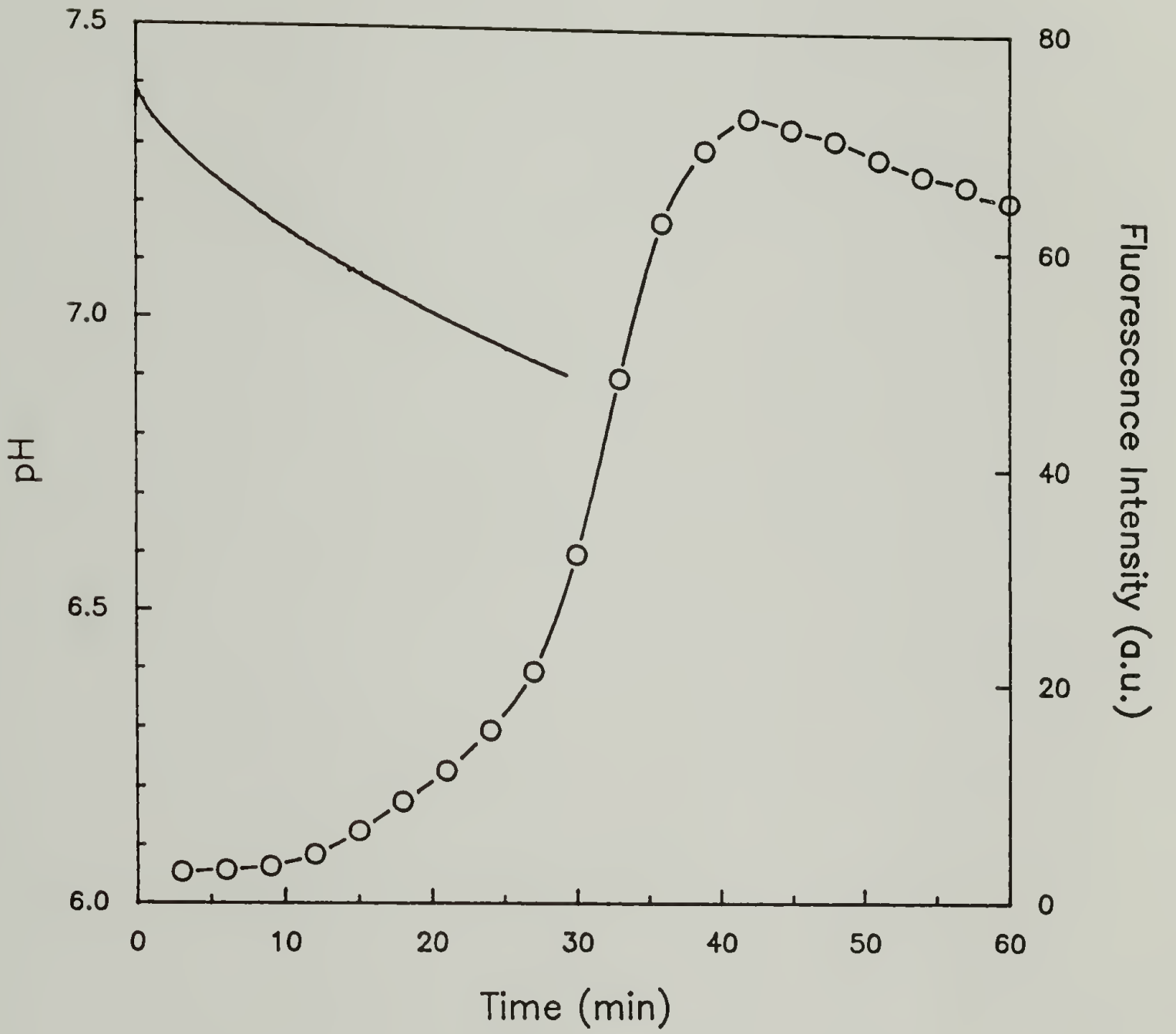

Figure 3.43 Comparison of the decrease in pH (solid line) with the dye release (O) in GO solutions (0.125 mg/ml) in the presence of PEAA (1 mg/ml) upon addition of glucose at a concentration of 200 mg%. Dye release experiments were performed with calcein loaded EYPC SUV's..

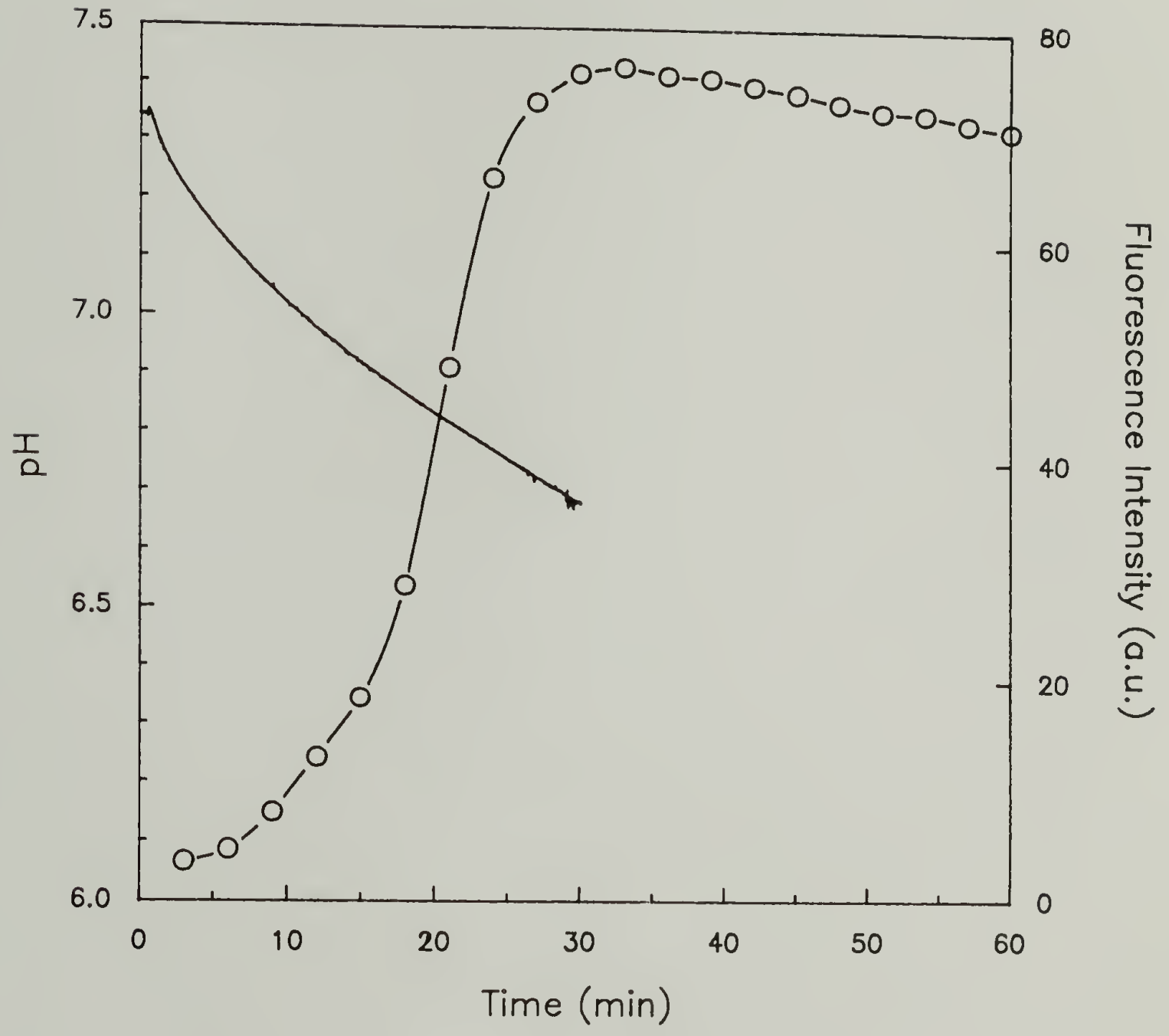

Figure 3.44 Comparison of the decrease in pH (solid line) with the dye release (O) in GO solutions (0.125 mg/ml) in the presence of PEAA (0.5 mg/ml) upon addition of glucose at a concentration of 100 mg%. Dye release experiments were performed with calcein loaded EYPC SUV's..

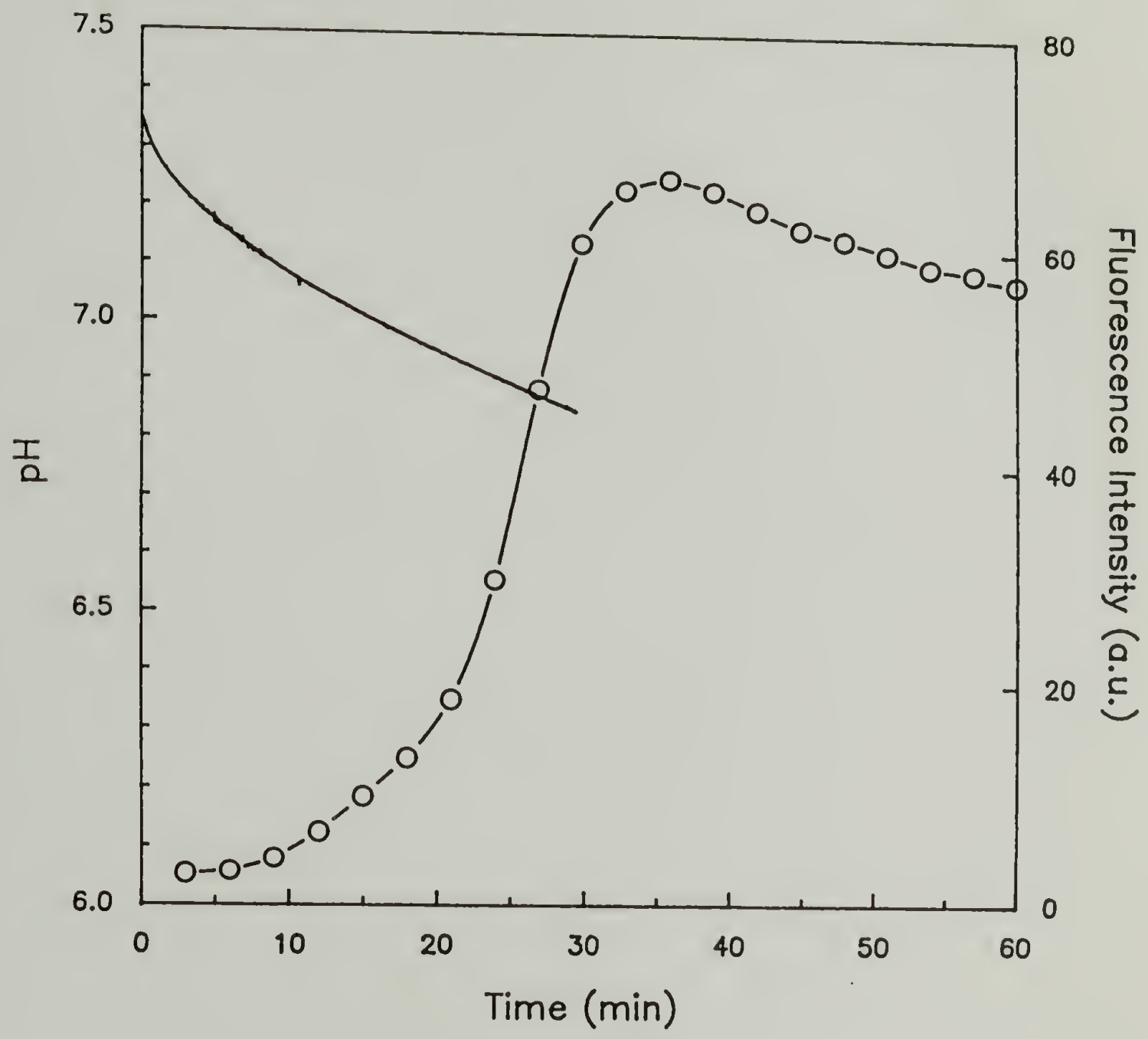

Figure 3.45 Comparison of the decrease in pH (solid line) with the dye release (O) in GO solutions (0.250 mg/ml) in the presence of PEAA (1 mg/ml) upon addition of glucose at a concentration of 100 mg%. Dye release experiments were performed with calcein loaded EYPC SUV's..

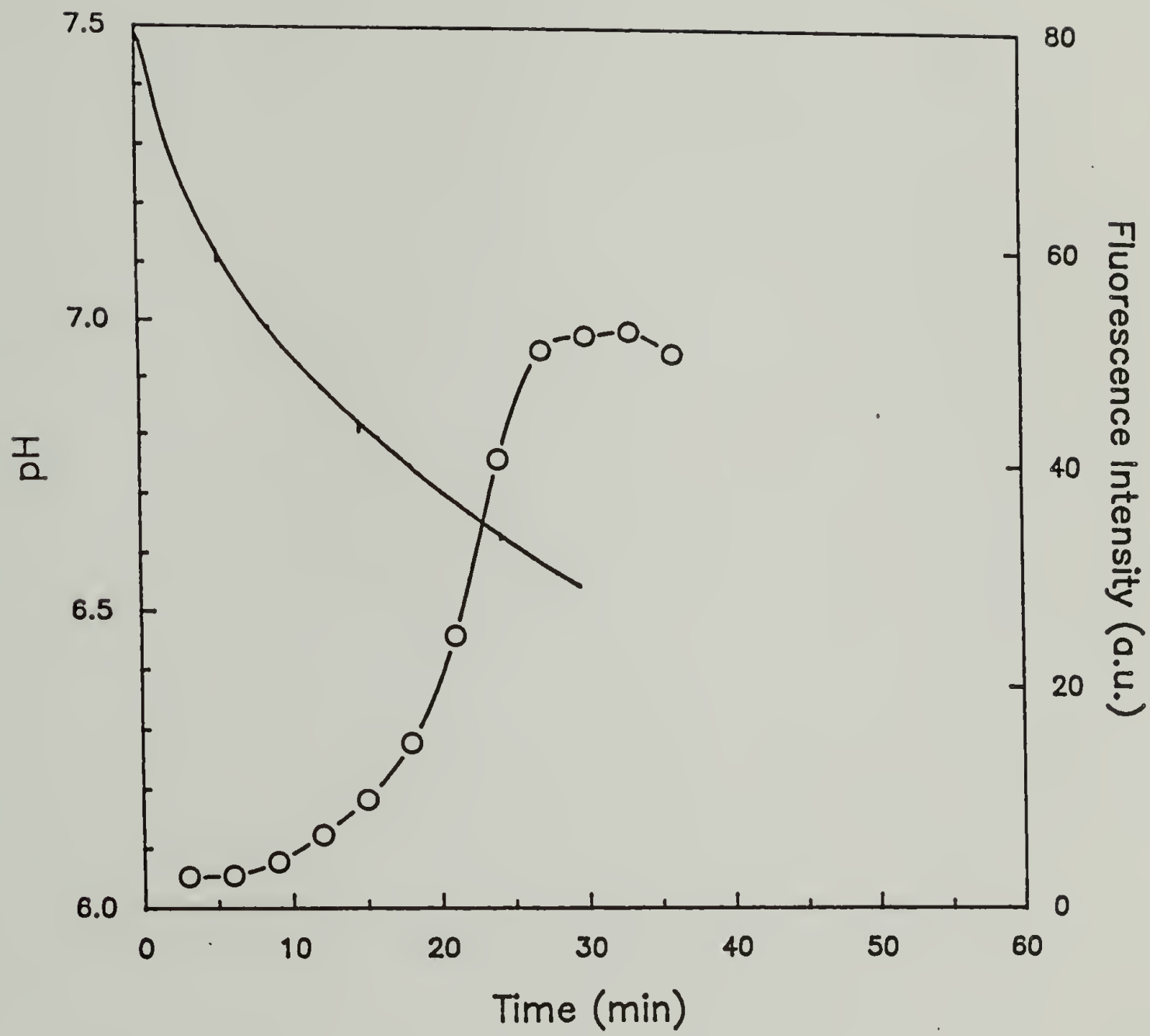

Figure 3.46 Comparison of the decrease in pH (solid line) with the dye release (O) in oxygenated GO solutions (0.125 mg/ml) in the presence of PEAA (1 mg/ml) upon addition of glucose at a concentration of 100 mg%. Dye release experiments were performed with calcein loaded EYPC SUV's..

E. Conclusions

The kinetics of the structural reorganization of phospholipid vesicles induced by the conformational transition of PEAA were examined by following changes in the turbidity of vesicle supensions. Reorganization of phosphatidylcholine vesicles was found to be temperature sensitive. Below the phase transition of the lipid, no reorganization was observed to occur. However, the rate of reorganization was found to be at a maximum at the phase transition temperature due to the presence of defects in the lipid bilayer at this temperature.

The process was found to be sensitive to the pH of the solution. Reorganization of DPPC vesicles was found to occur slowly above a 'critical' pH, and to increase in rate with decreasing pH below the 'critical' pH. The critical pH coincides with the pH of the onset of the conformational transition for PEAA as measured by potentiometric titration.

The reorganization was found to be affected by the state of the bilayer. Vesicles composed of different lipids exhibited different rates of reorganization as well as different pH and temperature dependences of the rate. Binary mixtures of lipids in the bilayer that introduce phase boundaries or defects cause the bilayers to disrupt faster. Conversely, incorporation of bilayer-stabilizing agents can prevent the reorganization from occurring.

Comparisons of dye release with optical density behavior of multilamellar vesicles revealed that PEAA induces

permeability of the membrane before it solubilizes the membrane.

Examination of the fluorescence behavior of PEAA labeled with dansyl groups showed that in solutions above pH 6.8, the polarity of the environment around the polymer chain is similar to the polarity of water. As the pH is decreased, the polarity of the environment near the chain decreases. Using the dansyl labeled PEAA, the reorganization process was visualized under a fluorescence microscope. Vesicles appeared highly fluorescent at pH values up to pH 10.0 indicating that PEAA associates with the vesicles at these pH values. As the pH was decreased, vesicle reorganization was viewed as a breakup of the vesicular structure into many smaller particles with a diffusion of the fluorescence.

The structure and integrity of EYPC vesicles were sensitized to the presence of glucose by addition of the enzyme, glucose oxidase. The rate of pH depression could be controlled by adjusting glucose, enzyme, PEAA and oxygen concentration and was found to be most sensitive to changes in PEAA and oxygen concentration. Using the glucose oxidase-glucose system, the release kinetics from SUV's could be controlled.

REFERENCES

1. Fendler, J.H., Membrane Mimetic Chemistry, John Wiley & Sons, New York, 1982, pp. 3-5.

2. Bangham, A.D., *Prog. Biophys. Mol. Biol.*, **18**, 29 (1968).

3. Tyrrell, D.A.; Heath, T.D.; Colley, C.M.; Ryman, B.E., *Biochim. Biophys. Acta*, **457**, 259 (1976).

4. Chapman, D. in: Membrane Structure and Function, John Wiley, New York, 1980 pp. 103-152.

5. Quinn, P.J.; Chapman, D., *CRC Crit. Rev. Biochem.*, **8**, 1-117 (1980).

6. Bangham, A.D.; Standish, N.M.; Watkins, J.C., *J. Mol. Biol.*, **13**, 238 (1965).

7. Israelachvili, J.N., Intermolecular and Surfaces Forces, Academic Press: New York, 1985 pp. 229-275.

8. Bangham A.; Horne R.W., *J.Mol.Biol.*, **8**, 386, (1964).

9. Bangham, A., *Chem. Phys. Lipids*, **8**, 237 (1972).

10. Wickner, W., *Ann. Rev. Biochem.*, **48**, 23 (1979).

11. Huang, C., *Biochemistry*, **8**, 344 (1969).

12. Mabrey-Gaud, S., in: Liposomes: From Physical Structure to Therapeutic Applications, C. Knight, Ed., Elsevier/North-Holland Biomedical Press: New York, 1981 pp. 105-138.

13. Gregoriadis, G., in: Drug Carriers in Biology and Medicine, Academic Press, London, 1979, pp. 287-341.

14. Fendler, J.H.; Romero, A., *Life Sci.*, **20**, 1109 (1977).

15. Finkelstein, M.C.; Weissmann, G., *J. Lipid Res.*, **19**, 289 (1978).

16. Kimelberg, H.K.; Mayhew, E., *CRC Crit. Rev. Toxicol.*, **6**, 25 (1978).

17. Ryman, B.E.; Tyrrell, D.A., *Essays Biochem.*, **16**, 49 (1980).

18. Fendler, J.H. in: Liposomes in Biological Systems, John Wiley and Sons, Chichester, 1980, pp. 87-100.

19. Trauble, H.; Haynes, D.H., *Chem. Phys. Lipids*, **7**, 324 (1971).

20. Oldfield, E.; Chapman, D., *FEBS Lett.*, **21**, 302 (1972).

21. Levine, Y.K., *Prog. Surf. Sci.*, **3**, 279 (1973).

22. Wilkinson, D.A.; Nagle, J.F., *Biochemistry*, **18**, 4244 (1979).

23. Chapman, D.; Williams, R.M.; Ladbrooke, B.D., *Chem. Phys. Lipids*, **1**, 445 (1967).

24. Phillips, M.C., *Prog. Surf. Membr. Sci.*, **5**, 139 (1972).

25. Chapman, D., *Quart. Rev. Biophys.*, **8**, 185 (1975).

26. Lee, A.G., *Prog. Biopys. Mol. Biol.*, **29**, 3 (1975).

27. Lee, A.G., *Biochim. Biophys. Acta.*, **422**, 237 (1977).

28. Lee, A.G., *Biochim. Biophys. Acta.*, **472**, 345 (1977).

29. Papahadjopoulos, D.; Kimelburg, H.K., *Prog. Surf. Sci.*, **4**, 141 (1975).

30. Mabrey, S.; Sturtevant, J.M., *Proc.Natl.Acad.Sci.*, **73(11)**, 3862 (1976).

31. Shimshick, E.; McConnell, H., *Biochemistry*,**12**, 2351, (1973).

32. Galla, H.; Sackmann, E., *J.Membr.Biol.*, **48**, 215, (1979).

33. Jacobson, K.; Papahadjopoulos, D., *Biochemistry*, **14**, 152, (1975).

34. Hackenbrock, C.; Hochli, M.; Chau, R., *Biochim.Biophys.Acta.*, **455**, 466, (1976).

35. Israelachvili, J.N.; Mitchell, J.; Ninham, B., *J. Chem. Soc. Faraday Trans.II*, **72**, 1525 (1976).

36. Mandersloot, J.; Reman, F.; VanDeenen,L.; DeGier, J., *Biochim.Biophys.Acta.*, **382**, 22, (1975).

37. Mabrey, S.; Mateo, P.; Sturtevant, J., *Biochemistry*, **17**, 2464, (1978).

38. Katchalsky, A., *J. Polym. Sci.*, **7**, 393 (1951).

39. Katchalsky, A.; Eisenberg, H., *J. Polym. Sci.*, **6**, 145 (1951).

40. Arnold, R., *J. Colloid Sci.*, **12**, 549 (1957).

41. Leyte, J.; Mandel, M., *J. Polym. Sci., Pt. A*, **2**, 1879 (1964).

42. Anufrieva, E.; Birnstein, T.; Nekrasova, T.; Ptitsyn, O.; Sheveleva, T., *J. Polym. Sci., Pt. C*, **16**, 3519 (1968).

43. Lando, J.; Koenig, J.; Semen, J., *J. Macromol. Sci., Phys.*, **B7**, 319 (1973).

44. Cutnell, J.; Glasel, J., *Macromolecules*, **9**, 71 (1976).

45. Crescenzi, V.; Quadrifoglio, F.; Delben, F., *J. Polym. Sci., Pt. A2*, **10**, 357 (1972).

46. Schaefer, J., *Macromolecules*, **4**, 98 (1971).

47. Nagasawa, M., *Pure Appl. Chem.*, **26**, 519 (1971).

48. Crescenzi, V., *Adv. Polym. Sci.*, **5**, 358 (1968).

49. Braud, C.; Muller, G.; Fenyo, J.; Selegny, E., *J. Polym. Sci. Polym. Chem. Ed.*, **12**, 2767 (1974).

50. Conio, G.; Patrone, E.; Russo, S.; Trefiletti, V., *Makromol. Chem.*, **177**, 49 (1976).

51. Chu, D.; Thomas, J., *Macromolecules*, **17**, 2412 (1984).

52. Sugai, S.; Nitta, K.; Ohno, N.; Nakano, H., *Colloid and Polym. Sci.*, **261**, 159 (1983).

53. Joyce, D.E.; Kurucsev, T., *Polymer*, **22**, 415 (1981).

54. Fichtner, F.; Schonert, H., *Colloid and Polym. Sci.*, **255**, 230 (1977).

55. Borden, K., Ph.D. Thesis, University of Massachusetts, 1989.

56. Schroeder, U.; Tirrell, D., *Macromolecules*, **22**, 765 (1989).

57. Borden, K.; Eum, K.; Langley, K.; Tirrell, D., *Macromolecules*, **20**, 454 (1987).

58. Eum, K., Ph.D. Thesis, University of Massachusetts, 1988.

59. Eum, K.; Langley, K.; Tirrell, D., *Macromolecules*, **22**, 2755 (1989).

60. Barone, G.; Crescenzi, V.; Pispisa, B.; Quadrifoglio, F., *J. Macromol. Chem.*, **1**, 767 (1966).

61. Barone, G.; Crescenzi, V.; Liquori, A.; Quadrifoglio, F., *J. Phys. Chem.*, **71**, 2341 (1967).

62. Meyer, K.; Kummerling, E.; Altman, L.; Iller, M.; Hoffman, S., *Cancer Res.*, **8**, 513, (1948).

63. Kahler, H.; Robertson, W., *J.Natl.Cancer Inst.(U.S.)*, **34**, 857, (1965).

64. Ellens, H.; Bentz, J.; Szoka, F., *Biochemistry*, **23**, 1532, (1984).

65. Nayer, R.; Schroit, A., *Biochemistry*, **24**, 5967, (1985)

66. Seki, K.; Tirrell, D.A., *Macromolecules*, **17**, 1692, (1984).

67. Tirrell, D.A.; Takigawa, D.Y.; Seki, K., *Ann. N.Y. Acad. Sci.*, **446**, 237, (1985).

68. Takigawa, D.Y.; Tirrell, D.A., *Macromolecules*, **18**, 338, (1985).

69. Arora, K.; Hwang, K.; Turro, N., *Macromolecules*, **19**, 2806 (1986).

70. Tall, A.R.; Small, D.M.; Deckelbaum, R.J.; Shipley, G., *J. Biol. Chem.*, **252**, 4701, (1977).

71. Carey, M.; Small, D., *Am.J.Med.*, **49**, 150 (1970).

72. Mazer, N.; Benedek, G.; Carey, M., *Biochemistry*, **19**, 601, (1980).

73. Ferritto, M.S., Ph.D. Thesis, University of Massachusetts, 1990.

74. Muller, D., *Biochem. Z.*, **199**, 136 (1928).

75. Franke, W.; Deffner, M., *Liebigs Ann.*, **541**, 117 (1939).

76. Franke, W.; Lorenz, F., *Liebigs Ann.*, **532**, 1 (1937).

77. Pazur, J.H., *Methods in Enzymology*, **9**, 82 (1966).

78. Kusai, K.; Sekuzu, I.; Hagihara, B.; Okunuki, K.; Yamauchi, S.; Nakai, M., *BBA*, **40**, 555 (1960).

79. Keilin, D.; Hartee, E.F., *Nature*, **157**, 801 (1946).

80. Bentley, R.; Neuberger, A., *Biochem. J.*, **45**, 584 (1949).

81. Keilin, D.; Hartee, E.F., *Biochem.J.*, **42**, 221 (1948).

82. Kusai, K., *Ann. Rept. Sci. Works, Fac. Sci. Osaka Univ.*, **8**, 43 (1960).

83. Cahill, G.F.; Etzweiler, D.D.; Freinkel, N., *Diabetes*, **25**, 137 (1976).

84. Chick, W.L.; Perna, J.J.; Lauris, V.; Low, D.; Galletti, P.M.; Panol, G.; Whittermore, A.D.; Like, A.A.; Colton, C.K.; Lysaght, M.J., *Science*, **197**, 780 (1977).

85. Leung, Y.F.; O'Shea, G.M.; Goosen, M.F.A.; Sun, A.M., *Art. Org.*, **7**, 208 (1983).

86. Elliot, J., *J. Am. Med. Assoc.*, **241**, 223 (1979).

87. Horbett, T.A.; Ratner, B.D.; Kost, J.; Singh, M., in: Recent Advances in Drug Delivery Systems, Plenum, New York, 1984, pp.204-220.

88. Ishihara, K.; Kobayashi, M.; Shionohara, I., *Makromol. Chem. Rapid Commun.*, **4**, 327 (1983).

89. Jeong, S.Y.; Kim, S.W.; Eenink, M.J.D.; Feijen, J., *J. Controlled Release*, **1**, 57 (1984).

90. Overberger, C.G.; O'Shaughnessy, M.T.; Shalit, H., *JACS*, **71**, 2661 (1949).

91. Ferritto, M.S.; Tirrell, D.A.; Ponticello, I.S., Macromolecular Syntheses, in press.

92. Kondo, H.; Takaki, K.; Kuroki, R.; Tada, A.; Fukumoto, K.; Sunamoto, J., *Bull. Chem. Soc. Jpn.*, **57**, 2957 (1984).

93. Chen, R.F., *Anal. Biochem.*, **25**, 412 (1968)..

94. DePecol, M.E.; McCormick, D.B., *Anal. Biochem.*, **101**, 435 (1980).

95. Mandel, M., *Eur. Polym. J.*, **6**, 807 (1970).

96. Tsong, T.Y.; Kanehisa, M.I., *Biochemistry*, **16**, 2674 (1977).

97. Pownall, H.J.; Massey, J.B.; Kusserow, S.K.; Gotto, A.M., Jr., *Biochemistry*, **17**, 1183 (1978).

98. Tall, A.R.; Shipley, G.G.; Small, D.M., *J. Biol. Chem.*, **251**, 3749 (1976).

99. Gwynne, J.; Brewer, H.B., Jr.; Edelhoch, H., *J. Biol. Chem.*, **250**, 2269 (1975).

100. Gwynne, J.; Brewer, H.B., Jr.; Edelhoch, H., *J. Biol. Chem.*, **219**, 1411 (1974).

101. Assman, G.; Brewer, H.B., Jr., *Proc. Natl. Acad. Sci. U.S.A.*, **71**, 989 (1974).

102. Marsh, D.; Watts, A.; Knowles, P.F., *Biochemistry*, **15**, 3570 (1976).

103. Carnie, S.; Israelachvili, J.N.; Pailthorpe, B.A., *Biochim. Biophys. Acta*, **554**, 340 (1979).

104. Hayden, D.A.; Taylor, J., *J. Theor. Biol.*, **4**, 281 (1963).

105. Lucy, J.A., *Nature*, **227**, 815 (1970).

106. Dekruijff, B.; van der Besselaar, A.M.H.P.; van Deenan, L.L.M. *Biochim. Biophys. Acta*, **465**, 443 (1977).

107. Hauser, H.; Barret, M.D., *Biochem. Biophys. Res. Commun.*, **53**, 399 (1973).

108. Phillips, M.C.; Williams, R.N.; Chapman, D., *Chem. Phys. Lipids*, **3**, 234 (1969).

109. Morris, D.A.N.; McNeil, R.; Castellino, F.J.; Thomas, J.K., *Biochim. Biophys. Acta*, **599**, 380 (1980).

110. Rand, R.P.; Panghorn, W.A.; Purdon, A.D.; Tinker, D.O., *Can. J. Biochem.*, **53**, 189 (1975).

111. Kleemann, W.; McConnell, H.M., *Biochim. Biophys. Acta.*, **419**, 206 (1976).

112. Shimshick, E.J.; McConnell, H.M., *Biochem. Biophys. Res. Commun.*, **53**, 446 (1973).

113. Pownall, H.J.; Van Winkle, W.B.; Pao, Q.; Rhode, M.; Gotto, A.M., Jr., *Biochim. Biophys. Acta*, **713**, 496 (1982).

114. Op den Kamp, J.A.F.; Kauerz, M.T.; van Deenen, L.L.M., *Biochim. Biophys. Acta*, **406**, 169 (1975).

115. Allen, T.M., in Liposome Technology, Gregoriadis, G., Ed., CRC PRess: Boca Raton, FL, 1984 Vol.3, pp.177-182.

116. Turro, N.J.; Arora, K.S., *Polymer*, **27**, 783 (1986).

117. Chen, H.L.; Morawetz, H., *Eur. Polym. J.*, **19**, 923 (1983).

118. Himel, C.M.; Mayer, R.T.; Cook,L.L.J., *J. Polym. Sci., Part A-1*, **8**, 2219 (1970).

119. Li, Y.-H.; Chan, L.-M.; Tyer, L.; Moody, R.T.; Himel, C.M.; Hercules, D.M., *J. Am. Chem. Soc.*, **97**, 3118 (1975).

120. Strauss, U.P.; Vesnaver; G., *J. Phys. Chem.*, **79**, 1558, (1975).

121. Bentley, R., *Methods in Enzymology*, **IX**, 86 (1966).

122. Gibson, Q.H.; Swoboda, B.E.P.; Massey, V., *J. Biol. Chem.*, **239**, 3927 (1964).

123. Lehninger, A.L., Biochemistry, Worth Publishers, New York, 1975, p. 831.

124. Dixon, M., *Discussions Faraday Soc.*, **20**, 301 (1955).

125. Ingraham, L.L., *Discussions Faraday Soc.*, **20**, 304 (1955).

126. Bentley, R., in The Enzymes, vol.7, Academic Press, New York, 1963, pp. 567-586.

APPENDIX A

REFERENCE ^{1}H NMR SPECTRA FOR THE CHARACTERIZATION OF POLYMERS AND INTERMEDIATES

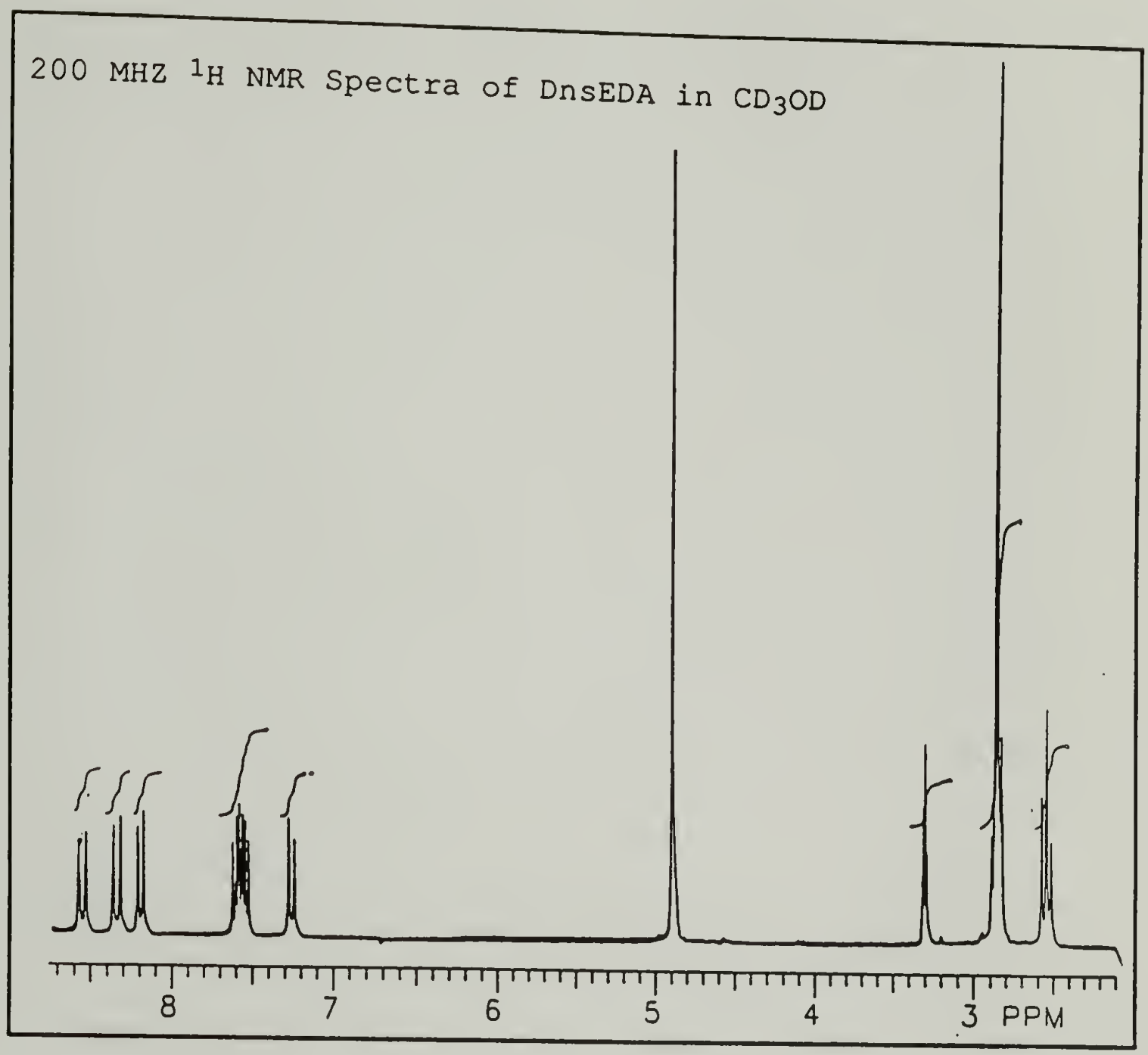
200 MHZ ^{1}H NMR Spectra of DnsEDA in CD_3OD
8
7
6
5
4
3 PPM

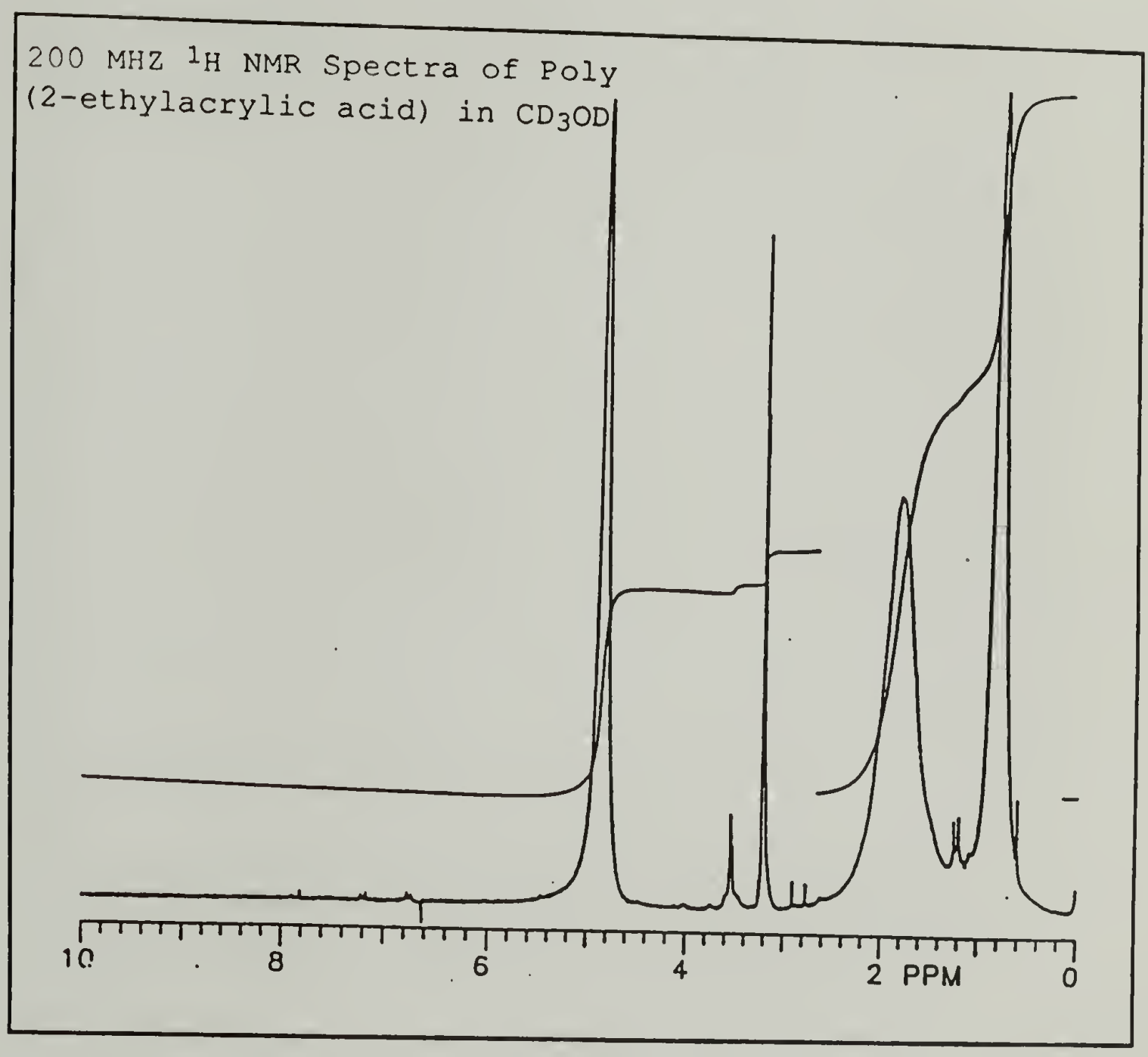
200 MHZ ^{1}H NMR Spectra of Poly (2-ethylacrylic acid) in CD_3OD
10
8
6
4
2 PPM
0

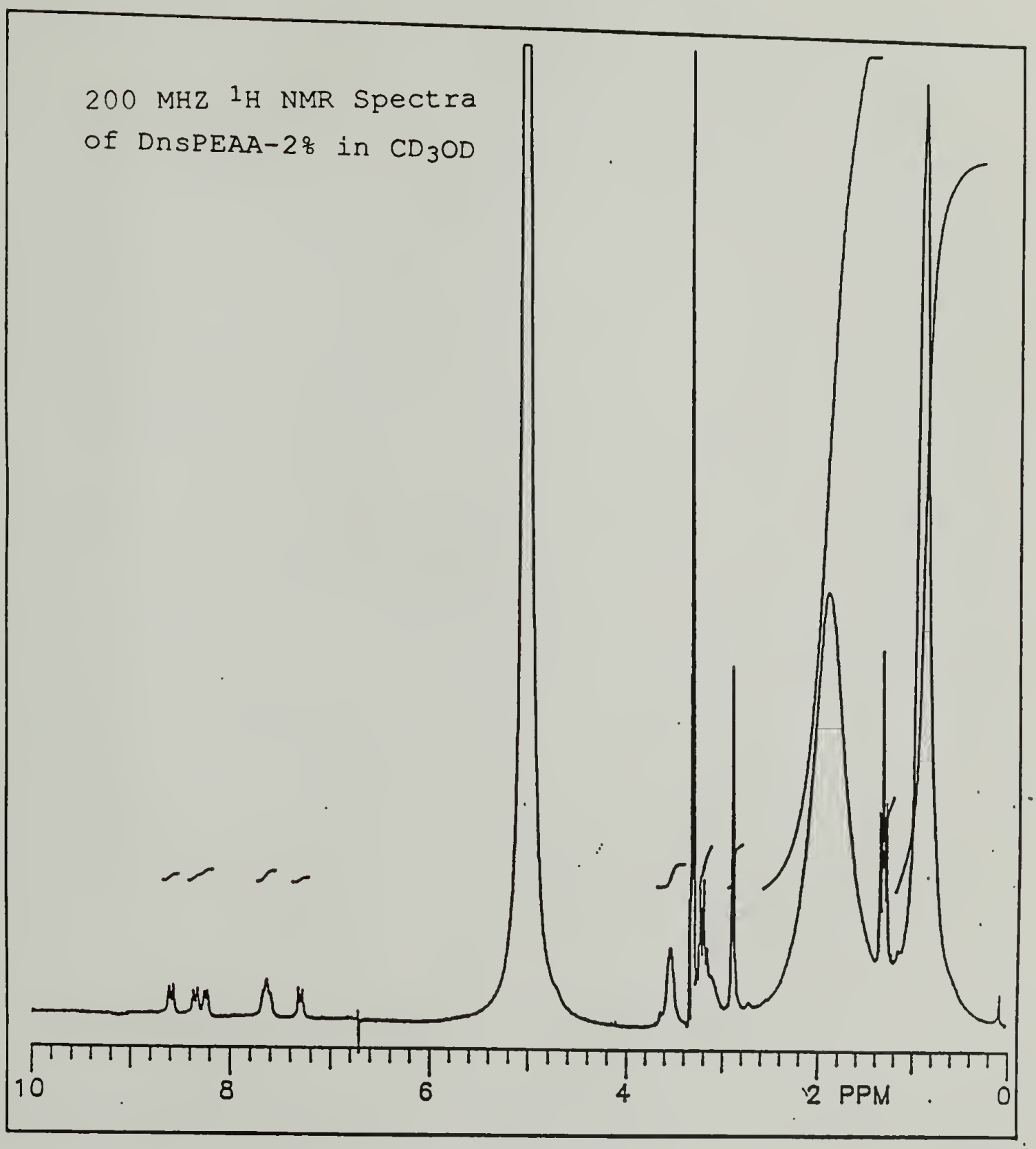
200 MHZ 1H NMR Spectra
of DnsPEAA-2% in CD3OD
10
8
6
4
2 PPM
0

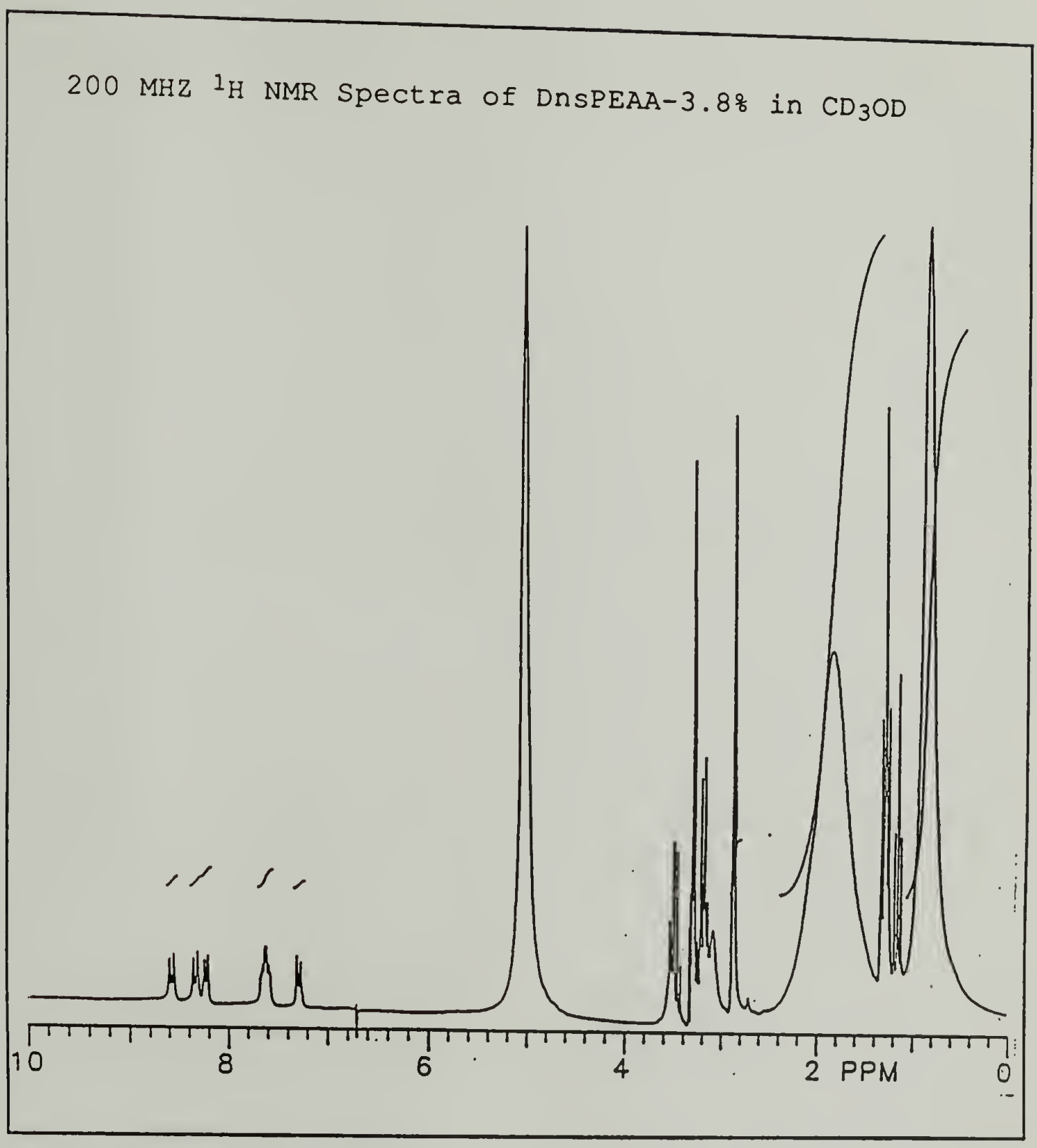
200 MHZ ^{1}H NMR Spectra of DnsPEAA-3.8% in CD_3OD
10
8
6
4
2 PPM
0

APPENDIX B

EPI-FLUORESCENCE AND TRANSMITTED LIGHT MICROGRAPHS OF DNSPEAA/VESICLE MIXTURES

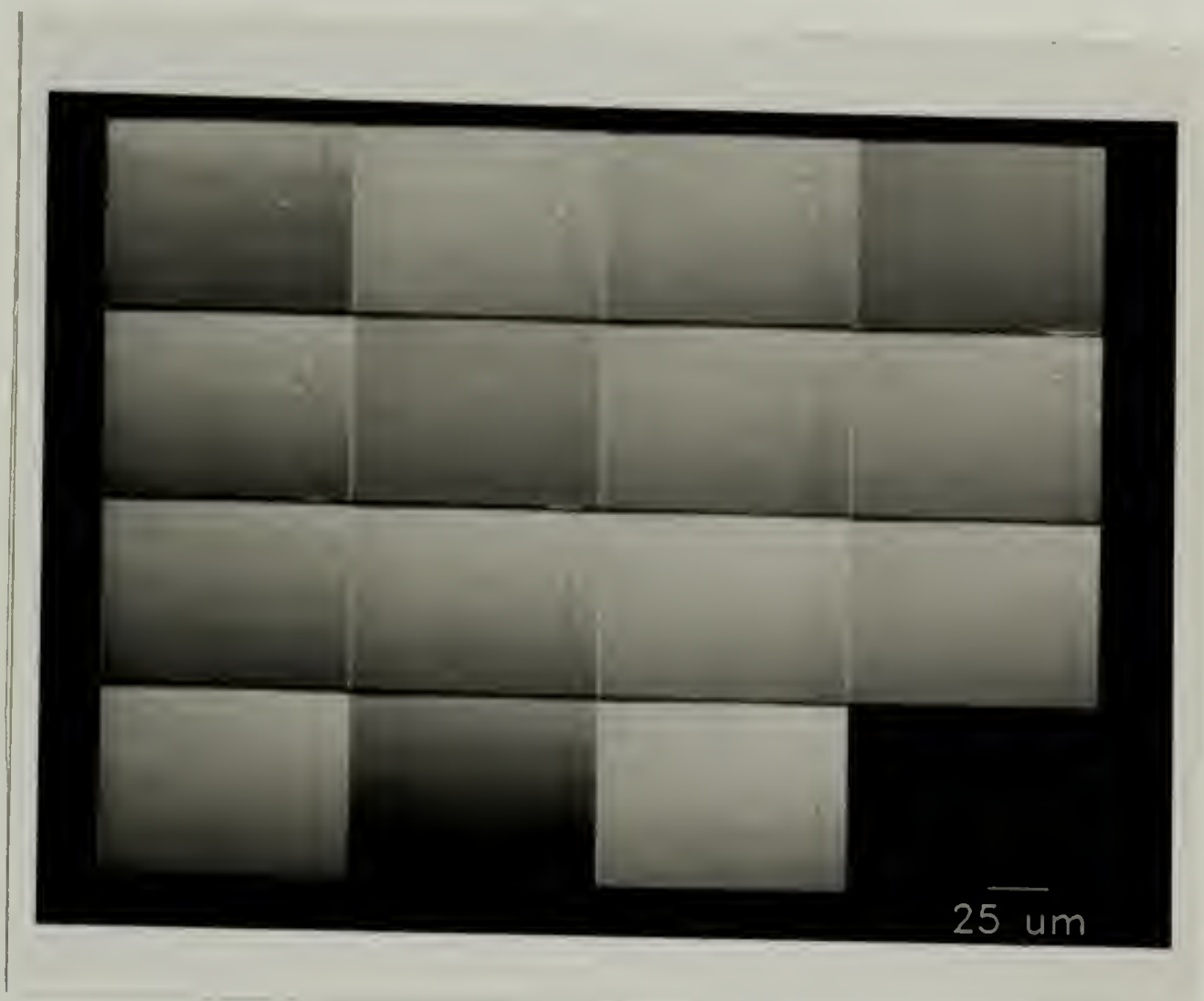

Figure B.1 Transmitted light micrographs of a suspension of EYPC MLV's (1 mg/ml) in the presence of DnsPEAA-2% (1mg/ml) at pH 6.4 in 50 mM phosphate/50 mM NaCl. Frames were taken one minute apart (left to right, top to bottom) starting at 3.5 minutes after acidification from pH 7.4.

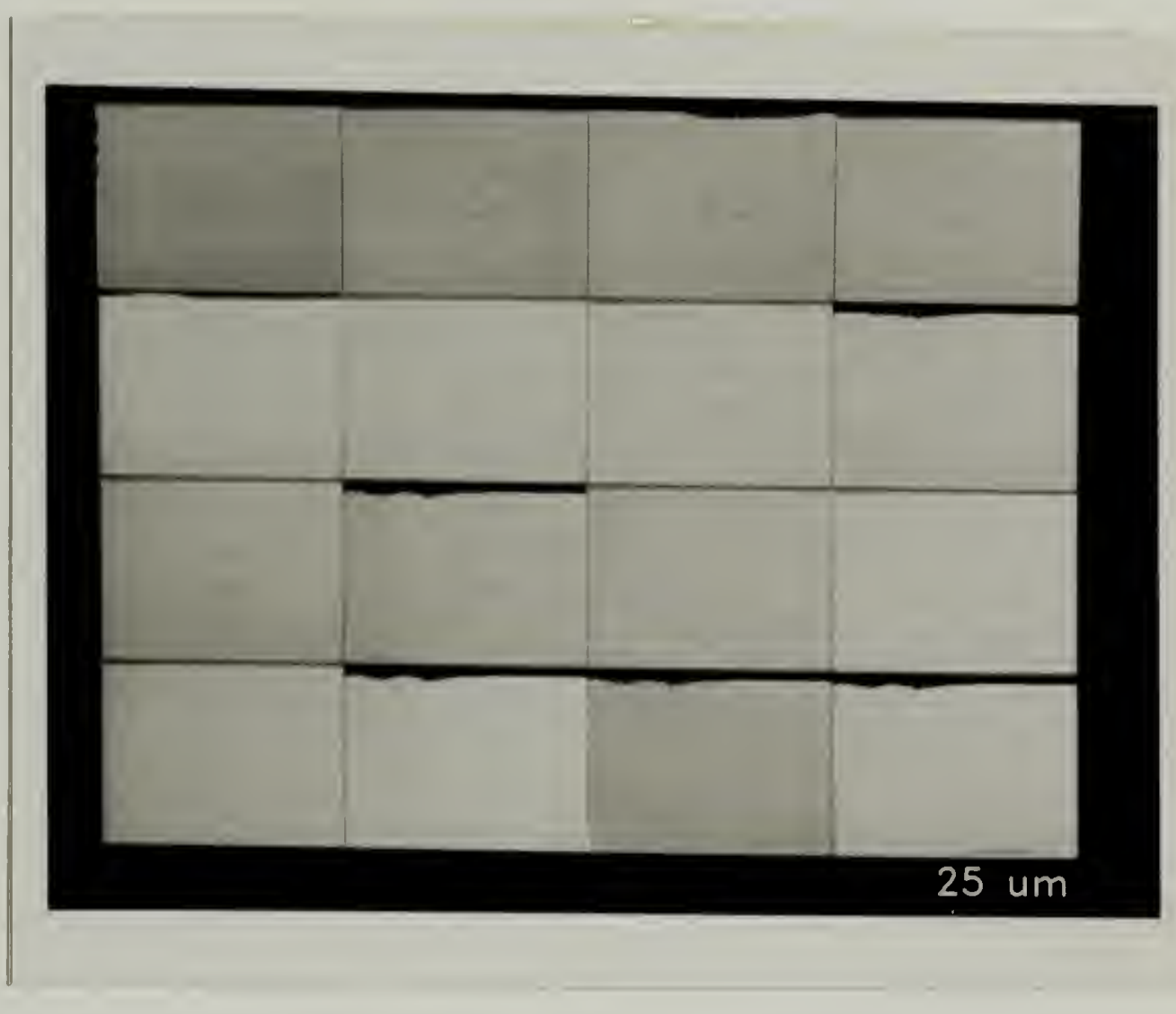

Figure B.2 Transmitted light micrographs of a suspension of EYPC MLV's (1 mg/ml) in the presence of DnsPEAA-3.8% (1mg/ml) at pH 6.4 in 50 mM phosphate/50 mM NaCl. Frames were taken one minute apart (left to right, top to bottom) starting at 4.5 minutes after acidification from pH 7.4.

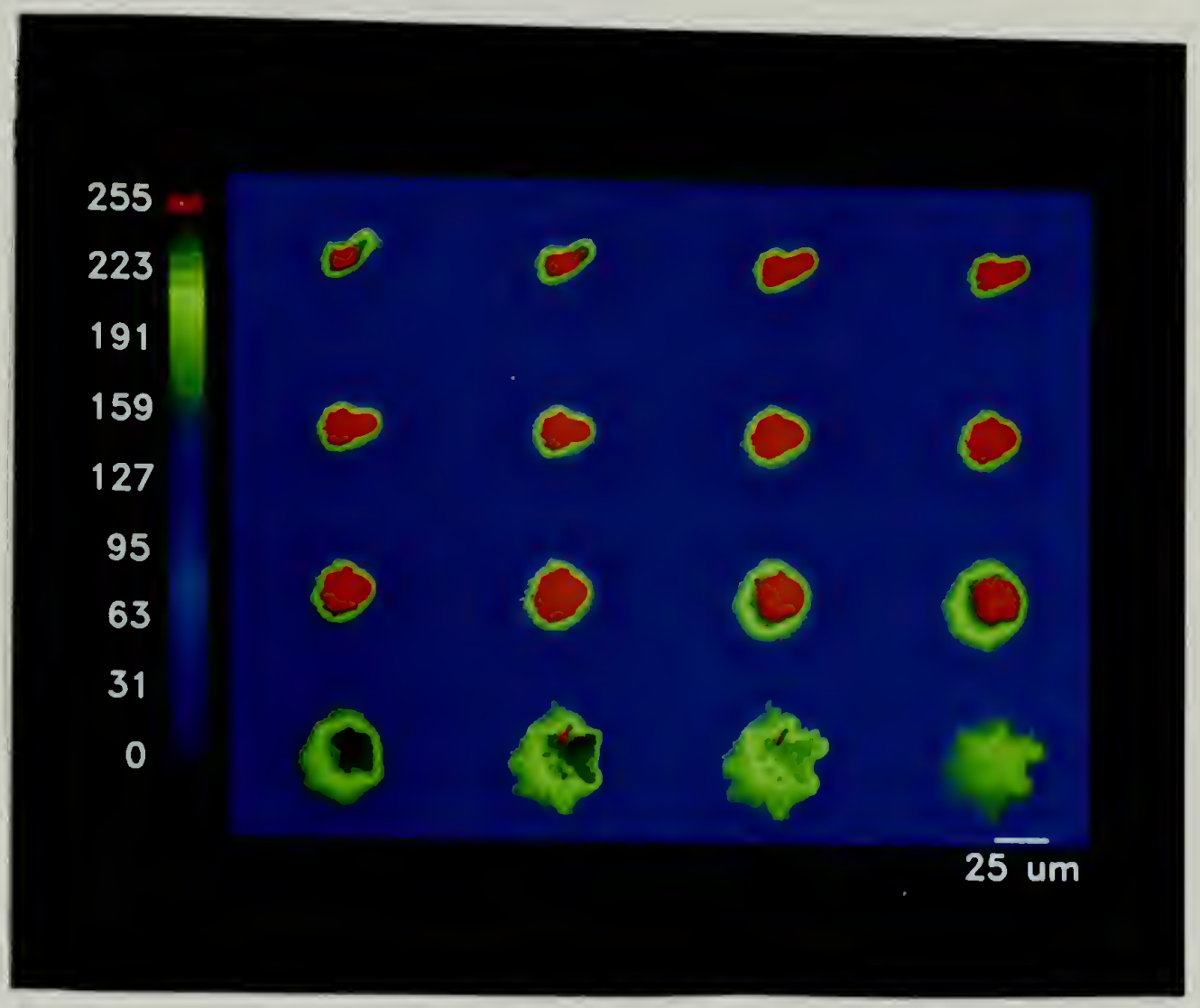

Figure B.3 Epi-fluorescence micrographs (λ_{ex}=334 nm) of a suspension of EYPC MLV's (1 mg/ml) in the presence of DnsPEAA-2% (1mg/ml) at pH 6.4 in 50 mM phosphate/50 mM NaCl. Frames were taken one minute apart (left to right, top to bottom) starting at 3.5 minutes after acidification from pH 7.4.

Figure B.4 Epi-fluorescence micrographs (λ_{ex}=334 nm) of a suspension of EYPC MLV's (1 mg/ml) in the presence of DnsPEAA-3.8% (1mg/ml) at pH 6.4 in 50 mM phosphate/50 mM NaCl. Frames were taken one minute apart (left to right, top to bottom) starting at 4.5 minutes after acidification from pH 7.4.

BIBLIOGRAPHY

Allen, T.M., in Liposome Technology, Gregoriadis, G., Ed., CRC PRess: Boca Raton, FL, 1984 Vol.3, pp.177-182.

Anufrieva, E.; Birnstein, T.; Nekrasova, T.; Ptitsyn, O.; Sheveleva, T., *J. Polym. Sci., Pt. C*, **16**, 3519 (1968).

Arnold, R., *J. Colloid Sci.*, **12**, 549 (1957).

Arora, K.; Hwang, K.; Turro, N., *Macromolecules*, **19**, 2806 (1986).

Assman, G.; Brewer, H.B., Jr., *Proc. Natl. Acad. Sci. U.S.A.*, **71**, 989 (1974).

Bangham A.; Horne R.W., *J.Mol.Biol.*, **8**, 386, (1964).

Bangham, A., *Chem. Phys. Lipids*, **8**, 237 (1972).

Bangham, A.D., *Prog. Biophys. Mol. Biol.*, **18**, 29 (1968).

Bangham, A.D.; Standish, N.M.; Watkins, J.C., *J. Mol. Biol.*, **13**, 238 (1965).

Barone, G.; Crescenzi, V.; Liquori, A.; Quadrifoglio, F., *J. Phys. Chem.*, **71**, 2341 (1967).

Barone, G.; Crescenzi, V.; Pispisa, B.; Quadrifoglio, F., *J. Macromol. Chem.*, **1**, 767 (1966).

Bentley, R., in The Enzymes, vol.7, Academic Press, New York, 1963, pp. 567-586.

Bentley, R., *Methods in Enzymology*, **IX**, 86 (1966).

Bentley, R.; Neuberger, A., *Biochem. J.*, **45**, 584 (1949).

Borden, K., Ph.D. Thesis, University of Massachusetts, 1989.

Borden, K.; Eum, K.; Langley, K.; Tirrell, D., *Macromolecules*, **20**, 454 (1987).

Braud, C.; Muller, G.; Fenyo, J.; Selegny, E., *J. Polym. Sci. Polym. Chem. Ed.*, **12**, 2767 (1974).

Cahill, G.F.; Etzweiler, D.D.; Freinkel, N., *Diabetes*, **25**, 137 (1976).

Carey, M.; Small, D., *Am.J.Med.*, **49**, 150 (1970).

Carnie, S.; Israelachvili, J.N.; Pailthorpe, B.A., *Biochim. Biophys. Acta*, **554**, 340 (1979).

Chapman, D. in: Membrane Structure and Function, John Wiley, New York, 1980 pp. 103-152.

Chapman, D., *Quart. Rev. Biophys.*, **8**, 185 (1975).

Chapman, D.; Williams, R.M.; Ladbrooke, B.D., *Chem. Phys. Lipids*, **1**, 445 (1967).

Chen, H.L.; Morawetz, H., *Eur. Polym. J.*, **19**, 923 (1983).

Chen, R.F., *Anal. Biochem.*, **25**, 412 (1968)..

Chick, W.L.; Perna, J.J.; Lauris, V.; Low, D.; Galletti, P.M.; Panol, G.; Whittermore, A.D.; Like, A.A.; Colton, C.K.; Lysaght, M.J., *Science*, **197**, 780 (1977).

Chu, D.; Thomas, J., *Macromolecules*, **17**, 2412 (1984).

Conio, G.; Patrone, E.; Russo, S.; Trefiletti, V., *Makromol. Chem.*, **177**, 49 (1976).

Crescenzi, V., *Adv. Polym. Sci.*, **5**, 358 (1968).

Crescenzi, V.; Quadrifoglio, F.; Delben, F., *J. Polym. Sci., Pt. A2*, **10**, 357 (1972).

Cutnell, J.; Glasel, J., *Macromolecules*, **9**, 71 (1976).

Dekruijff, B.; van der Besselaar, A.M.H.P.; van Deenan, L.L.M. *Biochim. Biophys. Acta*, **465**, 443 (1977).

DePecol, M.E.; McCormick, D.B., *Anal. Biochem.*, **101**, 435 (1980).

Dixon, M., *Discussions Faraday Soc.*, **20**, 301 (1955).

Ellens, H.; Bentz, J.; Szoka, F., *Biochemistry*, **23**, 1532, (1984).

Elliot, J., *J. Am. Med. Assoc.*, **241**, 223 (1979).

Eum, K., Ph.D. Thesis, University of Massachusetts, 1988.

Eum, K.; Langley, K.; Tirrell, D., *Macromolecules*, **22**, 2755 (1989).

Fendler, J.H. in: Liposomes in Biological Systems, John Wiley and Sons, Chichester, 1980, pp. 87-100.

Fendler, J.H., Membrane Mimetic Chemistry, John Wiley & Sons, New York, 1982, pp. 3-5.

Fendler, J.H.; Romero, A., *Life Sci.*, **20**, 1109 (1977).

Ferritto, M.S., Ph.D. Thesis, University of Massachusetts, 1990.

Ferritto, M.S.; Tirrell, D.A.; Ponticello, I.S., Macromolecular Syntheses, in press.

Fichtner, F.; Schonert, H., *Colloid and Polym. Sci.*, **255**, 230 (1977).

Finkelstein, M.C.; Weissmann, G., *J. Lipid Res.*, **19**, 289 (1978).

Franke, W.; Deffner, M., *Liebigs Ann.*, **541**, 117 (1939).

Franke, W.; Lorenz, F., *Liebigs Ann.*, **532**, 1 (1937).

Galla, H.; Sackmann, E., *J.Membr.Biol.*, **48**, 215, (1979).

Gibson, Q.H.; Swoboda, B.E.P.; Massey, V., *J. Biol. Chem.*, **239**, 3927 (1964).

Gregoriadis, G., in: Drug Carriers in Biology and Medicine, Academic Press, London, 1979, pp. 287-341.

Gwynne, J.; Brewer, H.B., Jr.; Edelhoch, H., *J. Biol. Chem.*, **219**, 1411 (1974).

Gwynne, J.; Brewer, H.B., Jr.; Edelhoch, H., *J. Biol. Chem.*, **250**, 2269 (1975).

Hackenbrock, C.; Hochli, M.; Chau, R., *Biochim.Biophys.Acta.*, **455**, 466, (1976).

Hauser, H.; Barret, M.D., *Biochem. Biophys. Res. Commun.*, **53**, 399 (1973).

Hayden, D.A.; Taylor, J., *J. Theor. Biol.*, **4**, 281 (1963).

Himel, C.M.; Mayer, R.T.; Cook,L.L.J., *J. Polym. Sci., Part A-1*, **8**, 2219 (1970).

Horbett, T.A.; Ratner, B.D.; Kost, J.; Singh, M., in: Recent Advances in Drug Delivery Systems, Plenum, New York, 1984, pp.204-220.

Huang, C., *Biochemistry*, **8**, 344 (1969).

Ingraham, L.L., *Discussions Faraday Soc.*, **20**, 304 (1955).

Ishihara, K.; Kobayashi, M.; Shionohara, I., *Makromol. Chem. Rapid Commun.*, **4**, 327 (1983).

Israelachvili, J.N., Intermolecular and Surfaces Forces, Academic Press: New York, 1985 pp. 229-275.

Israelachvili, J.N.; Mitchell, J.; Ninham, B., *J. Chem. Soc. Faraday Trans.II*, **72**, 1525 (1976).

Jacobson, K.; Papahadjopoulos, D., *Biochemistry*, **14**, 152, (1975).

Jeong, S.Y.; Kim, S.W.; Eenink, M.J.D.; Feijen, J., *J. Controlled Release*, **1**, 57 (1984).

Joyce, D.E.; Kurucsev, T., *Polymer*, **22**, 415 (1981).

Kahler, H.; Robertson, W., *J.Natl.Cancer Inst.(U.S.)*, **34**, 857, (1965).

Katchalsky, A., *J. Polym. Sci.*, **7**, 393 (1951).

Katchalsky, A.; Eisenberg, H., *J. Polym. Sci.*, **6**, 145 (1951).

Keilin, D.; Hartee, E.F., *Biochem.J.*, **42**, 221 (1948).

Keilin, D.; Hartee, E.F., *Nature*, **157**, 801 (1946).

Kimelberg, H.K.; Mayhew, E., *CRC Crit. Rev. Toxicol.*, **6**, 25 (1978).

Kleemann, W.; McConnell, H.M., *Biochim. Biophys. Acta.*, **419**, 206 (1976).

Kondo, H.; Takaki, K.; Kuroki, R.; Tada, A.; Fukumoto, K.; Sunamoto, J., *Bull. Chem. Soc. Jpn.*, **57**, 2957 (1984).

Kusai, K., *Ann. Rept. Sci. Works, Fac. Sci. Osaka Univ.*, **8**, 43 (1960).

Kusai, K.; Sekuzu, I.; Hagihara, B.; Okunuki, K.; Yamauchi, S.; Nakai, M., *BBA*, **40**, 555 (1960).

Lando, J.; Koenig, J.; Semen, J., *J. Macromol. Sci., Phys.*, **B7**, 319 (1973).

Lee, A.G., *Biochim. Biophys. Acta.*, **422**, 237 (1977).

Lee, A.G., *Biochim. Biophys. Acta.*, **472**, 345 (1977).

Lee, A.G., *Prog. Biopys. Mol. Biol.*, **29**, 3 (1975).

Lehninger, A.L., Biochemistry, Worth Publishers, New York, 1975, p. 831.

Leung, Y.F.; O'Shea, G.M.; Goosen, M.F.A.; Sun, A.M., *Art. Org.*, **7**, 208 (1983).

Levine, Y.K., *Prog. Surf. Sci.*, **3**, 279 (1973).

Leyte, J.; Mandel, M., *J. Polym. Sci., Pt. A*, **2**, 1879 (1964).

Li, Y.-H.; Chan, L.-M.; Tyer, L.; Moody, R.T.; Himel, C.M.; Hercules, D.M., *J. Am. Chem. Soc.*, **97**, 3118 (1975).

Lucy, J.A., *Nature*, **227**, 815 (1970).

Mabrey, S.; Mateo, P.; Sturtevant, J., *Biochemistry*, **17**, 2464, (1978).

Mabrey, S.; Sturtevant, J.M., *Proc.Natl.Acad.Sci.*, **73(11)**, 3862 (1976).

Mabrey-Gaud, S., in: Liposomes: From Physical Structure to Therapeutic Applications, C. Knight, Ed., Elsevier/North-Holland Biomedical Press: New York, 1981 pp. 105-138.

Mandel, M., *Eur. Polym. J.*, **6**, 807 (1970).

Mandersloot, J.; Reman, F.; VanDeenen,L.; DeGier, J., *Biochim.Biophys.Acta.*, **382**, 22, (1975).

Marsh, D.; Watts, A.; Knowles, P.F., *Biochemistry*, **15**, 3570 (1976).

Massey, J.B.; She, H.S.; Gotto, A.M., Jr.; Pownall, H.J., *Biochemistry*, **24**, 7110 (1985).

Mazer, N.; Benedek, G.; Carey, M., *Biochemistry*, **19**, 601, (1980).

Meyer, K.; Kummerling, E.; Altman, L.; Iller, M.; Hoffman, S., *Cancer Res.*, **8**, 513, (1948).

Morris, D.A.N.; McNeil, R.; Castellino, F.J.; Thomas, J.K., *Biochim. Biophys. Acta*, **599**, 380 (1980).

Muller, D., *Biochem. Z.*, **199**, 136 (1928).

Nagasawa, M., *Pure Appl. Chem.*, **26**, 519 (1971).

Nayer, R.; Schroit, A., *Biochemistry*, **24**, 5967, (1985)

Oldfield, E.; Chapman, D., *FEBS Lett.*, **21**, 302 (1972).

Op den Kamp, J.A.F.; Kauerz, M.T.; van Deenen, L.L.M., *Biochim. Biophys. Acta*, **406**, 169 (1975).

Overberger, C.G.; O'Shaughnessy, M.T.; Shalit, H., *JACS*, **71**, 2661 (1949).

Papahadjopoulos, D.; Kimelburg, H.K., *Prog. Surf. Sci.*, **4**, 141 (1975).

Pazur, J.H., *Methods in Enzymology*, **9**, 82 (1966).

Phillips, M.C., *Prog. Surf. Membr. Sci.*, **5**, 139 (1972).

Phillips, M.C.; Williams, R.N.; Chapman, D., *Chem. Phys. Lipids*, **3**, 234 (1969).

Pownall, H.J.; Massey, J.B.; Kusserow, S.K.; Gotto, A.M., Jr., *Biochemistry*, **17**, 1183 (1978).

Pownall, H.J.; Van Winkle, W.B.; Pao, Q.; Rhode, M.; Gotto, A.M., Jr., *Biochim. Biophys. Acta*, **713**, 496 (1982).

Quinn, P.J.; Chapman, D., *CRC Crit. Rev. Biochem.*, **8**, 1-117 (1980).

Rand, R.P.; Panghorn, W.A.; Purdon, A.D.; Tinker, D.O., *Can. J. Biochem.*, **53**, 189 (1975).

Ryman, B.E.; Tyrrell, D.A., *Essays Biochem.*, **16**, 49 (1980).

Schaefer, J., *Macromolecules*, **4**, 98 (1971).

Schroeder, U.; Tirrell, D., *Macromolecules*, **22**, 765 (1989).

Seki, K.; Tirrell, D.A., *Macromolecules*, **17**, 1692, (1984).

Shimshick, E.; McConnell, H., *Biochemistry*,**12**, 2351, (1973).

Shimshick, E.J.; McConnell, H.M., *Biochem. Biophys. Res. Commun.*, **53**, 446 (1973).

Strauss, U.P.; Vesnaver; G., *J. Phys. Chem.*, **79**, 1558, (1975).

Sugai, S.; Nitta, K.; Ohno, N.; Nakano, H., *Colloid and Polym. Sci.*, **261**, 159 (1983).

Takigawa, D.Y.; Tirrell, D.A., *Macromolecules*, **18**, 338, (1985).

Tall, A.R.; Shipley, G.G.; Small, D.M., *J. Biol. Chem.*, **251**, 3749 (1976).

Tall, A.R.; Small, D.M.; Deckelbaum, R.J.; Shipley, G., *J. Biol. Chem.*, **252**, 4701, (1977).

Tirrell, D.A.; Takigawa, D.Y.; Seki, K., *Ann. N.Y. Acad. Sci.*, **446**, 237, (1985).

Trauble, H.; Haynes, D.H., *Chem. Phys. Lipids*, **7**, 324 (1971).

Tsong, T.Y.; Kanehisa, M.I., *Biochemistry*, **16**, 2674 (1977).

Turro, N.J.; Arora, K.S., *Polymer*, **27**, 783 (1986).

Tyrrell, D.A.; Heath, T.D.; Colley, C.M.; Ryman, B.E., *Biochim. Biophys. Acta*, **457**, 259 (1976).

Wickner, W., *Ann. Rev. Biochem.*, **48**, 23 (1979).

Wilkinson, D.A.; Nagle, J.F., *Biochemistry*, **18**, 4244 (1979).